

**EXPRESSION OF AN ANTI-AGGREGANT TAU  
MUTANT (Tau<sup>RD/ΔK280PP</sup>) IS NEUROPROTECTIVE  
IN ORGANOTYPIC HIPPOCAMPAL SLICE CULTURES**

---

Dissertation

Zur Erlangung der Würde des Doktors der Naturwissenschaften  
des Department Biologie, der Fakultät für Mathematik, Informatik  
und Naturwissenschaften,

der Universität Hamburg

vorgelegt von

Chris Maria Renny Joseph

aus Tamil Nadu, India

Hamburg 2014

Tag der Disputation: 06.02.2015

Gutachter:

1. Prof. Dr. Eckhard Mandelkow
2. Prof. Dr. Christian Lohr

## SUMMARY

Tau protein is a key factor in the pathogenesis of Alzheimer disease and other neurodegenerative diseases. A number of transgenic mouse models have been generated in order to elucidate the role of Tau in disease progression. In the present study, transgenic organotypic hippocampal slice cultures (OHSC) were used to investigate the changes in the hippocampus of transgenic mice induced by overexpression of the anti-aggregant Tau repeat domain (Tau<sup>RDA-PP</sup>). The slice cultures were prepared from inducible anti-aggregant Tau<sup>RDA-PP</sup> mice at days P8-P10 and kept in culture for 4 weeks. A sensitive bioluminescence reporter gene assay (luciferase) was used to monitor the expression of the Tau transgene over time and in different hippocampal subregions. The expression of anti-aggregant Tau<sup>RDA-PP</sup> leads to a larger volume of the hippocampus at young age due to neurogenesis, which was confirmed by an increase of neuronal number as determined by stereology. The number of astrocytes did not change, whereas the number of microglia was reduced. Increased BrdU incorporation demonstrated a strong proliferation of neural stem cells and immunostaining for Ki67, doublecortin (DCX), and NeuN showed that most stem cells differentiated into mature neurons. There were no signs of activation of microglia and astrocytes, indicating the absence of an inflammatory reaction. The density of dendritic spines was unchanged during the whole culturing period. Expression of anti-aggregant Tau<sup>RDA-PP</sup> also leads to a 50% higher level of endogenous Tau and this increase was independent of the increase in the total number of neurons in the anti-aggregant Tau<sup>RDA-PP</sup> mice. Investigation of signaling pathways showed that Wnt-5a was strongly decreased whereas GSK3 $\beta$  was activated. The data suggest that the expression of anti-aggregant Tau<sup>RDA-PP</sup> enhances hippocampal neurogenesis mediated by a Wnt signaling pathway, without an inflammatory reaction.

## ZUSAMMENFASSUNG

Tau-Protein ist ein Schlüsselement bei der Entstehung der Alzheimerkrankheit und anderer neurodegenerativer Erkrankungen. Verschiedene Autoren haben transgene Mausmodelle hergestellt, um die Rolle vom Tau-Protein im Krankheitsprozess zu untersuchen. In der hier vorgelegten Arbeit wurden organotypische Hirnschnitte verwendet, um Änderungen im Hippocampus von transgenen Mäusen zu untersuchen, die durch Überexpression des anti-aggreganten Tau Proteins  $\text{Tau}^{\text{RDA-PP}}$  hervorgerufen wurden. Die organotypischen Hirnschnitte wurden aus dem Hippocampus von 8- bis 10-Tage alten induzierbaren  $\text{Tau}^{\text{RDA-PP}}$ -Mäusen präpariert und für vier Wochen in Kultur gehalten. Mit Hilfe eines sensitiven Reporter-gen-Assays (Luciferase) konnte die Expression des transgene Tau-Proteins über die Zeit in den verschiedenen Hippocampus-Regionen verfolgt werden. Die Expression von  $\text{Tau}^{\text{RDA-PP}}$  führte zu einer Volumenvergrößerung des Hippocampus durch Neurogenese, was durch eine erhöhte Anzahl von Neuronen in der stereologischen Untersuchung bestätigt wurde. Die Anzahl an Astrozyten blieb unverändert, während die Anzahl der Mikroglia reduziert war. Ein erhöhter Einbau von Bromdesoxyuridin wies auf eine stark erhöhte Proliferation von neuronalen Stammzellen hin. Die immunhistochemische Identifizierung von Ki67, Doublecortin und NeuN bestätigte, dass die meisten Stammzellen zu reifen Neuronen differenzierten. Über den gesamten Zeitraum der *in vitro* Kultivierung blieb die Dichte der dendritischen Dornenfortsätze unverändert. Die Expression von  $\text{Tau}^{\text{RDA-PP}}$  führte außerdem zu einem 50% Anstieg des endogenen Tau Proteins. Untersuchungen von Signalwegen zeigten eine Reduzierung von Wnt-5a, während gleichzeitig  $\text{GSK}\beta$  aktiviert war. Diese Daten zeigen, dass die Expression von  $\text{Tau}^{\text{RDA-PP}}$  die hippocampale Neurogenese

über einen Wnt-abhängigen Signalweg verstärkt, ohne jedoch zu einer entzündlichen Reaktion zu führen.

## Contents

SUMMARY.....	3
ZUSAMMENFASSUNG.....	4
1) ABBREVIATION.....	15
2) AIMS OF THIS STUDY.....	19
3) INTRODUCTION.....	21
3.1. Alzheimer disease (AD) .....	21
3.2. Tauopathies .....	22
3.3. Tau: A microtubule-associated protein. ....	24
3.4. Isoforms of Tau.....	26
3.5. Tau and its mutations. ....	29
3.6. Tau aggregation. ....	30
3.7. Soluble Tau levels and its importance. ....	30
3.8. Transgenic Tauopathy model. ....	31
3.9. The hippocampus.....	34
3.9.1. Structural features.....	34
3.9.2. Functional features.....	36
3.9.3. The hippocampus and neurodegenerative diseases.....	37
3.10. Organotypic hippocampal slice cultures.....	39
3.11. Neurogenesis .....	41
3.11.1. Postnatal hippocampal neurogenesis in OHSC's.....	43
3.11.2. Adult hippocampal neurogenesis.....	43

3.11.3. Stages of adult hippocampal neurogenesis.....	46
3.12.    Tau in neurogenesis .....	49
4) MATERIALS .....	51
4.1. List of chemicals.....	51
4.2. List of equipments.....	52
4.3. List of antibodies. ....	54
4.4. List of buffers and solutions.....	55
4.4.1. Slice culture media.....	55
4.4.2. Solutions for Immunohistochemistry in organotypic hippocampal slice cultures.....	55
4.4.3. Western Blotting.....	56
4.4.4. Solutions for Agarose gel electrophoresis.....	59
4.4.5. 6x Sample Loading buffer.....	59
4.4.6. Sample preparation for free floating vibratome brain section.....	60
5) METHODS.....	61
5.1.    The transgenic mice.....	61
5.2.    Origin of the Tau <sup>RD</sup> constructs and principle of the switch-off system.....	62
5.3.    Genotyping of Tau <sup>RDΔ-PP</sup> transgenic mice.....	63
5.4.    Assessment of luciferase activity.....	64
5.5.    Preparation of organotypic hippocampal slice culture. ....	64
5.6.    Suppression of anti-aggregant Tau <sup>RDΔ-PP</sup> expression by DOX. ....	66
5.7.    Immuno-histochemistry of slice cultures. ....	67

5.7.1.	Immunostaining.....	67
5.7.2.	DAB staining for bright field microscopy and stereology microscopy.....	67
5.7.3.	Confocal microscopy of slice cultures.....	68
5.8.	Diolistic labelling of organotypic slice cultures.....	69
5.9.	Assessment of spine density.....	70
5.10.	Bromodeoxy uridine incorporation assay in organotypic hippocampal slice cultures.....	71
5.11.	Bromodeoxy uridine incorporation assay in P8 pups.....	72
5.12.	Western blot analysis. ....	73
5.13.	Assessment of neuronal cell number in area DG, CA1 and CA3. ....	73
5.14.	Statistical analysis. ....	74
6)	RESULTS.....	75
6.1.	General aspects of slice cultivation.....	75
6.2.	Bioluminescence measurements on organotypic hippocampal slice cultures to determine transgenic Tau <sup>RDA-PP</sup> expression.....	76
6.3.	Increased neuronal number (NeuN positive cells) in the anti- aggregant Tau <sup>RDA-PP</sup> slice at DIV30.....	81
6.4.	Physiologically active microglia are observed in the anti-aggregant Tau <sup>RDA-PP</sup> slices at DIV 30.....	84
6.5.	Physiologically active astrocytes are observed in the anti-aggregant Tau <sup>RDA-PP</sup> slices at DIV 30. ....	89
6.6.	No change in spine density. ....	93
6.7.	Increase in the total number of proliferating BrdU positive cells. ....	94



6.8.	Neuronal stem cells at different proliferating stages are seen in aged anti-aggregant Tau <sup>RDA-PP</sup> slices (DIV30) but are absent in the age matched control littermates. ....	103
6.8.1.	Ki67 positive cells are observed in the anti-aggregant Tau <sup>RDA-PP</sup> slices but are absent in the control slices at DIV 30.....	103
6.8.2.	Doublecortin (DCX) positive cells are observed in the anti-aggregant Tau <sup>RDA-PP</sup> slices at DIV 30 but are absent in the control slices.....	105
6.9.	Tau distribution in organotypic hippocampal slice cultures. ....	109
6.10.	Increased endogenous mouse Tau levels are seen in the anti-aggregant Tau <sup>RDA-PP</sup> slices. ....	113
6.11.	Switch-off experiments with doxycycline. ....	114
6.11.1.	Switch-off of the anti-aggregant Tau <sup>RDA-PP</sup> by doxycycline causes a reduction of endogenous mouse Tau level in the anti-aggregant Tau <sup>RDA-PP</sup> slices. ....	115
6.11.2.	Switch-off of the anti-aggregant Tau <sup>RDA-PP</sup> decreases the total number of neurons in the anti-aggregant Tau <sup>RDA-PP</sup> slices.....	117
6.11.3.	Switch-off of the anti-aggregant Tau <sup>RDA-PP</sup> decreases the total number of BrdU positive cells in the anti-aggregant Tau <sup>RDA-PP</sup> groups...	118
6.12.	The rate of proliferation (BrdU positive cells) was increased in the anti-aggregant Tau <sup>RDA-PP</sup> animals at P8.....	120
6.13.	Increased proliferation in the anti-aggregant Tau <sup>RDA-PP</sup> animals at P8 in the CA3 region of the hippocampus.....	122
6.14.	Increased hippocampal volume in the anti-aggregant Tau <sup>RDA-PP</sup> animals at post-natal day 8. ....	124

6.15.	No change in hippocampal volume in the anti-aggregant Tau <sup>RDA-PP</sup> animals at 17-22 months of age.....	125
6.16.	Expression of the endogenous mouse Tau was high in the anti-aggregant Tau <sup>RDA-PP</sup> animals at 17-22 months of age.....	126
6.17.	GSK3 $\beta$ and its role in neurogenesis.....	127
6.18.	Decreased Wnt5a levels in the anti-aggregant Tau <sup>RDA-PP</sup> slices.....	130
7.	DISCUSSION.....	133
7.1.	Expression of the anti-aggregant Tau <sup>RDA-PP</sup> in organotypic hippocampal slice cultures causes enhanced proliferation and differentiation of neuronal stem cells into neurons.....	133
7.2.	Expression of anti-aggregant Tau <sup>RDA-PP</sup> decreases microglia number, but not astrocytes.....	135
7.3.	Expression of the anti-aggregant Tau <sup>RDA-PP</sup> increases the rate of hippocampal stem cell proliferation and the total hippocampal volume in young mice.....	137
7.4.	Anti-aggregant Tau <sup>RDA-PP</sup> enhances the expression of the endogenous mouse Tau.....	138
7.5.	GSK3 $\beta$ and its role in neurogenesis.....	141
7.6.	Anti-aggregant Tau <sup>RDA-PP</sup> suppresses Wnt5a levels.....	143
8)	CONCLUSIONS.....	144
9.	REFERENCE.....	145
	Acknowledgment.....	166

FIGURE 1: PATHOLOGICAL HALLMARKS OF ALZHEIMER DISEASE.....	22
FIGURE 2: STRUCTURE OF TAU. ....	24
FIGURE 3: DOMAIN STRUCTURE OF THE SIX TAU ISOFORMS THAT ARE EXPRESSED IN THE ADULT HUMAN BRAIN.. ....	27
FIGURE 4: TAU DOMAINS, MUTATIONS, PHOSPHORYLATION SITES AND KINASES. .....	29
FIGURE 5: BASIS OF TRANSGENE EXPRESSION IN THE INDUCIBLE TRANSGENIC MOUSE MODELS. ....	33
FIGURE 6: BASIC CIRCUIT OF THE HIPPOCAMPUS USING A MODIFIED DRAWING BY RAMON Y CAJAL.....	35
FIGURE 7: CHANGES IN THE VIEW OF ADULT NEUROGENESIS OVER THE PAST 15 YEARS.....	42
FIGURE 8: STAGES OF ADULT HIPPOCAMPAL NEUROGENESIS.....	47
FIGURE 9: THE HUMAN TAU REPEAT DOMAIN CONSTRUCTS CARRYING THE FTDP- 17 MUTATION $\Delta$ K280.....	61
FIGURE 10: DOXYCYCLINE DEPENDENT SWITCH-OFF SYSTEM.....	63
FIGURE 11: SLICE SELECTION AND CULTURE ARRANGEMENT IMAGED WITH INCREASING MAGNIFICATION.....	66
FIGURE 12: ASSESSMENT OF APICAL DENDRITIC SPINE DENSITY IN STRATUM RADIATUM OF AREA CA1.....	71
FIGURE 13: BRDU INJECTION IN P8 ANIMALS.....	72
FIGURE 14: BIOLUMINESCENCE MEASUREMENT DONE ON BRAINS FROM P8 ANIMALS. ....	78
FIGURE 15: BIOLUMINESCENCE IMAGE OF A SINGLE HIPPOCAMPAL SLICE FROM THE ANTI-AGGREGANT TAU <sup>RDA-PP</sup> MOUSE AT DIV 1.....	79
FIGURE 16: EXPRESSION LEVEL OF THE EXOGENOUS HUMAN TAU <sup>RDA-PP</sup> CONSTRUCT IN THE HIPPOCAMPAL SLICE CULTURES PREPARED FROM ANTI-AGGREGANT TAU <sup>RDA-PP</sup> ANIMALS, MEASURED BY BIOLUMINESCENCE.....	80
FIGURE 17: LARGER HIPPOCAMPUS WAS OBSERVED IN THE ANTI-AGGREGANT TAU <sup>RDA-PP</sup> SLICES AT DIV 30.....	81
FIGURE 18: INDIVIDUAL REGIONS OF THE HIPPOCAMPUS, THE CA1, CA3 AND DG. .....	82

<b>FIGURE 19: NEUN COUNTING DONE ON ORGANOTYPIC HIPPOCAMPAL SLICE CULTURES AT DIV 30 IN THE CONTROL AND THE ANTI-AGGREGANT TAU<sup>RDA-PP</sup> GROUPS.....</b>	<b>83</b>
<b>FIGURE 20: DIFFERENT STAGES OF MICROGLIAL ACTIVATION AS SEEN IN ORGANOTYPIC HIPPOCAMPAL SLICE CULTURES.....</b>	<b>85</b>
<b>FIGURE 21: NO ACTIVATION OF MICROGLIA WAS SEEN IN THE ANTI-AGGREGANT TAU<sup>RDA-PP</sup> SLICES AT DIV30.....</b>	<b>87</b>
<b>FIGURE 22: DECREASE OF THE TOTAL NUMBER OF MICROGLIA CELLS IN THE ANTI-AGGREGANT TAU<sup>RDA-PP</sup> SLICES AT DIV30.....</b>	<b>88</b>
<b>FIGURE 23: DIFFERENT FORMS OF ASTROCYTES SEEN IN ORGANOTYPIC HIPPOCAMPAL SLICE CULTURES AT DIV30. ....</b>	<b>90</b>
<b>FIGURE 24: ACTIVATED ASTROCYTES WERE NOT PRESENT AT DIV30 IN THE ANTI-AGGREGANT TAU<sup>RDA-PP</sup> SLICES.....</b>	<b>90</b>
<b>FIGURE 25: ASTROCYTIC GFAP PROTEIN LEVELS IN WESTERN BLOTS SHOW NO SIGNIFICANT INCREASE IN THE ANTI-AGGREGANT TAU<sup>RDA-PP</sup> SLICES AT DIV30. ....</b>	<b>91</b>
<b>FIGURE 26: NO CHANGE IN SPINE DENSITY IN THE APICAL AND BASAL DENDRITES OF THE CA1 PYRAMIDAL NEURONS.....</b>	<b>93</b>
<b>FIGURE 27: BRDU GETS INCORPORATED INTO THE PROLIFERATING CELLS WHICH CAN BE DETECTED BY IMMUNOSTAINING WITH ANTI-BRDU ANTIBODY AS SEEN IN OHSC'S AT DIV30.....</b>	<b>96</b>
<b>FIGURE 28: CONTROL AND ANTI-AGGREGANT TAU<sup>RDA-PP</sup> SLICES TREATED WITH BRDU FROM DIV 15 TO DIV 30. ....</b>	<b>97</b>
<b>FIGURE 29: RATE OF PROLIFERATION: NUMBER OF BRDU POSITIVE CELLS IN THE CONTROL AND THE ANTI-AGGREGANT TAU<sup>RDA-PP</sup> SLICES AT DIV 30. ....</b>	<b>98</b>
<b>FIGURE 30: PERCENTAGE OF THE CELLS THAT ARE BRDU POSITIVE ARE ALMOST DOUBLED IN THE ANTI-AGGREGANT TAU<sup>RDA-PP</sup> SLICES WHEN COMPARED TO THE CONTROLS. ....</b>	<b>99</b>
<b>FIGURE 31: RATE OF DIFFERENTIATION.....</b>	<b>102</b>
<b>FIGURE 32: KI67 POSITIVE NEUROBLAST CELLS FROM THE NEURONAL STEM CELL LINEAGE WERE SEEN IN THE ANTI-AGGREGANT TAU<sup>RDA-PP</sup> SLICES AT DIV 30. ....</b>	<b>104</b>

FIGURE 33: DCX POSITIVE NEUROBLAST CELLS FROM THE NEURONAL STEM CELL LINEAGE WERE SEEN IN THE ANTI-AGGREGANT TAU <sup>RDA-PP</sup> SLICES AT DIV 30.	107
FIGURE 34: DCX POSITIVE CELLS CO-STAINED WITH NEUN IN THE DG OF THE ANTI-AGGREGANT TAU <sup>RDA-PP</sup> GROUPS AT DIV30.....	109
FIGURE 35: MISLOCALIZATION OF TAU INTO THE SOMATO DENDRITIC COMPARTMENT IN SLICE CULTURES.....	110
FIGURE 36: MISLOCALIZATION OF TAU IN THE SOMATO-DENDRITIC COMPARTMENT OF THE CA1 PYRAMIDAL NEURONS OF PRO-AGGREGANT TAU <sup>RDA</sup> MICE AS SEEN IN ORGANOTYPIC HIPPOCAMPAL SLICE CULTURES....	111
FIGURE 37: DISTRIBUTION OF TAU IN CONTROL AND ANTI-AGGREGANT TAU <sup>RDA-PP</sup> SLICES AT DIV 30.....	112
FIGURE 38: LEVELS OF THE ENDOGENOUS MOUSE TAU WAS INCREASED IN THE ANTI-AGGREGANT TAU <sup>RDA-PP</sup> SLICES AT DIV 30.....	113
FIGURE 39: ENDOGENOUS MOUSE TAU WAS DECREASED AFTER APPLICATION OF DOXYCYCLINE TO THE ANTI-AGGREGANT TAU <sup>RDA-PP</sup> SLICES. ....	116
FIGURE 40: DOXYCYCLINE TREATMENT DECREASES THE TOTAL NUMBER OF NEURONS IN THE ANTI-AGGREGANT TAU <sup>RDA-PP</sup> SLICES.....	117
FIGURE 41: DOXYCYCLINE TREATMENT DECREASES THE TOTAL NUMBER OF BRDU POSITIVE CELLS IN THE ANTI-AGGREGANT TAU <sup>RDA-PP</sup> SLICES.....	119
FIGURE 42: BRDU INCORPORATION IN THE HIPPOCAMPUS OF P8 CONTROL ANIMALS. ....	121
FIGURE 43: INCREASED NUMBER OF BRDU POSITIVE PROLIFERATING CELLS IN THE CA3 REGION IN THE ANTI-AGGREGANT TAU <sup>RDA-PP</sup> GROUPS.....	123
FIGURE 44: TOTAL HIPPOCAMPAL VOLUME IS INCREASED IN THE ANTI-AGGREGANT TAU <sup>RDA-PP</sup> PUPS AT P8 AS MEASURED BY STEREOLOGY.....	124
FIGURE 45: NO DIFFERENCE IN THE TOTAL HIPPOCAMPAL VOLUME AT 17-22 MONTHS OF AGE.....	125
FIGURE 46: NO SIGNIFICANT DIFFERENCE IN THE DENSITY OF HIPPOCAMPAL NEURONS AT 17-22 MONTHS OF AGE. ....	126
FIGURE 47: INCREASE IN THE ENDOGENOUS MOUSE TAU LEVELS IN THE ANTI-AGGREGANT TAU <sup>RDA-PP</sup> GROUPS AT 17-22 MONTHS OF AGE.....	127
FIGURE 48: DECREASE IN THE INACTIVE FORM OF GSK3 $\beta$ LEVELS IN THE ANTI-AGGREGANT TAU <sup>RDA-PP</sup> GROUPS AT 17 MONTH OF AGE.....	129

**FIGURE 49: THE WNT5A LEVELS WERE SIGNIFICANTLY REDUCED IN THE ANTI-AGGREGANT TAU<sup>RDA-PP</sup> SLICES. THESE LEVELS WERE FURTHER SIGNIFICANTLY REDUCED WHEN THE EXPRESSION OF ANTI-AGGREGANT TAU<sup>RDA-PP</sup> WAS SWITCHED OFF BY THE APPLICATION OF DOXYCYCLINE. ....131**

## 1) ABBREVIATION

3R- 3 Repeats

4R- 4 Repeats

Anti-agg- Anti-aggregant

AD- Alzheimer disease

AMP- Adenosine monophosphate

APP- Amyloid precursor protein

ATP- Adenosine Triphosphate

A $\beta$ - Amyloid beta

BLI- Bioluminescence Imaging

bp- Base pairs

BrdU- Bromo deoxy uridine

CA- Cornu amonis

CaMKII $\alpha$ - Calcium/Calmodulin-dependent protein kinase alpha

CBD- Corticobasal degeneration

CNS- Central nervous system

Ca<sup>2+</sup>- Calcium

C-ter- Carboxy Terminus

Ctrl- Control

DCX- Doublecortin

DG- Dentate gyrus

DIV- Days In-vitro

DNA- Deoxyribonucleic acid

DOX- Doxycycline

E 10- Embryonic day 10

EC- Entorhinal cortex

FAD- Familial Alzheimer disease

FTDP17- Frontotemporal dementia with parkinsonism linked to chromosome 17

GFAP- Glial fibrillary acidic protein

GSK3 $\beta$ - Glycogen synthase kinase 3

g- Grams

HBSS- Hank's Buffered salt solution

HCl- Hydrochloride

h-CMV- human cytomegalo virus

Iba1- Ionised calcium binding adaptor molecule 1

KD- KiloDalton

KOKI- Knock-out knock-in

LDH- Lactate dehydrogenase

LPS- Lipopolysaccharide

LTP- Long-Term Potentiation

M- Molar

MARK1- MAP/microtubule affinity-regulating kinase 1

MAP- Microtubule associated protein

MAPT- Microtubule associated protein Tau

MEM- Minimum essential media

MF- Mossy fiber

mg- Milligram

$\mu$ g- Microgram

ml- Milliliter

MT- Microtubules

mM- Millimolar

$\mu$ M- Micromolar

mRNA- messenger RNA



MT- microtubules  
MRI- Magnetic resonance imaging  
NeuN- Neuronal nuclei  
NAD<sup>+</sup>- Nicotinamide adenine dinucleotide  
NFT- Neurofibrillary tangles  
NIH- National institute of health  
NMDA- N-methyl-D-aspartate  
NPC- Neuronal progenitor cell  
NSC- Neuronal stem cell  
N-terminal- Amino terminal  
nTg- Non-Transgenic  
OHSC- organotypic hippocampal slice culture  
P8- Post-natal day 8  
PBS- Phosphate buffered saline  
PD- Parkinson disease  
PHF- Paired helical filaments  
PP2A- Protein Phosphatase 2A  
p/s – Photons per second  
P/S- Penicillin/ Streptomycine  
PSP- Progressive supranuclear palsy  
PS1- Presenilin1  
RGC- Radial glial cell  
RNA- Ribonucleic acid  
RT- Room temperature  
rTg- Regulatable transgene  
s.l.- Stratum lucidum  
s.m.- Stratum moleculare

s.p.- Stratum pyramidale

s.r.- Stratum radiatum

SAD- Synapse of the Amphide defective

SDS- Sodium Dodecylsulphate

SDS-PAGE- Sodium Dodecylsulphate- Polyacrylamide gel electrophoresis

SGZ- Sub-granular zone

SVZ- sub-ventricular zone

TET-O- Tet-operon response element

THS- Thioflavin S

T<sup>RD</sup>- Tau Repeat Domain

TRE- Tetracycline-responsive promoter element

Tet-R- Tet-repressor DNA binding protein

tTA- Transactivator

Tau<sup>RDA</sup>- Pro-aggregant mutant

Tau<sup>RDA-PP</sup>- Anti-aggregant mutant

TKO- Tau knock-out

U- Units

## 2) AIMS OF THIS STUDY

Pathological changes involving Tau protein are thought to contribute to neurodegenerative processes in Alzheimer disease and other tauopathies. The starting point of this study was the observation that mouse models expressing a pro-aggregant form of Tau develop Alzheimer-like pathology quickly, while an anti-aggregant form of Tau does not cause frank neurodegeneration and related cognitive deficits. This can be traced back to the propensity of Tau protein for  $\beta$ -sheet structure, and hence its ability to form pathological aggregates. The repeat domain of Tau is responsible for aggregation. The "pro-aggregant" deletion mutation in the repeat domain (Tau- $\Delta$ K280) causes enhanced  $\beta$ -structure and aggregation in vitro, and faster development of pathology in mouse models and in organotypic brain slices derived from them (Mocanu et al., 2008; Messing et al. 2012). By contrast, neutralizing the  $\beta$ -propensity of Tau by insertion of prolines ("anti-aggregant" mutations  $\Delta$ K280-I277P-I308P) prevents both Tau aggregation and pathology in mouse models. Building on these observations, the aim of this study was to contribute to an understanding of this protective effect by using the experimental model of organotypic slices to address the following questions:

1. Why is there no overt neuropathology even when the anti-aggregant Tau repeat domain is overexpressed?
2. What structural and biochemical changes take place upon expression of anti-aggregant Tau?
3. How does the expression of exogenous anti-aggregant Tau affect the functions of endogenous mouse Tau?
4. What changes occur with regard to inflammatory processes or neurogenesis?

5. What neuronal signaling pathways are affected by the expression of anti-aggregant Tau?

### 3) INTRODUCTION

#### 3.1. Alzheimer disease (AD).

The name Alzheimer disease (AD) comes from a German psychiatrist and pathologist Dr. Alois Alzheimer, who in 1907 described the case of a 51 year old female patient's death in a completely demented state (Alzheimer, 1907). AD, a progressive neurodegenerative disorder, is the leading cause of dementia among older people. An impaired memory is a general sign associated with AD. In 2010, there were more than 30 Million people suffering from AD. Alzheimer disease can be subdivided into the sporadic AD (SAD), which is late in onset (>65 years) and has not been linked to any mutation and familial AD (FAD), which has an early onset (<60 years) is linked to several mutations (Campion et al., 1999, Chartier-Harlin et al., 1991, Murrell et al., 1991). Most of the FAD cases are caused by mutations in two genes namely presenilin 1 (PS1) and presenilin 2 (PS2) but mutations in the Amyloid precursor protein (APP) gene are also found (Sherrington et al., 1995, Rogaev et al., 1995). In its initial phases the disease causes damage to specialized brain structures like entorhinal cortex, hippocampus and basal forebrain that are involved in memory formation (alzforum 2012). At the cellular level the brains of AD patients are characterized by the accumulation of two main types of protein (Figure 1), the extracellular neuritic amyloid plaques composed of A $\beta$ -peptides (Kosik, 1992, Glenner and Wong, 1984, Masters et al., 1985) and intracellular neurofibrillary tangles (NFT's) comprising hyperphosphorylated Tau (Grundke-Iqbal et al., 1986a) (Goedert et al., 1996, Lee, 1993, Mandelkow and Mandelkow, 1998, Mandelkow, 1999). However, in AD no mutations have been identified in the gene MAPT, which codes for Tau protein.

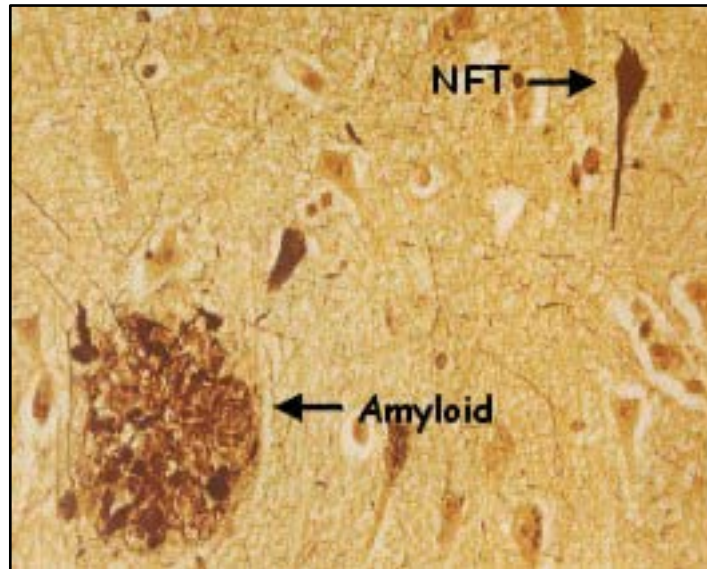


**Figure 1: Pathological hallmarks of Alzheimer disease.** Amyloid plaques are extracellular deposits of a 40- or 42-residue peptide called amyloid- $\beta$  protein ( $A\beta$ ) in the brain parenchyma and around the cerebral vessel walls, while tangles composed of twisted fibers of Tau protein (NFT) build up intracellularly in the degenerating neurons. The plaques and tangles get deposited in structures in the brain that play a critical role in memory. The plaques and tangles are the main hallmarks of Alzheimer disease. (Figure reproduced from <http://www.ahaf.org/alzheimers/about/understanding/plaques-and-tangles.html>).

In spite of the fact that both tangles and plaques are found in conjunction, it is difficult to correlate the appearance and distribution of  $A\beta$  deposits with the progression of the disease, whilst the appearance and distribution of tangles can be well correlated ("Braak stages") (Braak and Braak, 1991).

### 3.2. Tauopathies.

Tauopathies are a group of neurodegenerative disorders characterized by the presence of intracellular Tau inclusions (Lee et al., 2001). Among the microtubule associated proteins (MAP's) in the brain, Tau has received special attention because of its role in AD and other Tauopathies, where Tau protein is deposited within neurons in the form of NFT's (Grundke-Iqbal et al., 1986b, Grundke-Iqbal et al., 1986a, Lee et al., 1991, Ihara et al., 1986, Kosik et al., 1986,

Hyman, 1997). Besides AD, intraneuronal Tau aggregates also occur in patients suffering from frontotemporal dementia with parkinsonism linked to chromosome 17 (FTDP-17), progressive supranuclear palsy (PSP), corticobasal degeneration (CBD) and Pick disease (Ballatore et al., 2007). Tauopathies depict a range of clinical manifestations including memory and language impairments, extrapyramidal signs, and motor deficits (Foster et al., 1997). Whether Tau protein is causal to the diseases or just an effect of some disease process was debatable until 1998, when several mutations in the gene encoding Tau protein were discovered in FTDP-17, thereby confirming a causative role of Tau in neurodegeneration (Hutton et al., 1998, Poorkaj et al., 1998, Spillantini et al., 1998).

FTDP-17 differs from AD both in terms of symptoms and in pathology, especially due to the involvement of amyloid precursor protein (APP) in AD. But the demonstration that Tau pathology alone can cause neuronal loss and dementia (Mocanu et al., 2008, Santacruz et al., 2005) clearly indicates that Tau pathology is not just a marker of dying neurons in AD. Furthermore, recent studies have shown that A $\beta$  related toxicity is mediated by Tau and the deletion of Tau in TKO mice abolishes A $\beta$  induced toxicity (Roberson et al., 2007, Ittner et al., 2010, Zempel and Mandelkow, 2012, Zempel et al., 2013). The degree of NFT involvement in AD is defined by the Braak stages. When NFT involvement is confined mainly to the trans-entorhinal region we speak of Braak stages I and II. Stages III and IV involve the limbic region such as the hippocampus and stages V and VI additionally comprise the whole neocortex (Braak and Braak, 1991). Mutations in the Tau gene are linked to inherited FTDP 17 Tauopathy, demonstrating that Tau mutations are sufficient to trigger neurodegeneration (Llorens-Martin et al., 2011, Spillantini and Goedert, 2000).

### 3.3. Tau: A microtubule-associated protein.

Tau protein was discovered in 1975 in Marc Kirschner's laboratory at Princeton University (Weingarten et al., 1975) in an attempt to search for factors that promote the self-assembly of tubulin into microtubules (MT's). However, Tau only gained more interest, when it was found to be the component of protein aggregates called NFT's, one of the major hallmarks of AD (Brion et al., 1985, Grundke-Iqbal et al., 1986a) and has since then remained in the limelight. Microtubule associated proteins (MAP's) like Tau consist of several proteins among them Tau, MAP2 (Lewis et al., 1988) and MAP4 (Chapin and Bulinski, 1991), which occur throughout the animal kingdom.

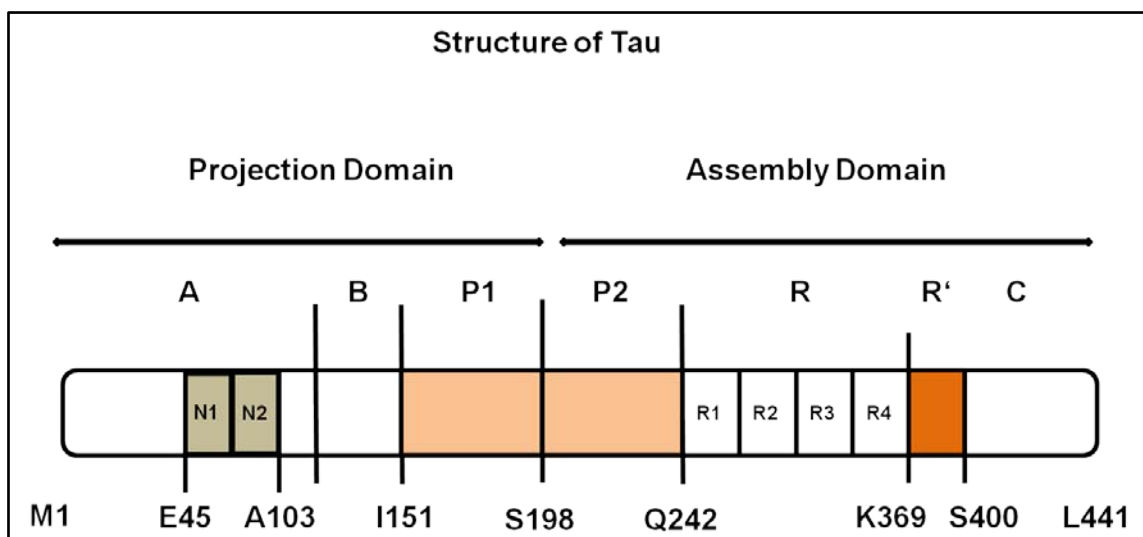


**Figure 2: Structure of Tau.** Bar diagram of Tau protein, isoform hTau40 (2N / 4R, 441 residues). The two 29-mer inserts (starting at E45) are in green and the four repeats are numbered 1-4 (Q244-N368). Definition of domains: projection domain, M1-Y197; assembly domain, S198-L441; N-terminal domains A (acidic), M1-G120, B (basic), G120-I151, and P (proline-rich and basic), I151-Q244, separated into P1 and P2 at Y197; repeats R1-R4, Q244-N368, "fifth" repeat R', K369-S400; and C= C-terminal tail, G401-L441. Modified from (Gustke et al., 1994)

Tau protein (Figure 2) can undergo several post-translational modifications including phosphorylation, acetylation, glycosylation and nitration. Tau protein contains 80 serine/threonine residues, of which 45 are



known to be phosphorylated (Hanger et al., 1992, Hanger et al., 2009). Tau protein is predominantly localized in the axonal compartment (Binder et al., 1985, Jinwal et al., 2010, Kowall and Kosik, 1987, Brion et al., 1988a, Brion et al., 1988b), but recent publications also postulated a dendritic function of Tau in stabilization of Fyn kinase (Ittner et al., 2010, Ittner and Gotz, 2011). Tau's main known biological function is to promote MT assembly and stabilization (Mandelkow et al., 2007). The MT network is key to the cellular transport machinery that allows vesicles and organelles (for example mitochondria), to travel along the axons (axonal transport). Interestingly, although the primary function of the MT-binding domain of Tau is the stabilization of MTs, investigators have found that it may also interact with other structures and enzymes, including RNA and PS1 (Takashima et al., 1998). The half-life of Tau protein is high (about 60 hours in HT22 cells) and can increase if it is in its phosphorylated aggregated form (Poppek et al., 2006).

Tau clearance may involve several processes like cathepsin-mediated Tau degradation, lysosomal or proteasomal degradation (Wang et al., 2007, Grune et al., 2010). Tau can also be digested by proteases such as puromycin-sensitive aminopeptidase (PSA) (Chow et al., 2010, Chesser et al., 2013)

### 3.4. Isoforms of Tau.

In adult human brain six Tau isoforms are expressed as a result of alternative mRNA splicing from a single gene localized on chromosome 17q21 composed of 16 exons (Figure 3) (Goedert et al., 1988, Goedert et al., 1989, Kosik et al., 1989). The six Tau isoforms differ in the presence of three (3R Tau) or four (4R Tau) repeats of 31 or 32 amino acids in the carboxy-terminal half (C-ter), as well as in the presence or absence of 1 or 2 inserts (29 or 58 amino acids) (Goedert et al., 1989). The tandem repeats in the C-ter are encoded by exons 9, 10, 11 and 12, and it is the alternative splicing of exon 10 that results in the generation of 4R Tau with exon 10 and 3R Tau without exon 10 mRNAs. The MT-binding domain of Tau protein consist of the repeat domain plus the flanking regions (Gustke et al., 1994). The 4R Tau has a much higher affinity for MT's and therefore plays a greater role in regulating the MT dynamics than 3R Tau. The alternative splicing of the six brain Tau isoforms are developmentally regulated. Developing brains require highly dynamic MT's which may be achieved by expressing only the shortest Tau isoforms with three repeats and no inserts. This isoform binds only weakly to MT's (Ikegami et al., 2000, Fuster-Matanzo et al., 2012). Isoforms appear to be differentially expressed during development; however the 3R and 4R Tau isoforms are expressed in a one-to-one ratio in most regions of the adult human brain.

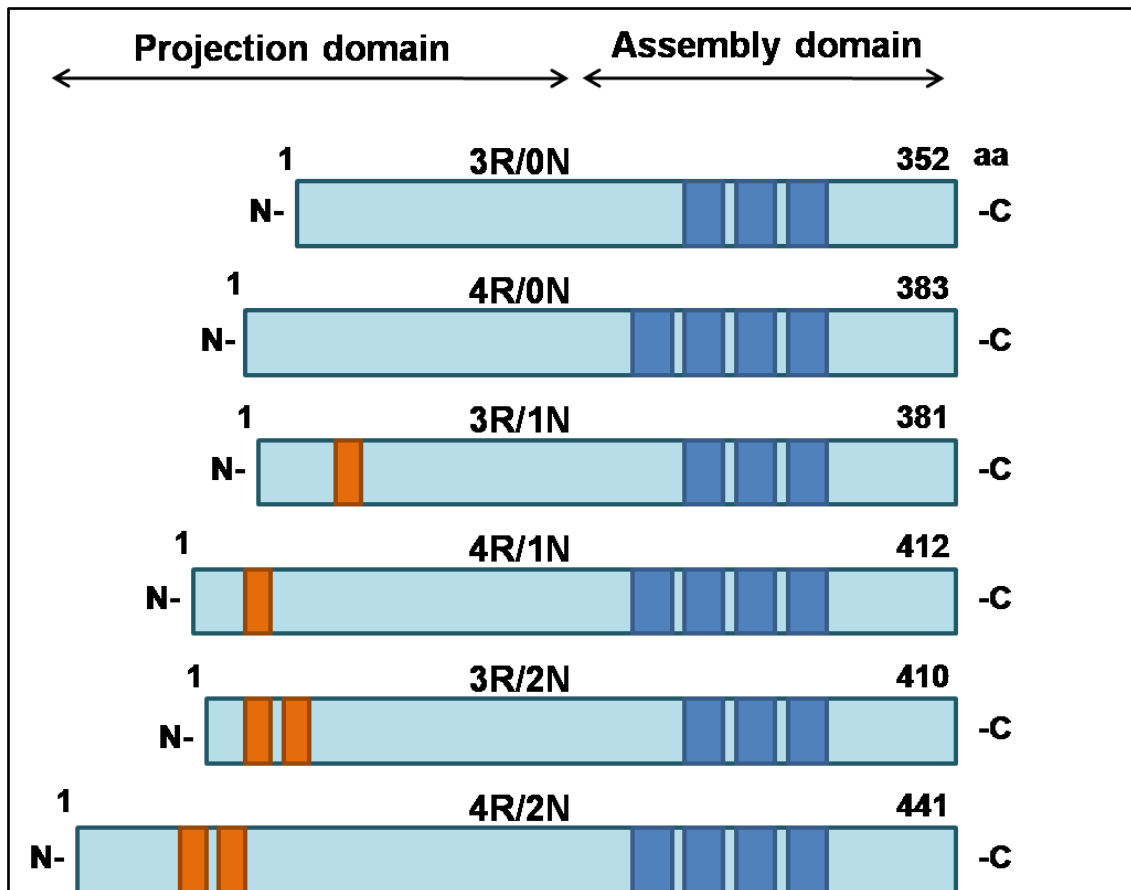


**Figure 3: Domain structure of the six Tau isoforms that are expressed in the adult human brain.** The different isoforms of Tau are depicted in this figure. The projection domain is in the N-terminal half and the assembly domain is located in the C-terminal half. The assembly domain is mainly involved in the attachment of Tau to the MT's. The number represents the total number of amino acids (aa) that are present in each Tau isoform. The 'N' in the name of the different isoforms represents the inserts in the N-terminus of the Tau protein that are represented in orange colour and 'R' in the name of the different isoforms represents the 'repeat region' in the Tau protein that is represented in dark blue (Gustke et al., 1994).

The gene encoding Tau protein is expressed predominantly in the neurons of the central nervous system (CNS) and the peripheral nervous system (PNS) (Andreadis et al., 1992). Tau is ubiquitously expressed in immature neurons. But as the neurons mature, its localization gets restricted almost entirely to the axonal compartment along with a shift toward higher-molecular-weight isoforms and reduced phosphorylation (Drubin and Kirschner, 1986, Kosik et al., 1989). In spite of this, low levels of Tau can still be found in other neuronal compartments after maturation, for example in the

nucleus (Loomis et al., 1990, Sultan et al., 2011, Lu et al., 2014), dendrites (Papasozomenos and Binder, 1987), and in other brain cells like oligodendrocytes (Goldbaum et al., 2003, LoPresti et al., 1995) and microglia (Odawara et al., 1995).

Tau regulates the assembly of MT's by binding to them and stabilizing them. MT's are protein polymers of the cytoskeleton that play a role in diverse cellular functions like cell morphology, mitosis or intracellular transport (Hirokawa, 1993, Hirokawa, 1994, Garcia and Cleveland, 2001). The evidence that supports the role of Tau in regulating assembly of MT's, stabilization and bundling came from the experiments, whereby purified bovine brain Tau protein, microinjected into rat fibroblasts deficient in endogenous Tau, lead to an increased MT mass and enhanced MT stability (Drubin and Kirschner, 1986). Additionally, neurons treated with antisense oligonucleotides to Tau mRNA (siRNA), to block expression of Tau, fail to extend axon-like processes (Caceres and Kosik, 1990, Caceres et al., 1991). This suggests a role of Tau protein in the establishment of neuronal polarity by stabilizing the MT's specifically in a particular compartment during development (Caceres and Kosik, 1990, Caceres et al., 1991).

### 3.5. Tau and its mutations.

FTDP-17 mutations within the Tau coding region are clustered in the vicinity of the MT repeat domain (Figure 4) and typically result in an enhancement of Tau assembly into NFTs (Barghorn et al., 2000, Gamblin et al., 2000) and in a decrease in MT binding (Hasegawa et al., 1998, Hong et al., 1998).

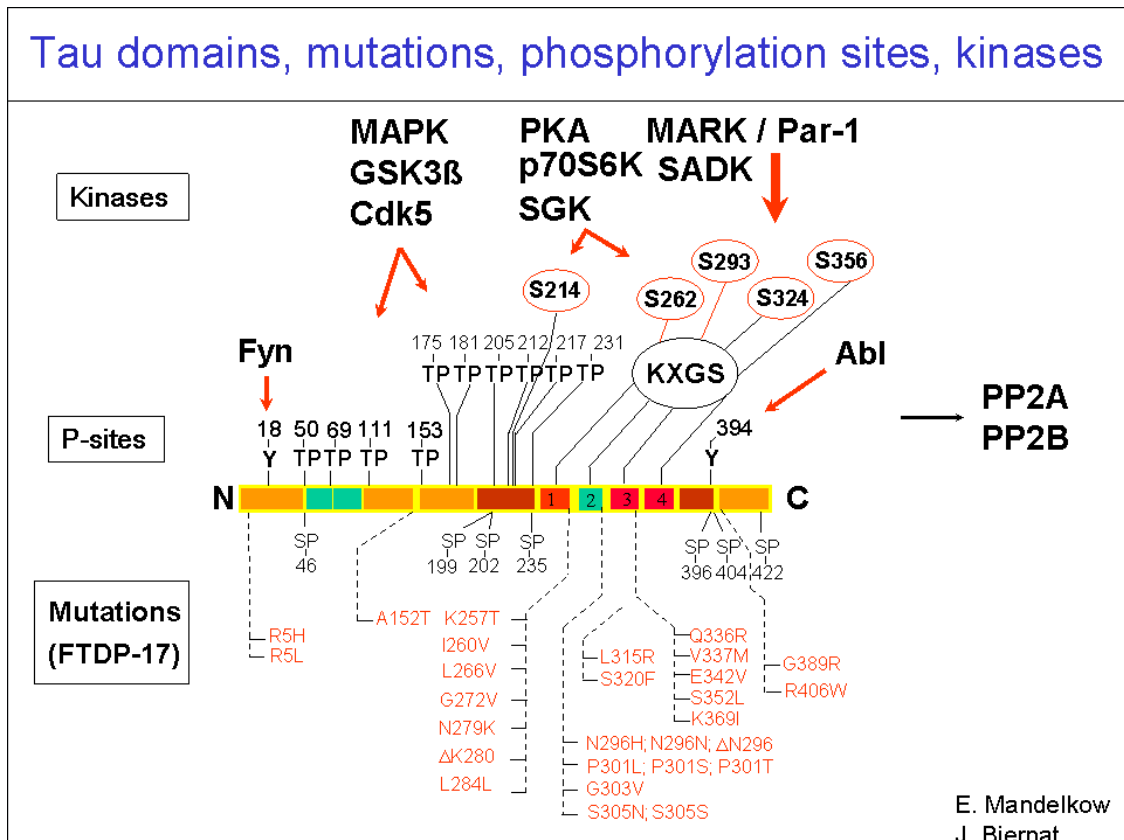


*Figure 4: Tau domains, mutations, phosphorylation sites and kinases.*

Until today forty Tau mutations have been identified including missense mutations like P301L (Proline (301) → Leucine), deletions like  $\Delta$ K280 (Lysine (280)) as well as silent mutations (Gasparini et al., 2007) or intronic mutations located close to the splice-donor site of the intron following the alternatively spliced exon 10 (R2) (van Swieten and Spillantini, 2007).

Tau mutations in FTDP-17 may act by two mechanisms. First, they may affect the alternative splicing of exon 10 resulting in a change of the ratio of 4R:

3R Tau. Second, the mutations (missense and deletions) may directly cause deficits in the abilities of Tau to bind to microtubules (MTs) and promote assembly and stability of MT's. Mutations such as  $\Delta$ K280 and P301L moderately decrease the affinity of Tau to microtubules, however, strongly enhance the aggregation of Tau into PHFs (Barghorn et al., 2000; Schneider and Mandelkow, 2008).

### **3.6. Tau aggregation.**

In all Tauopathies Tau aggregation is at the top of a pathological pathway which begins with the detachment of Tau from the MT's. The path from MT bound Tau to large aggregated structures such as NFTs is thought to be a multi-step phenomenon (Mandelkow et al., 2007). Changes in the equilibrium of Tau binding to the MTs, which can be triggered by numerous conditions (including increased rate of phosphorylation and/or decreased rate of dephosphorylation), results in an abnormal increase in the levels of the free (unbound) Tau fraction. It is likely that the resulting higher cytosolic concentrations of Tau increases the chance of pathogenic conformational changes (Kuret et al., 2005). Next, small non-fibrillary Tau deposits (normally referred to as 'pre-tangles') are formed, and these unlike NFTs cannot be detected by  $\beta$ -sheet specific dyes like thioflavine S or congo red (Maeda et al., 2006, Maeda et al., 2007, Galvan et al., 2001).

### **3.7. Soluble Tau levels and its importance.**

Tau shows no tendency to aggregate under physiological conditions because of its highly soluble nature (Wille et al., 1992). Despite this fact, Tau aggregates are found in several brain diseases collectively termed as Tauopathies (Lee et al., 2001) and the mechanism of Tau aggregation still needs to be elucidated. In vitro studies have shown that Tau aggregation is a multiple

step process which involves the formation of an oligomeric nucleus (rate-limiting nucleation step) followed by an elongation step whereby protein subunits add to this nucleus (Friedhoff et al., 1998). The two hexapeptide motifs [PHF6 (VQIVYK) and PHF6\* (VQIINK)], within the repeat domain of Tau, have a high propensity for  $\beta$ -structure and are responsible for Tau aggregation. During the aggregation process a transition from random coil to  $\beta$ -structure takes place (Barghorn et al., 2000, von Bergen et al., 2000). Tau aggregation can be suppressed by the introduction of two proline residues within these hexapeptide motifs (I277P and I308P), which produce kinks in the chain due to the cyclic structure of proline and hence act as  $\beta$ -breakers (anti-aggregant Tau<sup>RD $\Delta$ -PP</sup>) (von Bergen et al., 2001). Furthermore, the deletion of lysine in the position of 280 ( $\Delta$ K280), enhances this  $\beta$ -propensity and promotes Tau aggregation (pro-aggregant Tau<sup>RD $\Delta$</sup> ) (Khlistunova et al., 2006). Although it is not clear why a soluble protein like Tau forms insoluble fibers in various neurodegenerative diseases, various posttranslational modifications of Tau play a role in this process.

### **3.8. Transgenic Tauopathy model.**

#### **3.8.1. Inducible transgenic mouse model.**

The development of transgenic mice has allowed researchers to study gene function in the context of a whole mammalian organism. To overcome limitations of constitutive expression of genes in animal models researchers developed inducible expression systems like the Tet-On/Off system (Figure 5) (Furth et al., 1994). The Tet-Off and Tet-On expression systems are binary transgenic systems in which expression from a target transgene is dependent on the activity of an inducible transcriptional activator (Baron and Bujard, 2000, Urlinger et al., 2000, Baron et al., 1997, Mocanu et al., 2008, Eckermann et al.,

2007). In both the systems (Tet-Off and Tet-On), expression of the transcriptional activator can be regulated reversibly by exposing the transgenic animals/tissue to tetracycline or one of its derivatives like Doxycycline (DOX). In the Tet-Off system, transcription is inactive in the presence of DOX and active in its absence. A DOX-controlled transactivator protein (*tTA*), which is composed of the Tet repressor DNA binding protein (TetR) from *Escherichia coli* fused to the strong trans-activating domain of VP16 from Herpes simplex virus, regulates expression of a target gene that is under transcriptional control of a tetracycline-responsive promoter element (TRE). The TRE is made up of the Tet operator (*tetO*) sequence concatemers fused to a minimal promoter, from the human cytomegalovirus (hCMV). In the absence of DOX, *tTA* binds to the TRE and activates transcription of the target gene. In the presence of DOX, *tTA* cannot bind to the TRE, and expression from the target gene cannot take place. The vector design of the Tet-Off allows tissue-specific promoters to drive *tTA* expression, resulting in tissue-specific expression of the TRE-regulated target transgene.



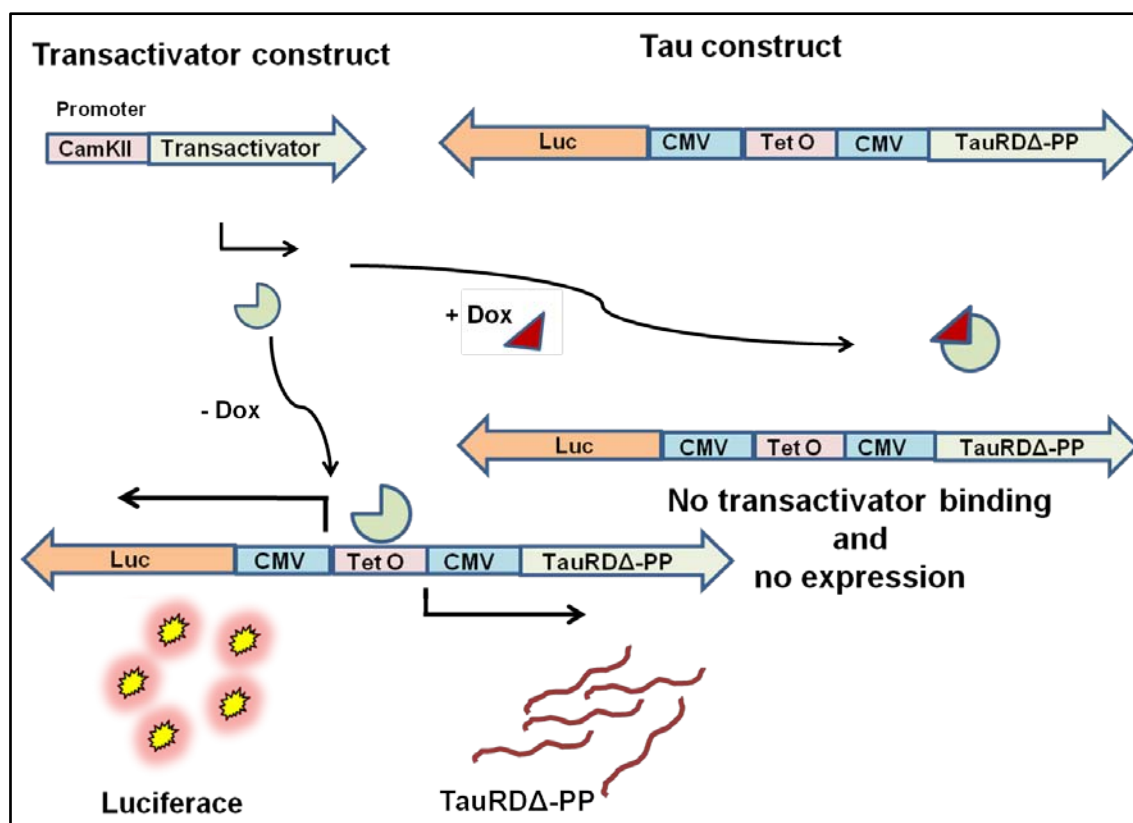


*Figure 5: Basis of transgene expression in the inducible transgenic mouse models.*

In the Tet-ON system, the transcription is active in the presence of DOX. There are several cell models of Tau pathology that are been generated in our lab with this Tet-ON system (Wang et al., 2007, Khlistunova et al., 2007)

### **3.9. The hippocampus.**

#### **3.9.1. Structural features.**

The hippocampus is perhaps the most studied structure in the brain; together with the amygdala it forms the central axis of the limbic system. This brain region is known to be critical for the formation of memory and object recognition (Williams et al., 1993, Bliss and Collingridge, 1993, Eichenbaum, 2000b, Reis et al., 1998, O'Keefe and Dostrovsky, 1971, O'Keefe et al., 1979). The forms of neuronal plasticity known as long-term potentiation (LTP) and long-term depression were first discovered to occur in the hippocampus and have been studied in this structure (Bliss and Collingridge, 1993, Lynch, 2004). LTP is widely believed to be one of the main neural mechanisms by which memory is stored in the brain.

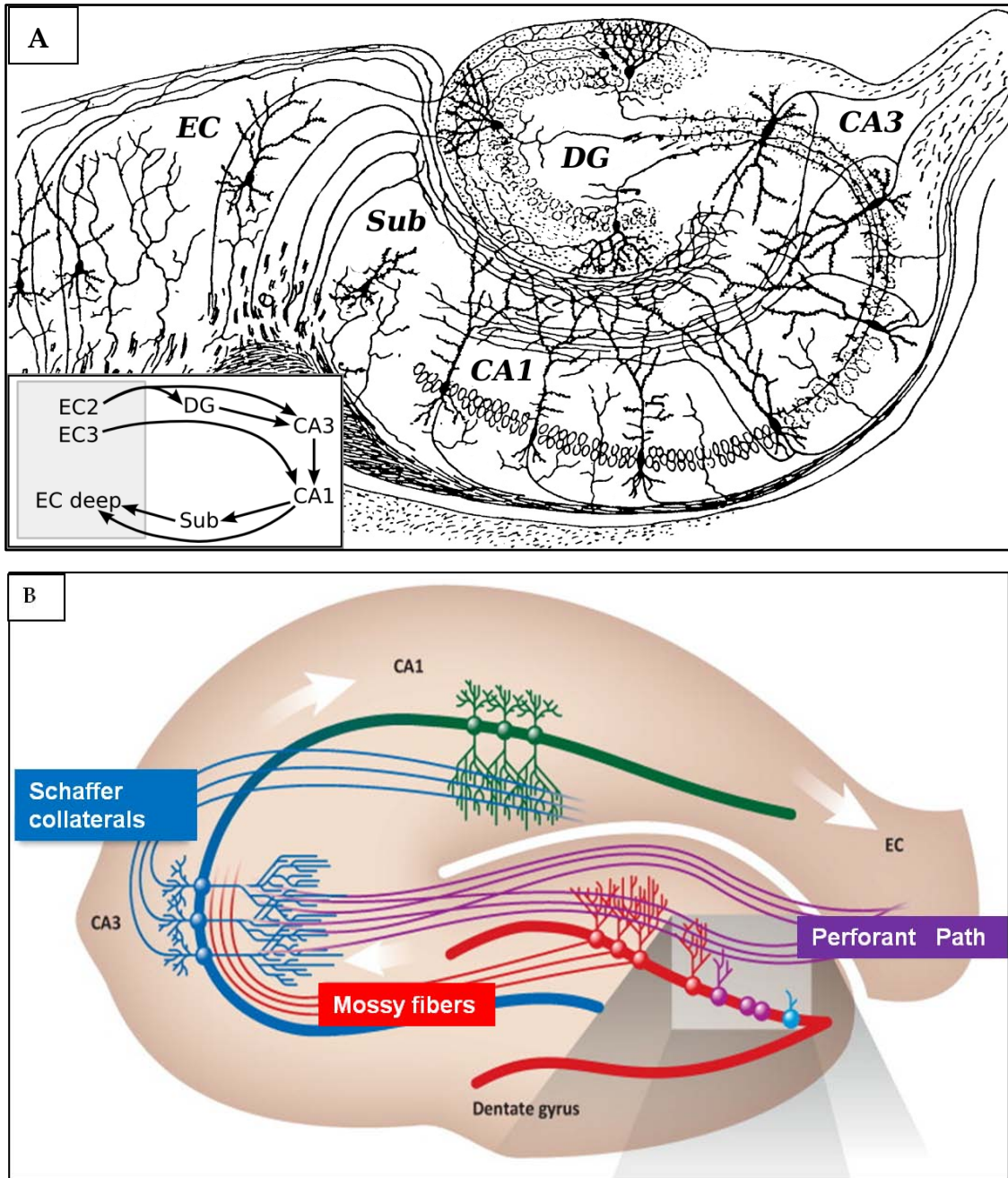


**Figure 6: Basic circuit of the hippocampus using a modified drawing by Ramon y Cajal.** DG: dentate gyrus. Sub: subiculum. EC: entorhinal cortex. CA: Cornu ammonis

- A) Modified drawing of the neural circuitry of rodent hippocampus.
- B) Cartoon of the synaptic circuit, modified from (Lucassen et al., 2013): The main hippocampal information-processing unit — connects EC–DG–CA3–CA1–EC (see arrows). The DG receives input from the EC via perforant path axons. From the DG, mossy fibers connect to CA3 pyramidal cells, which connect to CA1 pyramidal cells via Schaffer collaterals. The hippocampus has a high degree of plasticity throughout life.

Anatomically, the hippocampus is divided in different cell areas called Cornus Ammonis 1, 2 and 3 (CA1-CA3) and dentate gyrus (DG) (Figure 6 A) (Roche et al., 2005, Klausberger et al., 2005, Witter et al., 2000). The CA areas are filled with densely packed pyramidal cells and the DG is actually a separate structure formed by a tightly packed layer of granule cells (Figure 6 B). The perforant path is the major input to the hippocampus. The axons of the perforant path arise principally in layers II and III of the entorhinal cortex with minor contributions from the deeper layers IV and V. Axons from layers II project to the granule cells of the dentate gyrus and via the mossy fibers to the pyramidal cells of the CA3 region, while those from layers III project to the pyramidal cells of the CA1 and the subiculum.

### **3.9.2. Functional features.**

The hippocampus plays important roles in the formation of new memories about facts (declarative memory) and experienced events (episodic memory), in the consolidation of information from short-term memory to long-term memory and in spatial navigation (Morris et al., 1982, Morris et al., 1986, Eichenbaum, 2000a, Moser and Moser, 1998). The hippocampus is thereby part of a larger medial temporal lobe memory system (Squire, 1992, Fortin et al., 2002). The hippocampus is not involved in immediate or working memory processes and is not involved in a wide range of implicit or non-declarative long-term memory processes. The involvement of the hippocampus in episodic as well as declarative memory was discovered when the hippocampus was removed from a patient, known as H.M. to relieve epileptic seizures. H.M. was unable to remember episodes and events that had occurred in the last few years before the surgery. In addition, H.M. was not able to remember events that followed the surgery (O'Kane et al., 2004). These findings imply that the involvement of the hippocampus in declarative and episodic memory is time

limited since H.M. was able to remember events from earlier life. The hippocampal involvement in spatial memory was underlined by imaging studies, which have been shown that the hippocampus is more activated when individuals need to navigate through cities to locate specific places. These observations were underlined by findings that the posterior portion of the hippocampus is larger in experienced taxi drivers (Maguire et al., 2000). Functional and structural features are closely related in the hippocampus (VanElzakker et al., 2008): this brain region shows an impressive capacity for structural reorganization and plasticity. Preexisting neural circuits undergo lifelong modifications in dendritic complexity, in dendritic spine morphology and synapse number (Leuner and Gould, 2010). Additionally, the hippocampus is one of the few places of adult neurogenesis which occurs throughout life in the DG (Kempermann et al., 1997b) resulting in the continuous addition of new neurons into the existing neuronal network (Aimone et al., 2010). Incorporation of novel neurons as well as changes in dendritic spines enhances the capacity for new synapses which favors an increase of the neuronal network underlying memory formation.

### **3.9.3. The hippocampus and neurodegenerative diseases.**

Since memory loss is one of the major pathological changes in neurodegenerative diseases, it is not surprisingly, that the hippocampus plays a crucial role in various neurodegenerative diseases like AD (Braak and Braak, 1991), depression (Campbell and Macqueen, 2004) or temporal lobe epilepsy (French et al., 1993). Additionally the hippocampus is notable for its particular vulnerability to damage as a consequence of ischemia, trauma and hypoglycemia. The role of the hippocampus in AD and epilepsy has been intensively investigated. As early as 1906 Alois Alzheimer described pathological changes in the hippocampus of his first patient Auguste Deter

suffering from AD. In temporal lobe epilepsy, the pathological damage is often restricted to the hippocampus in the form of hippocampal sclerosis (loss of neurons in various hippocampal regions depending on the specific type of epilepsy (Van Paesschen et al., 1997). The hippocampus is thereby sensitive to damage by seizure activity but can also act as origin of epileptic seizure generation (Sander and Shorvon, 1996). Several changes in hippocampal organization, connectivity, receptors, intrinsic neuronal properties, and astrocyte function have been found to contribute to epileptogenicity (Wahab et al., 2010). AD is the most common cause of dementia worldwide. Memory loss is the predominant feature of the disease, especially impairment of episodic memories. The neuropathological changes of Tau protein in AD are thought to occur initially in the entorhinal cortex and progressing from there to the hippocampus (Braak and Braak, 1991). The use of volumetric magnetic resonance imaging (MRI) measures the hippocampal atrophy as a surrogate marker of pathology in AD. This correlates with the decrease of volume and neuronal numbers in the hippocampus of AD. Data from cross-sectional studies indicate that AD is associated with an increased rate of hippocampal atrophy (Jack et al., 1998), observed already in patients even before clinical symptoms are observed, NFT's are formed in the hippocampus of patients (Braak and Braak, 1991) and transgenic mice (see chapter 1.5.2) and correlate with cognitive impairment. The loss of dendritic spines and synapses within the hippocampus is strongly correlated with cognitive impairment (Smith et al., 2009). The pro-aggregant Tau<sup>RDA</sup> mice also showed loss of neurons, loss of spines, cognitive decline in behavioral tasks and deficits in LTP (Mocanu et al., 2008, Sydow et al., 2011, Van der Jeugd et al., 2012, Messing et al., 2013). All together the hippocampus is a brain region which is seriously damaged in AD.

### **3.10. Organotypic hippocampal slice cultures.**

Organotypic hippocampal slice cultures (OHSC) have been employed for the study of normal brain function and brain development. Usually different regions of the brain are used for the preparation of the slice cultures like the hippocampus, cortex, striatum and others (Gahwiler, 1981). Rearrangements of neuronal circuitry often occur in the organotypic hippocampal slice cultures, in parallel with the substantial amount of cell death during the first days after the explants. Early post-natal periods (P0-P8) are ideal for slice culturing, because the cytoarchitectonic fundamentals are already established in most areas, the brain is larger and easier to manipulate, and nerve cells are more likely to survive explantation (Lossi et al., 2009).

#### **Advantages of the slice culture technique.**

The principle of membrane interface culture methods is to maintain brain slices on a porous membrane filter at the interface between medium and a humidified atmosphere. The medium provides adequate nutrition to tissues through the membrane via capillary action (Bergold and Casaccia-Bonnel, 1997, Noraberg et al., 2005).

It is important to note, however, that even in cultures prepared with the membrane interface method there are some properties that substantially differ from the characteristics acquired during the physiological brain maturation *in vivo*. For example fluorescent dye tracing of single neurons in OHSC's showed a more complex pattern of dendritic branching and consistently with this, a significant increase in the frequency of glutamatergic miniature synaptic currents, probably reflecting an increased number of total synapses (De Simoni and Yu, 2006). These observations strongly suggest, that cutting of projection axons, which inevitably occurs during slice preparation, leads to a compensatory response over the course of the culture period, and that damaged

axons have a chance to recover and reroute their processes to form new neural connections (Lossi et al., 2009).

The technique is ideal only for regions with a layered structure that can be aligned parallel to the plane of slicing and is ideally confined inside the thickness of the slice itself. Cultures can currently be produced mainly from embryonic or juvenile donor animals (typically up to 12 days postnatal). Production of slice cultures from older donors is possible, given that only around 5–10% remain viable for 3–4 weeks.



### **3.11. Neurogenesis.**

In 1960's Altman and colleagues described new cells with neuronal morphology in adult cat and rat brains, in the olfactory bulb, hippocampus and neocortex. Kaplan later found out by ultra-structural studies, that these new cells have neuronal characteristics. These studies about adult neurogenesis were later put to a halt by the report from Rakic, who showed that there was no adult neurogenesis in monkeys. In 1980's Nottebohm and colleagues published a series of studies which showed adult neurogenesis in song birds. Interest in adult neurogenesis increased, when it was demonstrated that new neurons were produced in the DG of adult humans. The study was done on very old cancer patients, thus the number of new neurons in the adult human brain was considered to be under-estimated. Two studies published in 2004 showed that there is robust neurogenesis taking place in rodents and from then on the terms "neurogenic" and "non-neurogenic" came into existence (Kempermann et al., 2004a, Kempermann et al., 2004b, Gage, 2004). The following figure (Figure 7) depicts these two regions of the brain which were considered to be neurogenic (red) and non-neurogenic (grey) till the year 2007 (Gould, 2007).

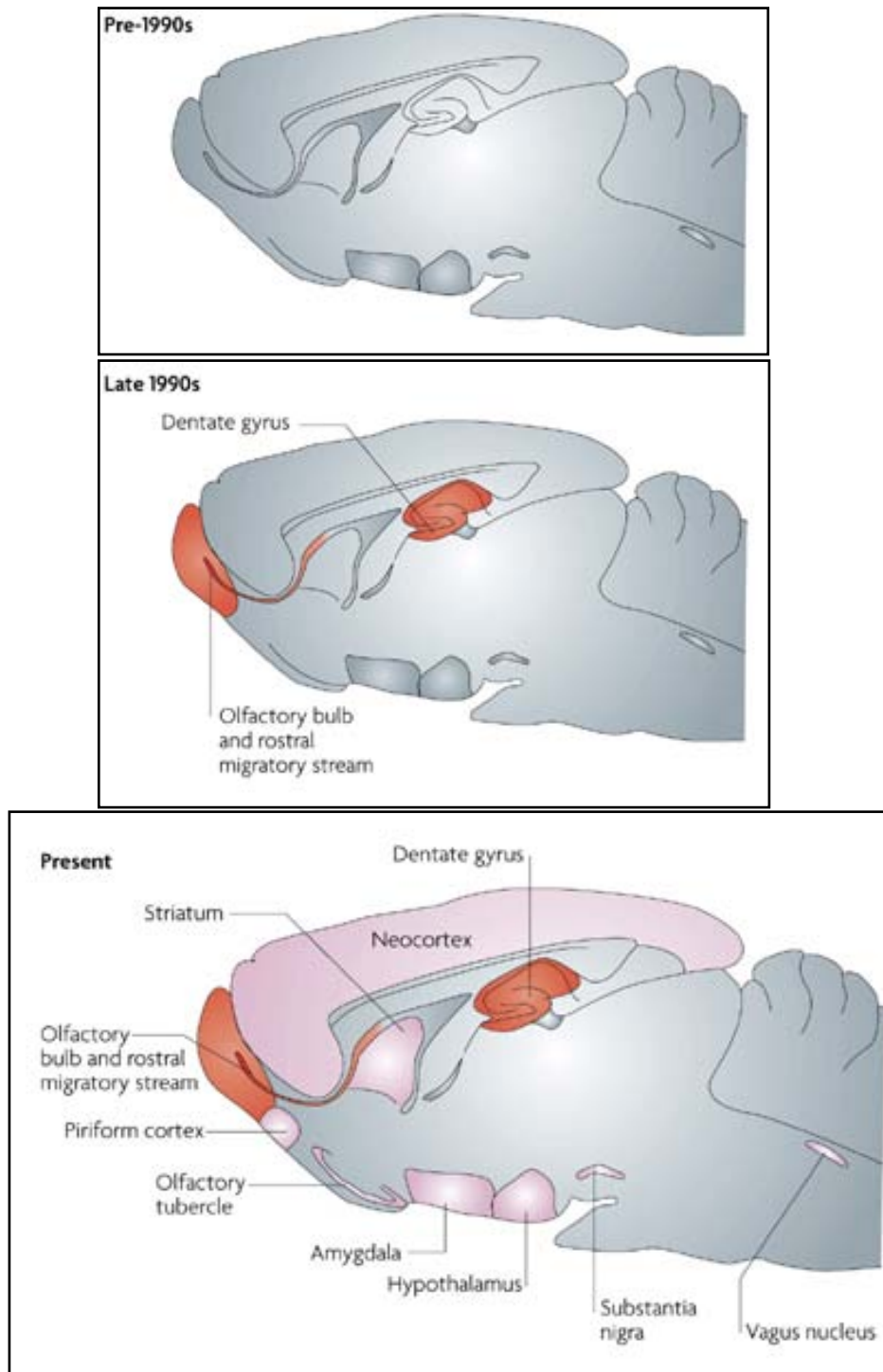


*Figure 7: Changes in the view of adult neurogenesis over the past 15 years.*

*(Modified from Gould E 2007)*

There is also adult neurogenesis taking place in the cerebellum. This is called cerebellar neurogenesis. There are very few stem cells in the adult mouse

cerebellum and these stem cells do not give rise to neurons or astrocytes (Su et al., 2014).

### **3.11.1. Postnatal hippocampal neurogenesis in organotypic hippocampal slice cultures.**

In the hippocampus the sub granular zone (SGZ) of the DG is considered highly neurogenic, even though the other regions of the hippocampus like CA1 subfield has been observed as a region of neurogenesis (Nakatomi et al., 2002). This is still under debate. When OHSC's from P5 rats, are labeled with BrdU 14 days in culture (DIV 14-DIV 21), almost 10% of the BrdU labeled cells express neuronal markers. Although in living rats, about 80% of the cells labeled with BrdU on P5 had become neurons by P19. When OHSC's were prepared from P5 animals that were injected with BrdU 30 minutes before the preparation, more than two-thirds of BrdU labeled cells expressed mature neuronal markers. These results show that the OHSC's are a suitable model to study postnatal neurogenesis and suggest that the capacity of neural precursors to differentiate into neurons is reduced during the culturing period (Namba et al., 2007). Electrophysiologically it has been demonstrated that the new granule cells arising from the DG in the OHSC's mature and integrate normally into the hippocampal circuit, thereby making the OHSC's a useful ex-vivo model to study the mechanism of proliferation and differentiation of neurons (Raineteau et al., 2006).

### **3.11.2. Adult hippocampal neurogenesis.**

Adult hippocampal neurogenesis is a unique form of neural circuit plasticity. Adult born neurons have a very high synaptic plasticity during their maturation and can account for up to 10% of the entire granule cell population. Many intrinsic and extrinsic factors regulate adult hippocampal neurogenesis

which include learning, environmental enrichment, exercise and chronic treatment with antidepressants. Thus by improving adult hippocampal neurogenesis we can improve hippocampal function. Genetic expansion of adult born hippocampal neurons in mice specifically enhances pattern separation which is a specific hippocampus dependent behavior. Further increasing adult hippocampal neurogenesis is observed by combining genetic modulations along with physical exercise and this increase the exploratory behavior in mice (Jacobs et al., 2000, Gould et al., 1999, Sahay et al., 2011, Kempermann et al., 1997a, Malberg et al., 2000). Thus enhancing adult hippocampal neurogenesis may have therapeutic potential. The DG region of the hippocampus is considered as the most important region of the hippocampus where adult neurogenesis takes place. Researchers have shown that the adult born neurons get functionally integrated into the hippocampal circuit (van Praag et al., 2002).

Adult hippocampal neurogenesis which is involved in learning and memory is impaired in Alzheimer disease. Reestablishing a functional population of hippocampal newborn neurons in adult AD mice rescues behavioral symptoms suggesting that adult neurogenesis may be a promising therapeutic target for alleviating behavioral deficits in AD patients (Shruster and Offen, 2014).

Adult born neurons are necessary for mediating specific cognitive functions, but it is unknown whether increasing the adult born neurons alone is sufficient to enhance cognition and mood. Genetic expansion of the population of adult-born neurons through enhancing their survival improves performance in a specific cognitive task. Mice with increased adult hippocampal neurogenesis show normal object recognition, spatial learning, contextual fear conditioning and extinction learning but are more efficient in differentiating

between overlapping contextual representations, which is indicative of enhanced pattern separation. Strategies designed to increase adult hippocampal neurogenesis specifically by targeting the cell death of adult-born neurons or by other mechanisms may have therapeutic potential for reversing impairments in pattern separation and dentate gyrus dysfunction such as those seen during normal ageing (Kheirbek et al., 2012, Sahay et al., 2011, Weber et al., 2011). Recent studies have implicated adult-born hippocampal neurons in pattern separation, a process by which similar experiences or events are transformed into discrete, non-overlapping representations. It was proposed that impaired pattern separation underlies the overgeneralization often seen in anxiety disorders, specifically post-traumatic stress disorder and panic disorder, and therefore represents an endophenotype for these disorders. The development of new, pro-neurogenic compounds may therefore have therapeutic potential for patients who display pattern separation deficits (Kheirbek et al., 2012, Sahay et al., 2011, Weber et al., 2011). Newly generated neurons of the adult hippocampus have their axons extending into the CA3 region of the hippocampus via the mossy fiber pathway. There are two types of mossy fibers, called as the suprapyramidal mossy fibers (SMF) and infrapyramidal mossy fibers (IMF). The newly generated neurons in the DG, tend to contribute more to the IMF and thereby are more involved in the modulation of its synaptic plasticity (Romer et al., 2011).

### **3.11.3. Stages of adult hippocampal neurogenesis.**

Recently there is evidence that the DG of the adult human brain has substantial levels of adult neurogenesis (Figure 8) (Spalding et al., 2013). Radial glia-like (RGL) neural stem cells, that reside in the sub-granular zone (SGZ) of the DG, proliferate and give rise to transit-amplifying progenitors (TAP) expressing the T-box brain gene 2 (Tbr2) antigen, which then give rise to doublecortin (DCX)-expressing immature neurons. After a phase of maturation, newly-formed neurons express the mature neuronal marker NeuN, functionally integrate into the hippocampal network and participate to mechanisms of learning and memory. The neurogenic niche is constituted by stem cells and their progenies, astrocytes, oligodendrocytes, endothelial cells, microglia, mature and immature neurons.

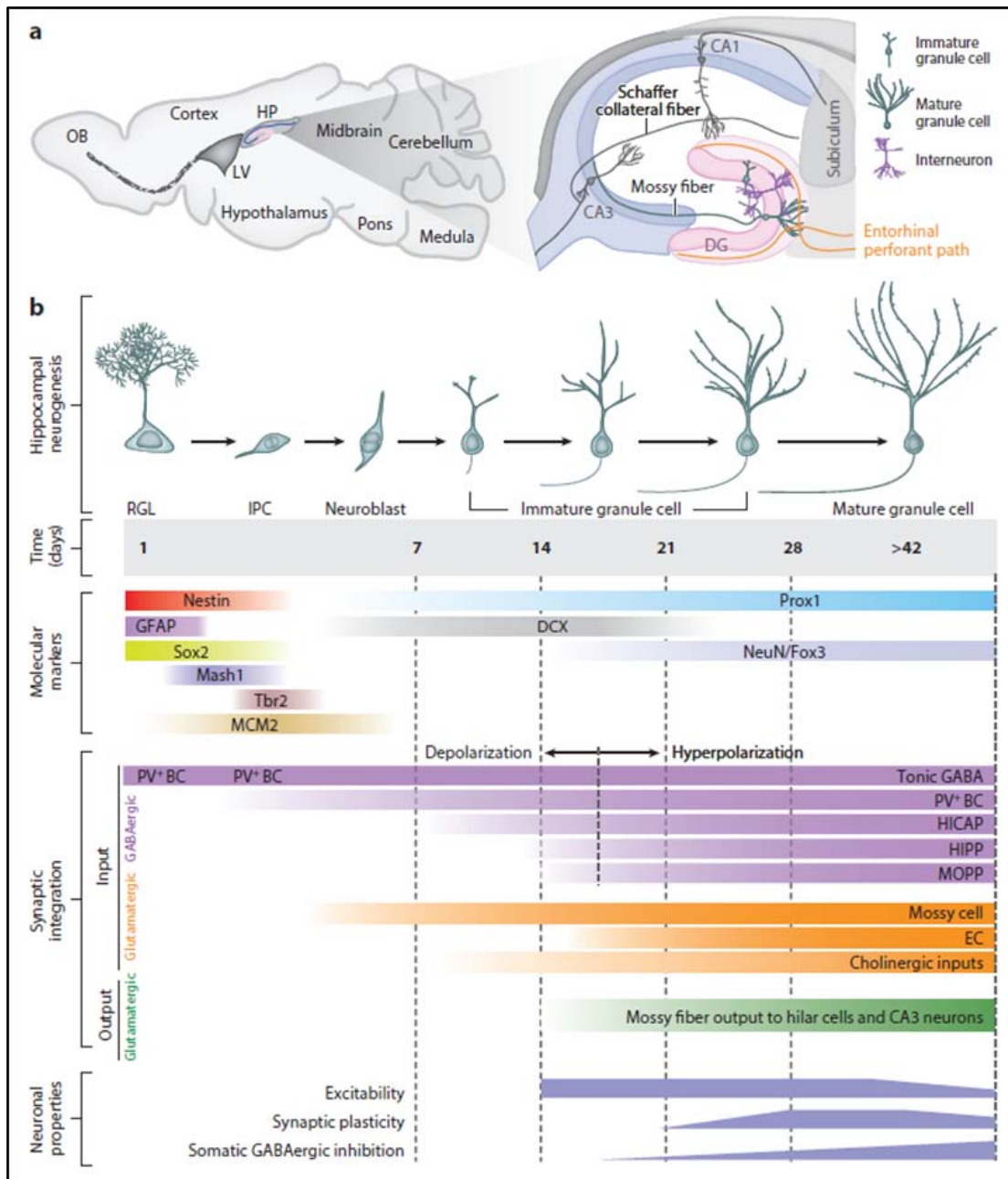


**Figure 8: Stages of adult hippocampal neurogenesis.** Figure 8a represents the canonical signaling network of the hippocampus which consists of synaptically connected principal neurons located in the three major subregions to form the trisynaptic circuit. Figure 8b shows the cell division of neuronal stem cells which give rise to intermediate progenitor cells which in turn give rise to proliferating neuroblasts, postmitotic immature neurons and finally mature DG cells. Figure obtained from Christian et al., 2014.

Two weeks old new-born cells in the SGZ develop dendritic spines (Zhao et al., 2006). They also send their axons to the CA3 region of the hippocampus

through the hilus region. These two weeks old new-born cells have 3R Tau in the axons and also in the somato-dendritic compartments (Fuster-Matanzo et al., 2012, Llorens-Martin et al., 2012). Four to six weeks later the new-born neurons get completely integrated into the hippocampal circuit (Fuster-Matanzo et al., 2009).

The existing stem cells are a subset of astrocytes (Doetsch and Hen, 2005). These astrocyte-like stem cells remain as a cluster of two or four stem cells in specific neurogenic niches (Alvarez-Buylla et al., 2002, Seri et al., 2001). Adult neurogenesis recapitulates neuronal development. Three days after birth there is an expression of 3R Tau isoforms (Bullmann et al., 2010, Bullmann et al., 2009, Bullmann et al., 2007). Retroviral injections were done on adult mouse brains to study the process of adult hippocampal neurogenesis. The retrovirus infects only the dividing cells. The viral infected cells were also co-labeled for the 3R-Tau isoform, which can be seen within a period of 7-21 days after the viral infection (Llorens-Martin et al., 2012).

New born neurons extend a single axon from the base of the cell body within 7 days and establish primary projection patterns within 21 days (Sun et al., 2013). They also show synaptic structures, associated with cells in both hilus and CA3 within 14 days and mossy fiber boutons reaching morphological maturation within 8 weeks (Toni et al., 2008, Faulkner et al., 2008). New born neurons form functional glutamatergic synaptic outputs onto hilar mossy cells and interneurons and CA3 neurons (Gu et al., 2012, Toni et al., 2007). 14 days old adult born neurons already exhibit functional glutamatergic synaptic inputs and outputs and can therefore participate in neuronal processing during immature stages (Liu et al., 1996, Zhao et al., 2006). Mature excitatory synapses are visualized at about 2 months of age. Spine density increases in the new neurons up to 6 months of age (Zhao et al., 2006). Axons from the new neurons



grow and establish either functional glutamatergic synapses with hilar interneurons (Toni and Sultan, 2011) or GABAergic inhibitory synapses with granule cells (Liu et al., 2003). The neurogenic markers remained unchanged at the anterior (at the level of basal ganglia) and temporal horn (at the level of the hippocampus) of the SVZ and the ependymal cell layer adjacent to those, when analyzed by Braak stages and by the presence of dementia (Ekonomou et al., 2014)

### **3.12. Tau in neurogenesis.**

New born granule cells generated in the SGZ grow dendrites into the molecular layer and send axons into the CA3 region, a process that occurs similar during neuronal polarization. The outgrowth of axons during embryonic neurogenesis is characterized by the expression of Tau isoforms with less affinity to microtubules. This Tau with three repeat domains (tau 3R) in these new neurons is in hyperphosphorylated form. This suggest that axonal outgrowth requires a dynamic microtubule network and Tau protein helps to maintain this microtubule dynamicity (Fuster-Matanzo et al., 2012). The 3R Tau present in the newborn neurons lack the N-terminal exons 2 and 3, which are thought to be involved in some associations with membranes (Brandt et al., 1995, Kosik et al., 1989). The phosphorylation of Tau is developmentally regulated. It is higher in fetal neurons and decreases with age during development. The 3R Tau expression starts within 3 days after the incorporation of BrdU in the new born neurons, meaning that there is a transient expression of the 3R isoform of Tau during adult neurogenesis. The 3R Tau is down regulated when the new born neurons start to develop fully differentiated long axonal processes after 1 week (Fuster-Matanzo et al., 2012, Brion et al., 1993). Phosphorylated Tau at sites pS396 and pS404 (recognized by PHF-1), pS202 and pT205 and pT231 phosphorylation sites recognized by AT-8

and AT-180 respectively were identified in DCX positive immature neurons (Fuster-Matanzo et al., 2009, Hong et al., 2010).

Induction of adult hippocampal neurogenesis in rats (3 months of age) resulted in enhancing proliferation of cells in the DG, by increasing the activity of GSK3 $\beta$  and the phosphorylation of Tau, but there was no survival or differentiation (Hong et al., 2010). Transgenic mice, expressing the pathological fragment of N-Tau (26-230aa) in nestin-positive stem/progenitor cells, showed reduced proliferation, reduced survival, followed by neuroinflammation and increased cell death by a caspase 3-independent mechanism. The studies from these transgenic mice showed that the expression of this type of Tau fragment greatly influences neurogenesis (Pristera et al., 2013). The HTau4R isoform expression in a Tau- Knockout, Knockin model (Tau-KOKI) suppressed proliferation and promoted neuronal differentiation and restored neurite and axonal outgrowth (Sennvik et al., 2007). The N-terminal exons 2 and 3 regulate the binding of Tau to membranes and are expressed during embryonic and early post-natal development (Kosik et al., 1989, Brandt et al., 1995), but the Tau expressed in the adult born neurons lack exons 2 and 3, indicating that this Tau cannot bind to membranes (Bullmann et al., 2007).

## 4) MATERIALS

### LIST OF MATERIALS

#### 4.1. LIST OF CHEMICALS

Chemicals	Company
3,3'- diaminobenzidine (DAB)	Vector Laboratories, Germany
Sodium Chloride (NaCl)	Carl Roth, Germany
Protease inhibitor mix Complete Mini	Roche, Indianapolis, USA
3-[(3-cholamidopropyl)- dimethylammonio]- 1- propanesulfonate (CHAPS)	Sigma, Germany
Benzonase	Sigma, Germany
Okadaic Acid	Sigma, Germany
Dithiothreitol (DTT)	Sigma, Aldrich
Doxycycline hydrochloride (DOX)	Sigma, Germany
Roti superglue	Carl Roth, Germany
Dulbecco's Phosphate Buffer Saline (PBS)	PAA, Austria
ECL Western Blot Detection Kit	GE Healthcare, USA
Ethanol	Sigma, Germany
Ethylene glycol tetraacetic acid (EGTA)	Sigma, Germany
D-Glucose	Sigma, Germany
Glycerol	Sigma, Germany
Glycine	Sigma, Germany
Hank's Balanced Salt solution (HBSS)	PAA, Austria
Horse Serum, heat inactivated	PAA, Austria
Minimum Essential Medium (MEM)	PAA; Austria

Penicillin/Streptomycin	PAA, Austria
Permaflour mounting solution	Beckman Coulter, France
Polyacrylamide	Serva, Germany
Potassium permanganate	Sigma, Germany
Propidium Iodide	BD Pharmingen, Germany
Rotisol	Roth, Germany
Sucrose	Sigma, Germany
Sodium Bicarbonate	Sigma, Germany
Sodium Chloride	Sigma, Germany
Sodium Dodecyl sulphate (SDS)-pellets	Sigma, Germany
Sodium Fluoride	Sigma, Germany
Sodium Orthovanadate	Sigma, Germany
Tris-Hydro Chloride	Sigma, Germany
Tris-X	Sigma, Germany
TritonX- 100	Sigma, Germany
Tween 20	Sigma, Germany
1',3'-diiodo-5-(diethylamino)carbocyanine perchlorate (DiI)	Invitrogen, Germany
N-lauroylsarcosine	Sigma, Germany
Milk powder (Low-Fat)	Roth, Germany
Millipore water (ddH <sub>2</sub> O)	Millipore

## 4.2. LIST OF EQUIPMENTS

<b>Equipments</b>	<b>Company/provider</b>
500 ml Bottle Top filter	Corning, Germany
Cell culture dishes 35 mm x 10 mm	Corning, Germany
Cell culture dishes 60 mm x 15 mm	Corning, Germany

Cellulose nitrate filter	Sartorius Stedim Biotech, Germany
Cover slips	Menzel-Glaeser, Germany
Glass Bottle 100 ml	VWR, Germany
Glass Bottle 500 ml	VWR, Germany
Millicell Organotypic Inserts, 0.45 $\mu\text{m}$	Millipore, USA
Glass-Microscope slides	VWR, Germany
Micron Gold 1.6 $\mu\text{m}$	Bio Rad, Germany
Pipette tips (0.2, 10, 20, 100, 200 $\mu\text{l}$ and 1 ml)	Sarstedt, Germany
Polyvinylidene fluoride (PVDF) membranes (pore size 0.45 $\mu\text{m}$ )	Millipore, Germany
Rupture Disc	Bio Rad, Germany
Razor Blades	Rotbart, Germany
Single use Latex gloves	Roth, Germany
Sterile 6 well plates	Corning, Germany
Stopping screens	Bio Rad, Germany
Tecan plate reader (Absorbance/fluorescence)	Tecan, Switzerland
Gel electrophoresis chamber	Pierce, Germany
Electrophoresis power supply EPS 3500	Pharamcia Biotec, USA
Gel run chamber	Hoefer, Germany
ImageJ software	National Institute of Health, USA
Incubator Heracell 150	ThermoScientific, Germany
IVIS (live imaging) software	Caliper, Germany
IVIS spectrum	Caliper, Germany
LAS 3000	Raytest, Germany
LAS 3000; AIDA software	Raytest, Germany
Office 2010	Microsoft, USA
Table-top Centrifuge (mini spin)	Eppendorf, Germany

Olympus laser -scanning microscope FV1000	Olympus, Japan
Pipette 10µl, 20µl, 100µl, 200µl, 1000 µl	Gilson, Germany
Helium pump (PSD100)	Bio Rad, Germany
Preparation Equipment	Sigma, Germany
Semi-Dry Blotting unit (Uniblot)	VWR, Germany
Stereo Microscope M76	Leica, Germany
Sterile Gard Hood	The Baker Company, USA
Sterile Working bench	ThermoScientific, Germany
Thermo mixer Compact	Eppendorf, Germany
Tissue Chopper	Gabler, Bad Schwabach, Germany
Ultracentrifuge	Beckmann TL-100
Vibratome VT1200S	Leica, Germany
Vortex Genie 2	Scientific Industries, Germany
Water Bath	GFL, Germany

### 4.3. LIST OF ANTIBODIES

<b>Antibodies against the following epitopes</b>	<b>Company</b>
GFAP	Sigma Aldrich, USA
Iba1	Wako chemicals, Germany
NeuN	R&D systems USA
β-Actin	Sigma, Germany
Nestin	Acris, USA
Ki67	Abcam, Cambridge, UK
DCX	Abcam, Cambridge, UK
Anti-BrdU	Dianova, Germany
K9JA	Dako, Germany

GSK3 $\beta$	Life Technologies, USA
pGSK3 $\beta$	Cell signaling, USA
Wnt5a	Abcam, UK
GAPDH	Santa Cruz, USA
FITC	Dianova, Germany
TRIC	Dianova, Germany
Alexa-488	Dianova, Germany

#### 4.4. LIST OF BUFFERS and SOLUTIONS

##### 4.4.1. Slice culture media.

Components	Volume in %
Minimal essential media (MEM)	50%
HBSS	25%
Horse serum (heat inactivated)	25%
Pen/Strep	0.04%
D-Glucose	25%

The pH of the slice culture medium was 7.4. The slice culture medium was stored at 4°C and was used within one month.

##### 4.4.2. Solutions for Immunohistochemistry in organotypic hippocampal slice cultures.

###### 4.4.2.1. Fixation Solution.

4% Formaldehyde solution was prepared by adding 10 ml Formaldehyde (37%) to 90 ml of 0.1M PBS (Phosphate buffer saline).

The fixation solution was freshly prepared before use.

###### 4.4.2.2. Antigen retrieval solution.

10 mM Sodium citrate buffer, 0.05 Triton X-100, pH 6

2.94 g of Tri-sodium citrate (dehydrate) was dissolved in 1000 ml of distilled water.

The pH was adjusted to 6.0 with 1M HCl.

0.5 ml of Triton X-100 was then added and the solution was stored at 4°C for a maximum of 6 months.

#### 4.4.2.3. Permeabilization solution.

40 µl of 10% Triton X-100 (v/v) was added up to 1000 µl with 0.1 M PBS. The permeabilization solution was stored at 4°C for further used

#### 4.4.2.4. Blocking Solution.

2 ml Horse serum and 0.3 ml Triton X-100 was mixed and adjusted to 100 ml with 0.1M PBS.

The blocking solution was aliquoted into 50 ml falcon tubes and stored at -20°C till further use.

#### 4.4.2.5. Washing solution.

2.7 g Sodium phosphate monobasic ( $\text{NaH}_2\text{PO}_4$ ), 11.5 g Sodium phosphate dibasic ( $\text{Na}_2\text{HPO}_4$ ) and 9 g Sodium chloride ( $\text{NaCl}$ ), were dissolved in 1000ml of distilled water. The pH was adjusted to 7.4.

### 4.4.3. Western Blotting.

#### 4.4.3.1. Preparation of 2x lysis buffer (Stock solution; Volume: 40ml) (aliquoted and stored at -20°C)

Reagents	Final Concentration
0.25M Tris HCl, pH 7.4	100 mM
Pure Glycerol	20%
Pure NP40 (detergent)	2%
0.5M DTT	10mM



0.5M NaEGTA/ EGTA	2mM
0.5M NaF (phosphatase inhibitor)	40mM
50mM Vanadate/ orthovanadate, (phosphatases inhibitor)	Sodium Na <sub>3</sub> VO <sub>4</sub> 2mM
H <sub>2</sub> O	-

#### 4.4.3.2. Preparation of 1x lysis buffer (Working solution) (Freshly prepared)

Reagents	Final Concentration
2x Lysis stock solution	-
5M NaCl	150mM
Protease inhibitor (Compleatete Mini)	1X
100 $\mu$ M CHAPS	5mM
Benzonase	100U/ml
1 $\mu$ M Okadaic Acid	5 $\mu$ M
Millipore water	-

The collected tissue samples were homogenized in 30 $\mu$ l of freshly prepared 1x lysis buffer.

#### 4.4.3.3. 10x Tris buffered saline (TBS) stock solution.

100 mM Tris HCL and 1.5 M NaCl was dissolved in 2.5 L of Millipore water. The pH was adjusted to 7.5. 1xTBST (Tris buffered saline + tween) was prepared by adding 100 ml of 10x TBS to 900 ml of Millipore water and 1 ml of Tween 20 was added to it.

#### 4.4.3.4. 10x Blotting.

480 mM Tris HCL, 390 mM Glycine and 10 mM SDS was measured and dissolved in 500 ml of Millipore water. The pH was adjusted to 8.9-9.1, finally adjusted to 1000 ml.

100 ml of 10x Blotting buffer solution was adjusted to 1000 ml with Millipore water.

#### 4.4.3.5. 2x SDS running buffer.

50 mM Tris HCl, 7 mM SDS and 384 mM Glycine was measured and dissolved in 500 ml of Millipore water. The pH was adjusted to 8.4, and the final volume was adjusted to 1000 ml with Millipore water.

100 ml of 2x SDS running buffer was further diluted with 100ml of Distilled water and the final 1xSDS running buffer was used as the working solution.

#### 4.4.3.6. Blocking solution.

5 g Low-Fat milk powder was dissolved in 100 ml 1xTBST and used as the blocking solution.

#### 4.4.3.7. Preparation of 17% Gels for SDS-PAGE electrophoresis.

Ingredients (Solutions)	17% Resolving Gel	4% Stacking Gel
30% Acrylamide	34ml	5,3ml
1 M Tris-HCl pH 8,8	22ml	-
0.25 M tris-HCl pH 6,8	-	20ml
H <sub>2</sub> O	3ml	14,10ml
10% SDS	0,6ml	0,4ml
TEMED	0,12ml	80µl
10% APS	0,065ml	150µl

#### 4.4.3.8. Preparation of 10% Gels for SDS-PAGE electrophoresis

Ingredients (Solutions)	10% Resolving Gel	4% Stacking Gel
30% Acrylamide	20ml	5,3ml
1 M Tris-HCl pH 8,8	22ml	-
0.25 M Tris-HCl pH 6,8	-	20ml

H <sub>2</sub> O	16,6ml	14,10ml
10% SDS	0,6ml	400µl
TEMED	0,12ml	80µl
10% APS	0,06ml	150µl

#### 4.4.4. Solutions for Agarose gel electrophoresis.

##### 4.4.4.1. 50xTAE buffer (stock solution).

2 mM Tris HCl, 950 mM Acetic acid and 100 ml 0.5 M EDTA (pH 8.0) was added together and the volume was adjusted to 1000 ml with Millipore water.

1xTAE buffer was prepared by dissolving 20 ml of 50xTAE buffer in 980 ml of Millipore water.

##### 4.4.4.2. 0.5x TAE buffer (running buffer).

500 ml of 1xTAE buffer was diluted to 1000 ml with Millipore water.

##### 4.4.4.3. 1.8% Agarose gel.

1.98 g of Agarose was dissolved in 110 ml of 0.5xTAE buffer.

The solution was allowed to boil in the microwave until it becomes clear.

##### 4.4.4.4. 6x Sample Loading buffer.

0.01 g Bromophenol blue (0.25%), 0.01 g Xylencyanol FF (0.25%) and 0.6 g Ficoll (Type 400) in water (15%) was all together dissolved in 4ml of Millipore water.

##### 4.4.4.5. Ethidium Bromide Solution.

8 µl of Ethidium Bromide (Stock conc. of 1%) was dissolved in 200 ml of Millipore water.

#### **4.4.5. Sample preparation for free floating vibratome brain section.**

##### **4.4.5.1. Fixation solution.**

4% FA solution: 5.4 ml of Formaldehyde solution (37%) was dissolved in 44.6 ml of 0.1 M PBS. This solution had to be prepared fresh, shortly before fixing the brain.

##### **4.4.5.2. Storage solution.**

30% Sucrose solution: 30 g of Sucrose was dissolved in 0.1 M PBS.

0.01% Azida was added to prevent contamination.

## 5) METHODS

### 5.1. The transgenic mice.

Mice which express either the human Tau four-repeat domain carrying the FTDP-17 mutation  $\Delta$ K280 (Rizzu et al., 1999) (called Tau<sup>RD $\Delta$</sup>  or pro-aggregant mice) or mice expressing Tau<sup>RD $\Delta$ K280PP</sup> with two additional proline mutations at positions 277 (I277P) and 308 (I308P), which prevent beta structure formation (called Tau<sup>RD $\Delta$ -PP</sup> or anti-aggregant mice) (Figure 9) and reporter gene Firefly luciferase under control of a bidirectional Tet-operon response element (tetO) (Mocanu et al., 2008), were crossed with CaMKII $\alpha$ -tTA mice (Mayford et al., 1996b). This results in an inducible Tet-off system. A detailed description of both mouse lines is given in the following chapter. The anti-aggregant Tau<sup>RD $\Delta$ -PP</sup> mouse line is used for this study.

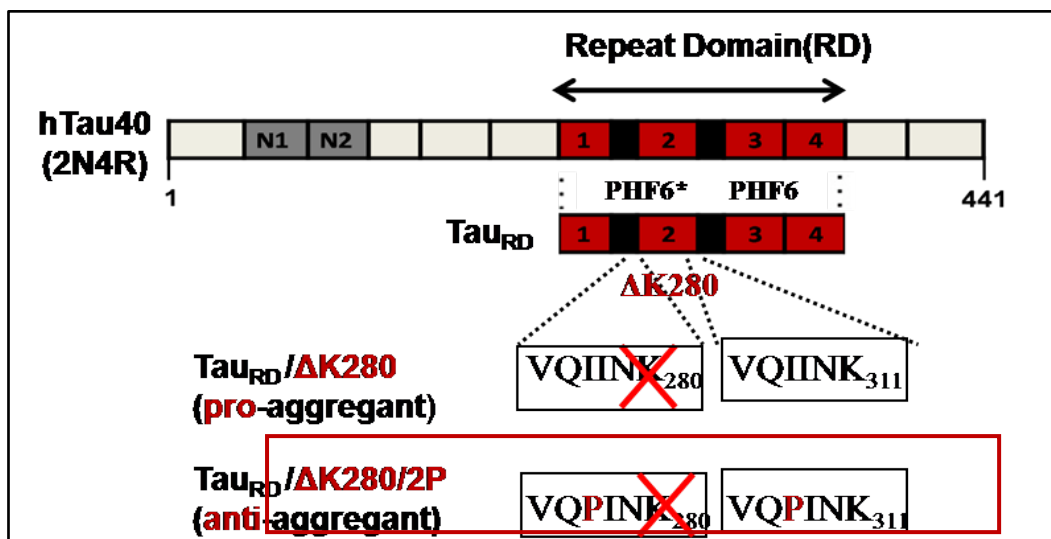


**Figure 9: The human Tau repeat domain constructs carrying the FTDP-17 mutation  $\Delta$ K280.** Four repeats located in the C-terminal half of Tau are highlighted in red (R1-R4). Two hexapeptide motifs at the beginning of R2 and R3 (shown in black) promote Tau aggregation into PHFs by inducing  $\beta$ -structure. The FTDP-17 mutation  $\Delta$ K280 localized within R2 strongly increases the propensity for  $\beta$ -structure. This mutation is called as the pro-aggregant Tau<sup>RD $\Delta$</sup>  mutation. The second line indicates the anti-aggregant Tau<sup>RD $\Delta$ -PP</sup> mutation. This mutation along with  $\Delta$ K280, also has two additional mutations of leucine to proline at sites 277 and 308 within the repeat domain. Fig modified from (von Bergen et al., 2001)

## 5.2. Origin of the Tau<sup>RD</sup> constructs and principle of the switch-off system.

Previous studies have shown that Tau<sup>RD $\Delta$</sup>  has a high propensity for  $\beta$ -structure and strongly promotes Tau aggregation *in vitro* (Barghorn et al., 2000, von Bergen et al., 2001), whereas Tau<sup>RD $\Delta$ -PP</sup> does not aggregate and causes no toxicity at least in transgenic mice (Khlistunova et al., 2006, Mocanu et al., 2008) (Figure 9). Mice were generated either expressing ~~Tau<sup>RD $\Delta$</sup>~~  Tau<sup>RD $\Delta$ K280PP</sup> under control of a Tet-operon response element (tetO) (Figure 10). Both mouse lines additionally carry the reporter gene Firefly luciferase under control of tetO. The switch-off system was achieved by crossing mice expressing a DOX depending transactivator (tTA) under control of the neuron specific CaMKII $\alpha$ -promoter (Mayford et al., 1996a) with transgenic Tau mice. The transactivator bound to DOX is inactive and cannot bind to the tetO element to promote transgene expression (switch-off modus, Figure 10; right panel). In the absence of DOX the transactivator binds to the tetO element and promotes transcription of Tau<sup>RD $\Delta$ -PP</sup> and luciferase messenger-RNAs (switch-on modus, Figure 10; left panel). Tau<sup>RD $\Delta$</sup>  expression caused aggregation, toxicity and reduced plasticity of the hippocampus whereas Tau<sup>RD $\Delta$ -PP</sup> expression leads to an increase in long term potentiation.

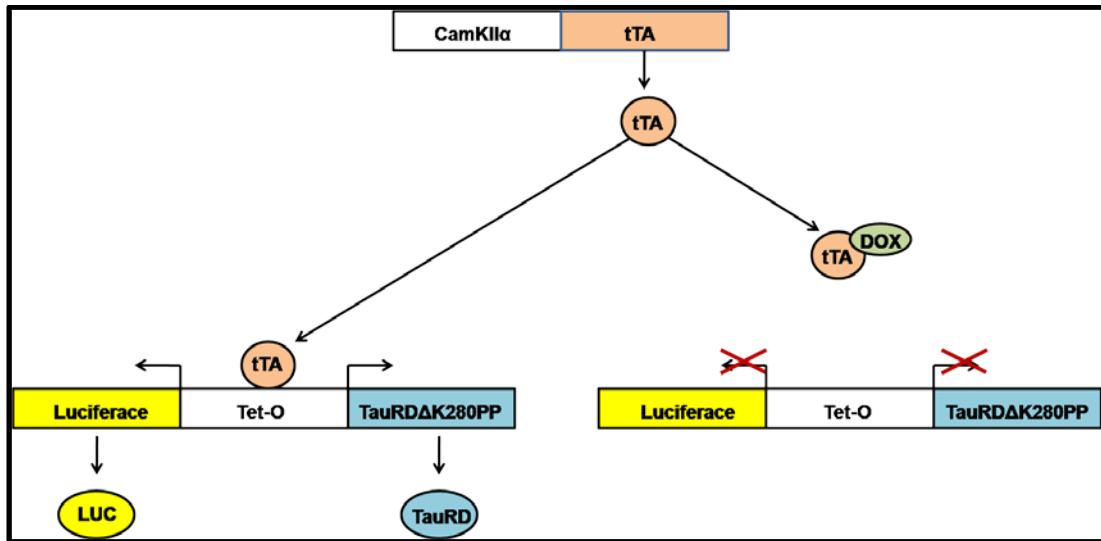


**Figure 10: Doxycycline dependent switch-off system.** Mice which express a Doxycycline (DOX) depending transactivator (tTA) under control of the neuron specific CaMKII $\alpha$ -promoter (Mayford et al., 1996) were crossed with mice expressing human Tau four-repeat domain carrying the FTDP-17 mutation  $\Delta$ K280 and two additional proline mutations (called TauRD $\Delta$ K28PP) and reporter gene Firefly luciferase (LUC) under control of a Tet-operon response element (tetO) (Mocanu et al., 2008) to generate an inducible expression system. The transactivator bound to DOX is inactive and cannot bind to the Tet-operon response element to promote transgene expression (scenario shown on the right site). In the absence of DOX the transactivator binds to Tet-O and promotes the transcription of TauRD and luciferase mRNAs (scenario shown on the left site). Result is the simultaneous expression of reporter gene LUC and Tau construct in neuronal cells of the mouse forebrain which can be switched off by application of DOX. Fig modified from (Mayford et al., 1996a)

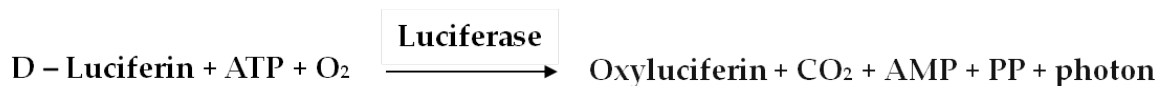
### 5.3. Genotyping of Tau<sup>RDA-PP</sup> transgenic mice.

Anti-aggregant Tau<sup>RDA-PP</sup> transgenic mice were identified by polymerase chain reaction (PCR) of genomic mouse tail DNA (DNA isolation; Invitex, Berlin, Germany) using the primer pairs

IK11n	CAT CGA TAT GCA GAC AGC CC
IK12n	CGT CGA CGG ATC CTA TTC AA
tTA-s3	TCA GCG CTG TGG GGC ATT TT
tTA-as3	AAA TCG TCT AGC GCG TCG GC

#### 5.4. Assessment of luciferase activity.

Since the anti-aggregant Tau<sup>RDΔ-PP</sup> transgenic mouse line was generated by using a bidirectional promoter to produce besides Tau<sup>RDΔ-PP</sup>, the reporter gene Firefly luciferase, its enzymatic activity can be used to investigate the regional distribution and strengths of transgene expression. Bioluminescence (photons / sec) was detected with a luminometer (IVIS, Spectrum; Caliper Life Sciences, Germany) after incubation of slice cultures with 5 µg / ml of the luciferase substrate D-luciferin (Caliper Life Sciences, Germany). Luciferase substrate was applied 30 min prior measurement. The substrate is cell permeable and Firefly luciferase reaction takes place inside the cytoplasm in two steps by using Adenosine Triphosphate (ATP) as a cofactor:



The reaction is very energetically efficient: nearly all of the energy input into the reaction is transformed into light.

#### 5.5. Preparation of organotypic hippocampal slice culture.

It was previously demonstrated that slices (300 - 400 µm thickness) from developing brain tissue can be grown in culture for several weeks (Gahwiler et al., 1997, Noraberg et al., 2005) in the form of organotypic hippocampal slice cultures (OHSC). Studies have shown that neuronal morphology, cellular and anatomical relations and network connections are maintained in slice cultures (Zimmer and Gahwiler, 1987, Sundstrom et al., 2005). The organotypic slice culture technique became an increasing popular tool with the development of the roller-tube technique in 1981 by Gähwiler (Gahwiler, 1981) and later the interface cultures in 1991 by Stoppini (Stoppini et al., 1991) modified by several other groups (Noraberg et al., 1999, De Simoni and Yu, 2006). These studies all took advantage of the isolated and well defined environment of the *in vitro*



preparations. The most used donor sources have been rats and mice, but rabbits, pigs and human fetuses have also been used. Most organotypic brain slice cultures have been derived from neonatal (P0-P10) animals. The brain areas that have been studied included the hippocampus, cerebellum, striatum or retina. Organotypic slice cultures were previously used to investigate mechanisms and treatment strategies for neurodegenerative disorders including Parkinson's disease (PD) (Madsen et al., 2003, Jakobsen et al., 2005, Larsen et al., 2008), Huntington's disease (HD) (Storgaard et al., 2000, Zhang et al., 2005) and epilepsy (Thompson, 1993, Poulsen et al., 2005, Albus et al., 2008). Furthermore, a number of pharmacological and genetic manipulations have been demonstrated to be reproducible in organotypic slices (Cho et al., 2004, Pringle et al., 1996, Ray et al., 2000, Lossi et al., 2009).

For the preparation of hippocampal slice cultures, 8 days-old mouse-pups were used. The brain was carefully removed after the skull was opened and then soon transferred into a plastic dish containing ice-cold culture medium on a 2 cm x 2 cm piece of sterile cellulose nitrate filter (Cho et al., 2004, Pringle et al., 1996, Ray et al., 2000, Lossi et al., 2009). Next, the cerebellum was removed from the explanted brain and the brain hemispheres were separated from each other with a scalpel. In the next step, the hippocampus was explanted along a blood vessel that demarcates the border between the hippocampus and the adjacent cortical areas. The tissue was then cut along this blood vessel with a scalpel while the hemisphere is pinned to the culture plate with a second scalpel. The explanted hippocampus was then placed on the cellulose nitrate filter and transferred on a McIlwain tissue chopper and cut perpendicular to its length axis. The slice thickness is adjusted to 400  $\mu\text{m}$ . The hippocampus is then automatically cut into twenty to thirty slices depending on the adjusted thickness and on the age of the animal. By means of a humidified

brush and the cellulose filter, the slices were transferred to a dish containing ice-cold nutrition medium). The slices were then carefully separated from each other and four to six single slices were placed on the membrane of a static tissue culture insert in a six-well plate containing 1ml nutrition medium per well (Figure 11). Only slices with an apparent and undamaged dentate gyrus (DG) and cornu ammonis (CA) region were taken for cultivation. Damaged slices were discarded. The six-well plates with the tissue culture inserts were then transferred to an incubator with a humidified atmosphere containing 5% CO<sub>2</sub> at 37°C. The medium was changed completely the day after the preparation and then every third day thereafter. A higher magnification of slice cultures lying on the culture insert's membrane *in vitro* is shown in Figure 11.

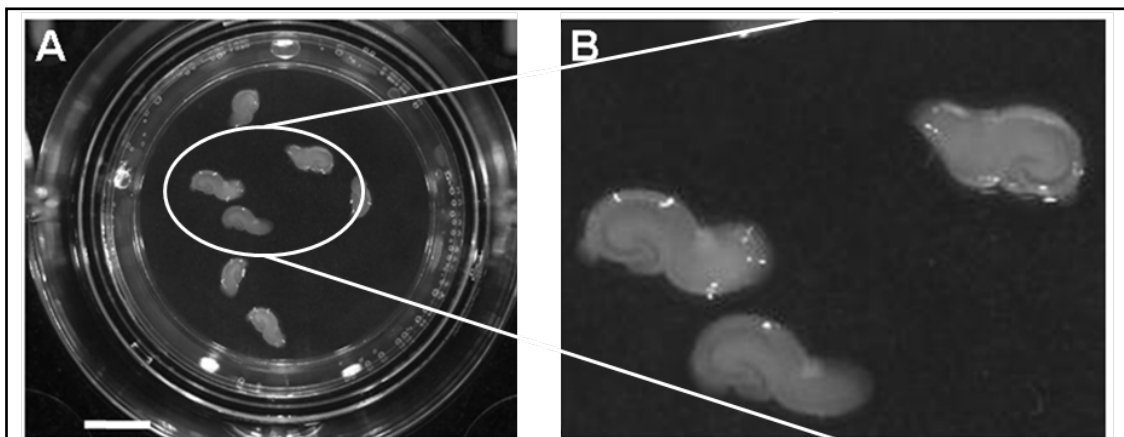


**Figure 11: Slice selection and culture arrangement imaged with increasing magnification.**

*A) Four to eight slices were placed onto the membrane of a static tissue culture insert in a six-well plate.*

*B) Magnification taken from image A. Only slices with an apparent and undamaged DG and CA region were selected.*

## **5.6. Suppression of anti-aggregant Tau<sup>RDA-PP</sup> expression by DOX.**

Doxycycline hydrochloride was dissolved in 1 ml of slice culture medium at a concentration of 2 mg / ml. This stock solution was stored at minus

20°C for several months. Suppression of the human Tau construct was achieved by application of 1 µl of stock solution to the culture media resulting in a final concentration of 2 µg / ml. This concentration was sufficient to inhibit transgene expression completely when refreshed with each full-medium change.

## **5.7. Immuno-histochemistry of slice cultures.**

### **5.7.1. Immunostaining.**

Slice cultures were left attached on the Millicell culture membrane and stained as free-floating sections in 6-well plates. Cultures were first fixed with 4% paraformaldehyde in PBS for two hours at 4 °C. After three times washing with cold 1 x PBS, slices were permeabilized for 90 minutes at RT. Slices were then blocked with 5 % BSA for 2 hours and afterwards incubated with the primary antibody diluted in 1 x PBS for 2-3 days at 4°C. After washing with 1 x PBS, slices were incubated with the secondary antibody for two days at 4 °C. After washing, slices were mounted with Permafluor mounting solution, coverslipped and dried before imaging. The following primary antibodies were used: monoclonal anti-neuronal nuclei (NeuN) antibody (Chemicon International, Temecula, CA) (1:500), anti-glial fibrillary acidic protein (GFAP) (Sigma-Aldrich, St. Louis, MO) (1:1000), K9JA (Dako, CA) (1:1000), anti-Iba1 (Wako Chemicals, Germany) (1:1000), Nestin (Acris, Germany) (1:500), Ki67 (Abcam,UK) (1:500), DCX (Abcam, UK) (1:500), Anti-BrdU antibody (Dianova,Germany) (1:1000). All fluorescent (goat anti-rabbit/mouse cyanine 2, 3 and 5)-labeled secondary antibodies were from Dianova (Hamburg, Germany) (1:1000).

### **5.7.2. Diaminobenzidine staining for bright field microscopy and stereology microscopy.**

Mice were anesthetized with 2-bromo-2-chloro-1,1,1-trifluoro ethane and killed by decapitation. The brains were removed and stored in 4% PFA at 4°C during 3 days. Brains were change in a gradient of sucrose (10, 20 and 30%) during 3 days. Brains were snap-frozen in liquid N<sub>2</sub> and stored at -80°C. Serial coronal sections (40 µm), obtained with a Cryostat NX-70 (ThermoFisher, MA), were processed for immunohistochemistry as free floating. For diaminobenzidine (DAB) immunohistochemistry experiments, endogenous peroxidases were blocked for 30–45 min in PBS containing 10% methanol and 3% H<sub>2</sub>O<sub>2</sub>. Then, nonspecific protein interactions were blocked with 10% horse serum for 30 min at room temperature. Tissue was incubated overnight at 4°C with NeuN (1:1000, neuronal marker; Millipore Bioscience Research Reagents) primary antibody. Secondary antibody was incubated for 30 min incubation at room temperature. For the secondary antibody and avidin-biotinylated peroxidase system, we used the Vectastain Universal Elite ABC kit (Vector Laboratories). NeuN (1:1000, neuronal marker; Millipore Bioscience Research Reagents) was used. Hippocampal volumes were measured by using Stereo Investigator software on fully motorized Nikon microscope. Consecutive sections (10-12 sections per animal) were visualized, and the borders of the hippocampus were outlined. The volumes were calculated by multiplying the sum of all sectional areas (square millimeters) by the distance between successive sections (0.32 mm).

### **5.7.3. Confocal microscopy of slice cultures.**

All images were acquired on an Olympus laser scanning microscope FV1000, equipped with a confocal laser scanning unit, argon (Ar; 488 nm) and helium/neon (He/Ne 543nm and 633 nm). The microscope was equipped with

following objectives: 20 x, 40 x and 63 x magnification. Two/three channel imaging images were acquired via sequential scanning mode. Image stacks were collected for the whole hippocampus at lower and for hippocampal subfields at higher magnifications. For imaging of dendritic spines the “zoom-in” function was used. Hippocampal regions were scanned at a step size ranging from 0.15  $\mu\text{m}$  (for dendritic spines) to 0.7  $\mu\text{m}$  (for low magnification images of the whole hippocampus). Maximum projection images were generated from the resulting Z stacks by using Image J or Olympus imaging software 2D function.

### **5.8. Diolistic labelling of organotypic slice cultures.**

The lipophilic tracer 1,1'-dioctadecyl-3,3',3'-tetramethylindocarbocyanine perchlorate (DiI, Invitrogen) was used to investigate dendritic spines in transgenic or control slice cultures. DiI uniformly labels neurons via lateral diffusion in the plasma membrane at a rate of about 0.2 – 0.6 mm per day in fixed tissue (Invitrogen manual). The dye allows imaging of whole neurons including small structures like dendritic spines when excited at 549 nm (resulting emission at 565 nm). When doing diolistic labelling, DiI-coated gold particles are shot under high pressure into the slice tissue. For the preparation of dye-coated gold particles 0.002 g of DiI were mixed with 20  $\mu\text{l}$  of dichloromethane and 250  $\mu\text{l}$  of double distilled water. The mixture was added to 0.00075 g of gold particles (radius 1.6  $\mu\text{m}$ ) and mixed in a standard 1.5 ml Eppendorf tube. The solution was sonicated for 20 min in a water bath at room temperature. Then 20  $\mu\text{l}$  of the solution was dried on macro-carriers (Biorad) at 37 °C for at least two hours. Macro-carriers were stored at 4 °C (protected from light) and used within one day. DiI coated gold particles were applied under high pressure in living slice cultures by using the BioRad PDS100/ helium pump with following settings: a) 2 cm distance between sample and macro-

carrier b) 650 psi rupture disks. After shooting slices were immediately fixed with fixation solution and stored at 4°C for at least 48 hours before imaging by using Tritc-filter settings.

### **5.9. Assessment of spine density.**

The spine density of apical dendrites of CA1 pyramidal neurons was estimated after 5, 10 and 20 days *in vitro* after DiI labeling apical dendritic primary and secondary branches (> 150  $\mu\text{m}$  away from the cell soma see (Fig. 16) were imaged by using high resolution confocal microscopy at a step size of 0.15  $\mu\text{m}$ . Spines were counted from resulting Z-stacks and estimated as spines /  $\mu\text{m}$  by using ImageJ plugin's Neuron Tracer and cell counter. Cell Counter was used to allow a proper spine counting and Neuron Tracer was used to measure the dendritic lengths.

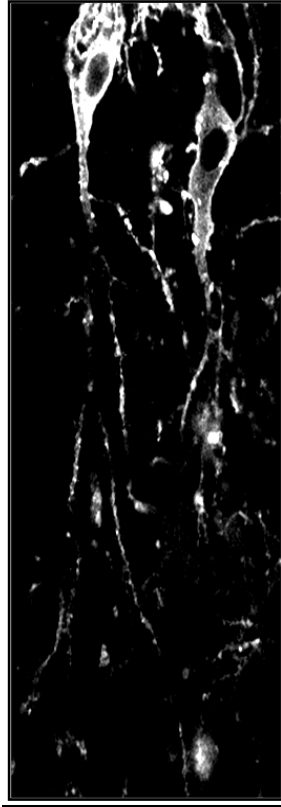


*Figure 12: Assessment of apical dendritic spine density in stratum radiatum of area CA1.*

### **5.10. Bromodeoxy uridine incorporation assay in organotypic hippocampal slice cultures.**

50  $\mu$ M of Bromodeoxy uridine (BrdU) was applied to the culture media in which the slices were cultured. The BrdU application was done from DIV 15 till DIV 30. The slices were then fixed with 4% FA overnight and permeabilized with 4% Triton X 100 in 0.1M PBS. After permeabilization the slices were incubated with 1N HCl for 10 min on ice to denature the DNA and thereby to expose the BrdU incorporated parts in the DNA. Next the slices were incubated in 2N HCl for 10 min at RT, later moved it to a 37<sup>0</sup>C incubator for 20 min. The denaturing effect of HCl was nullified by washing the slices with borate buffer for 12 min at RT. Slices were then washed with 0.1M PBS with 1% Triton X-100, 3 times 5 min each at RT. Next the slices were blocked

with 0.1M PBS + 1% Triton X-100 + 1M Glycine and 5% horse serum for 1 hour at RT. Then the slices were incubated with the respective primary antibodies for 3 days followed by the respective secondary antibodies for 2 days under constant shaking.

### 5.11. Bromodeoxy uridine incorporation assay in P8 pups.

Neurogenesis within the CNS is demonstrated using an exogenous cell tracer, BrdU. It is a thymidine analogue that incorporates into the dividing cells during DNA synthesis. BrdU is injected intraperitoneally and the dosage depends on the experimental requirements.

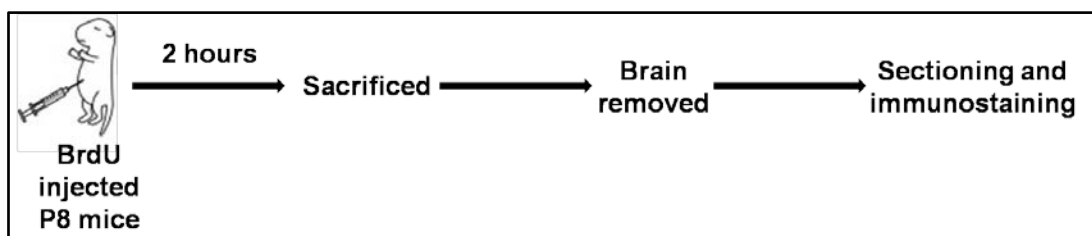


**Figure 13: BrdU injection in P8 animals.** Post-natal day 8 animals were used for the experiments. The animals from the control and the anti-aggregant Tau<sup>RDΔ-PP</sup> groups were injected with 50 mg/kg body weight and kept alive for 2 hours. After the two hour time window, the animals were sacrificed and their brains removed. The expression of the anti-aggregant Tau<sup>RDΔ-PP</sup> was measured by IVIS. Following which the brains were fixed and cut into 40μm thick, free floating vibratome sections. The free floating sections were immunostained for different markers for proliferation and differentiation.

For the experimental procedure post-natal day 8 animals from the control and the anti-aggregant Tau<sup>RDΔ-PP</sup> groups were selected. The body-weight of the animals was measured following which, 50 mg /Kg of BrdU dissolved in saline, was injected. Two hours post injection, the animals were sacrificed and the brains removed. The expression level of anti-aggregant Tau<sup>RDΔ-PP</sup> was measured by bioluminescence. The highest expressers were used for further analysis.



### **5.12. Western blot analysis.**

To estimate protein expression in the hippocampal lysates from slice cultures and also from the adult brain, the semi-dry western blot technique was used. Cultured hippocampal slices were homogenized in 10  $\mu$ l lysis buffer. Proteins were resolved by SDS-PAGE (10% or 17% polyacrylamide gels) and transferred to polyvinylidene fluoride (PVDF) membranes (size of the membrane: 9 cm x 6 cm = 54 cm<sup>2</sup>; during blotting 1.5 mA / cm<sup>2</sup> was used (81mA)). The membrane was incubated in 5 % non-fat milk in TBST for 1 h at room temperature, washed with TBST and incubated overnight in primary antibody solution at 4°C or for one hour at 37 °C. The membrane was washed with TBST and incubated with the secondary antibody (Dako, Germany) for 1 hour at RT which was coupled to horseradish peroxidase (HRP). The membrane was developed by using ECL Western Blotting Detection Kit (GE Healthcare, USA) and analyzed by densitometry (LAS 3000; AIDA software). The following antibodies were used: pan-Tau antibody K9JA (1:5000); pGSK3 $\beta$ (Y216) (Biosource) (1:1000), pGSK3 $\beta$ (S9) (Cell signaling, USA) (1:1000), Wnt5a (Abcam, UK) (1:1000), GFAP (Sigma-Aldrich, St.Louis, MO) (1:1000), GAPDH (Santa Cruz, USA) (1:1000) and secondary antibodies, HRP-anti-rabbit and HRP-anti- mouse (Dako, US).

### **5.13. Assessment of neuronal cell number in area DG, CA1 and CA3.**

For further investigation of neurotoxicity, immunohistochemistry of slice cultures against neuronal nuclei protein (NeuN) was done to visualize the neuronal cell layer of the dentate gyrus (DG) and cornu ammonis (CA) area. NeuN is a DNA-binding, neuron-specific protein, which is present in most excitatory neuronal cell types of the central nerve system (CNS). NeuN protein distribution is apparently restricted to neuronal nuclei, perikarya and some

proximal neuronal processes (Mullen et al., 1992, Wolf et al., 1996). Immunohistochemistry with antibodies against NeuN antigen was done in accordance to the description under 3.4.5. The number of neurons (NeuN expression cells) was counted in area CA1, CA3 as well as from the DG by using ImageJ software (NIH).

#### **5.14. Statistical analysis.**

Statistical analysis was done by using statistic-software Prism5 (GraphPad, California, US). Evaluation of data from neuronal number, microglial number, spines, western blot analysis and bioluminescence was performed using an unpaired Student's t-test. Correlation was tested in accordance to Pearson. Data are shown as mean +/- SEM. p values are as follows: \* $p < 0.05$ , \*\* $p < 0.01$ , \*\*\* $p < 0.001$  and \*\*\*\* $p < 0.0001$ .

## 6) RESULTS

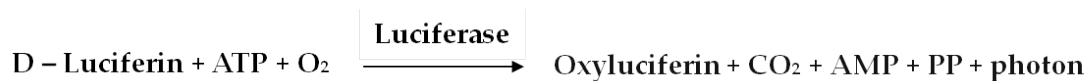
### 6.1. General aspects of slice cultivation.

Organotypic hippocampal slice cultures (OHSC's) were used to monitor the development of neuronal and non-neuronal cell types. The rate of preparation, age of pups, pH stability and glucose concentration of the culture media were identified as critical parameters of slice cultivation. Best preservation of the tissue architecture was achieved with animals not older than post-natal day ten, in minimal essential medium (MEM) including high serum (25 % v/v), 0.45 % (w/w) of glucose and pH 7.3 - 7.4. Under these conditions slices were viable for at least five weeks. Slice thickness was adjusted to 400  $\mu\text{m}$  to enable gas support of the inner cell layers. The hippocampus was separated from large parts of the entorhinal cortex although some cortical cells remained. During cultivation tissue thickness decreased to  $\sim 150 \mu\text{m}$  and simultaneously doubled in diameter ( $203 \pm 33 \%$  ( $n = 3$ )). Although tissue flattening and tissue extension occurred, the typical hippocampal morphology was still able to be visualized with immunohistochemistry in five week old cultures with an antibody against the neuronal nuclear protein (NeuN). All hippocampal sub regions including area CA1, CA3 and DG remained preserved. Immunolabeling for NeuN was not seen inside the slice rim indicating that slice extension is caused by cell movements other than neurons.

The first two post-natal weeks in rodents are a critical period with regard to naturally occurring neuronal death (NOND) in different brain areas (Lossi L et al., 2009). Fetal tissue survive very well in slice cultures but the organotypic organization is often distorted and/or poorly preserved, given that early in development massive neuronal migration and major rearrangements of neuronal circuits still occur (Hocke et al., 2007).

## 6.2. Bioluminescence measurements on organotypic hippocampal slice cultures to determine transgenic Tau<sup>RDA-PP</sup> expression.

Luminescence refers to the emission of light from a substance. If the reaction takes place within the living organism it is called bioluminescence (BLI). In the presence of adenosine-5-triphosphate (ATP) and molecular oxygen, luciferase generates an oxidized excited intermediate substrate which emits a photon when returning to the basic state. Thus, bioluminescence is based on the following reaction



The transmission of photons is optimal in the near-infrared spectrum beyond 600nm. The longer the wavelength, the greater is the penetration in living tissue. Firefly luciferase emits a high proportion of red light (>600nm) and this makes it favorable for in vivo imaging approaches, especially [C. A. 137](#). An increase of luciferase activity is observed with the peak emission of 612nm and ~64% of emitted light is >600nm. D-Luciferin is a low molecular weight organic-compound (318.41 g/mol). Importantly, human Tau variants are expressed together with a luciferase reporter on the same plasmid but not as a fusion protein under control of the bidirectional transactivator (tTA)-responsive promoter (Ptetbi-1). The bidirectional promoter element ensures co-regulation of both genes, whereas a forebrain-specific expression of tTA using the calcium/calmodulin-dependent protein kinase II (CaMKII $\alpha$ ) promoter ascertains expression of Tau and luciferase in AD-relevant brain structures. Gene expression can be switched off by application of DOX 150mg/kg body

weight of D-luciferin is injected into animals i.p and peak emission was observed 15 to 20 min post injection and quantified as total flux in photons per second (Hochgraefe and Mandelkow, 2013)

In mice, the expression of the anti-aggregant  $\text{Tau}^{\text{RDA-PP}}$  was switched-off for 8 months by the administration of DOX via drinking water, after which the administration of DOX was stopped. The withdrawal of DOX resulted in a delay in the start of expression of the human anti-aggregant  $\text{Tau}^{\text{RDA-PP}}$  protein (Hochgraefe and Mandelkow, 2013). Similarly, when OHSC's were prepared from pups born from pregnant animals treated with DOX, the slice cultures did not show any expression of the anti-aggregant  $\text{Tau}^{\text{RDA-PP}}$ . Because of this reason the pregnant animals were not administered with DOX to prevent the embryonic expression of the anti-aggregant  $\text{Tau}^{\text{RDA-PP}}$ . Therefore the expression of the anti-aggregant  $\text{Tau}^{\text{RDA-PP}}$  was from the embryonic stages onwards. Post-natal day 8 animals were used for the preparation of OHSC's. We wanted to investigate the expression level of anti-aggregant  $\text{Tau}^{\text{RDA-PP}}$  in P8 pups before we could start with the preparation of OHSC's. Therefore we measured the bioluminescence in whole brains of these P8 animals after sacrificing them and dissecting their brains (Figure 14). The brains from the anti-aggregant  $\text{Tau}^{\text{RDA-PP}}$  pups, showed enhanced bioluminescence signal as measured by IVIS. The expression was high in the forebrain region as seen by the red colour (Figure 14). The other regions of the brain, like cerebellum, show a lower amount of anti-aggregant  $\text{Tau}^{\text{RDA-PP}}$  expression.

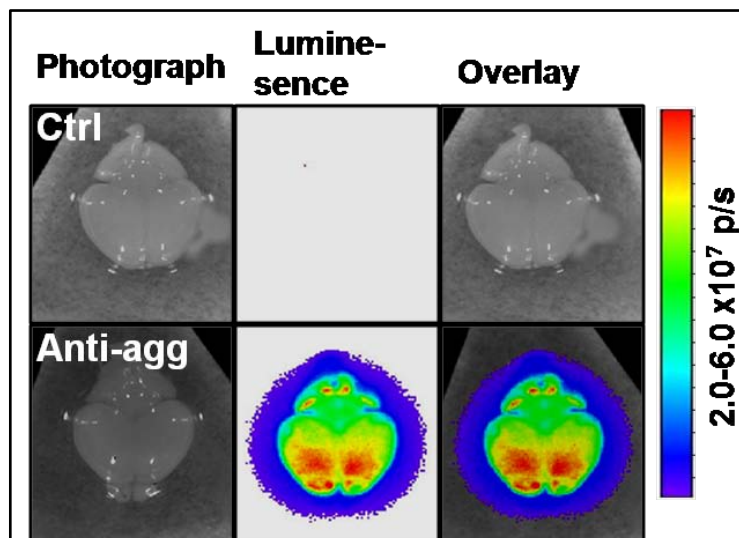


**Figure 14: Bioluminescence measurement done on brains from P8 animals.** Post-natal day 8 animals were killed by cervical decapitation. The brains were removed and placed on a petri-dish on ice. Immediately 5 $\mu$ l of 2 $\mu$ M D-luciferin was added on top of the brain and placed inside the bioluminescence chamber for measurements. The first panel shows a whole brain from a control animal where there is no bioluminescence signal. The second panel shows a whole brain from an anti-aggregant Tau<sup>RDA-PP</sup> animal, which had a high bioluminescence signal of 2.0-6.0x 10<sup>7</sup> photons per second. All the transgenic animals with high bioluminescence signals were selected for further study and used for the preparation of organotypic hippocampal slice cultures.

OHSC's were prepared from P8 pups from both the control and the anti-aggregant Tau<sup>RDA-PP</sup> groups. The slices were cultured under normal culturing conditions for the required time period in 6-well plates. When the cultures were one day in-vitro (at DIV1) we checked for the expression of the anti-aggregant Tau<sup>RDA-PP</sup> in the slices prepared from the anti-aggregant Tau<sup>RDA-PP</sup> groups (Figure 15). For analyzing the expression of the anti-aggregant Tau<sup>RDA-PP</sup> in slices, we directly applied D-luciferin into the culture media. The intensity of the bioluminescence signal was seen at its maximum in the CA1 region of the hippocampus (shown in red) (Figure 15) and also in the subiculum. The CA3 and the DG region showed lower expression of the anti-aggregant Tau<sup>RDA-PP</sup>.

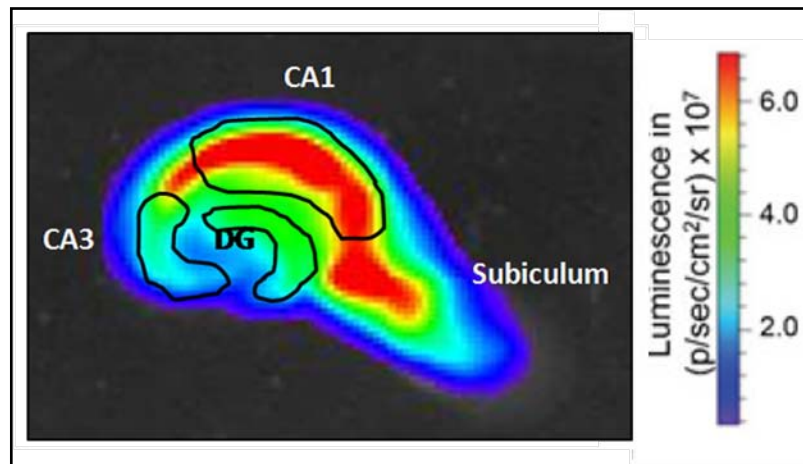


**Figure 15: Bioluminescence image of a single hippocampal slice from the anti-aggregant  $\text{Tau}^{\text{RDA-PP}}$  mouse at DIV 1.** The organotypic hippocampal slices were prepared from anti-aggregant  $\text{Tau}^{\text{RDA-PP}}$  pup at post-natal day 8 and its expression was measured via bioluminescence. The image depicts a single hippocampal slice with the expression pattern of the anti-aggregant  $\text{Tau}^{\text{RDA-PP}}$  along with the luciferase signal as seen by bioluminescence. The highest signal was seen in the CA1 and the subiculum region of the hippocampus; whereas a moderate amount of signal was seen in the CA3 and the DG regions of the hippocampus.

As mentioned before in Tau transgenic mice, luciferase and human  $\text{Tau}^{\text{RD}}$  are regulated simultaneously by a bidirectional promoter but are transcribed as individual mRNAs and not as a fusion construct. Therefore post-transcriptional modifications and translation of each mRNA occur independently, which may lead to disproportional protein levels. In addition, both proteins are degraded by different pathways: Tau is degraded by autophagy and proteasomal pathways, luciferase is targeted to peroxisomes. BLI signal intensities of  $\sim 1 \times 10^7$  p/s corresponded to a 40-50% overexpression of human  $\text{Tau}^{\text{RD}}$  over endogenous mouse Tau. The half life of luciferase is  $\sim 3-6$  hours, whereas for pro-aggregant  $\text{Tau}^{\text{RDA}}$  it is  $\sim 14$  days (Hochgraefe and Mandelkow, 2013).

The OHSC's were cultured until DIV30. The expression level of the anti-aggregant  $\text{Tau}^{\text{RDA-PP}}$  was monitored every fifth day until DIV30 (Figure 16). There was a reduction of the transgene expression as measured by bioluminescence during the culturing period.

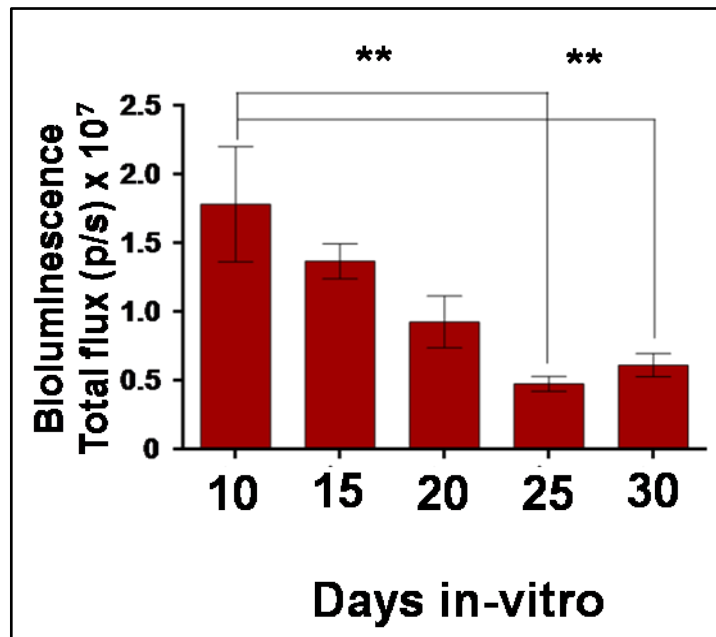


*Figure 16: Expression level of the exogenous human  $Tau^{RD\Delta-PP}$  construct in the hippocampal slice cultures prepared from anti-aggregant  $Tau^{RD\Delta-PP}$  animals, measured by bioluminescence. The bioluminescence measurement in the organotypic hippocampal slices was taken at different time points to observe the expression level of the anti-aggregant  $Tau^{RD\Delta-PP}$  in our model. The bioluminescence signal was reduced over the culturing period. Data was analyzed by Student t-test \*\*  $p$ -value < 0.01 \*\*\*\* $p$ <0.0001.*

There was a 30% reduction of the transgene expression as measured by bioluminescence. The reduction was significant only at later stages of the culturing period. This can be compared to similar bioluminescence signals seen in live animals (Hochgraefe and Mandelkow, 2013). In transgenic mice it is reported that initially there is a strong upregulation of the luciferase expression during the first two post-natal months. From three months onwards there is a stable expression of the transgene, which lasts up to 22 months. In the OHSC's there was a slight upregulation of the transgene expression from DIV1 to DIV10 (data not shown). From DIV10 to DIV30 there was a gradual decrease of the transgene expression by ~60% (Figure 16).



### 6.3. Increased neuronal number (NeuN positive cells) in the anti-aggregant $\text{Tau}^{\text{RDA-PP}}$ slice at DIV30.

OHSC's were immunostained for NeuN, a marker for matured neurons, as described in 4.4.2. Overview images of the slices were obtained. The slices showed intact hippocampal morphology in both the control and the anti-aggregant  $\text{Tau}^{\text{RDA-PP}}$  groups (Figure 17).

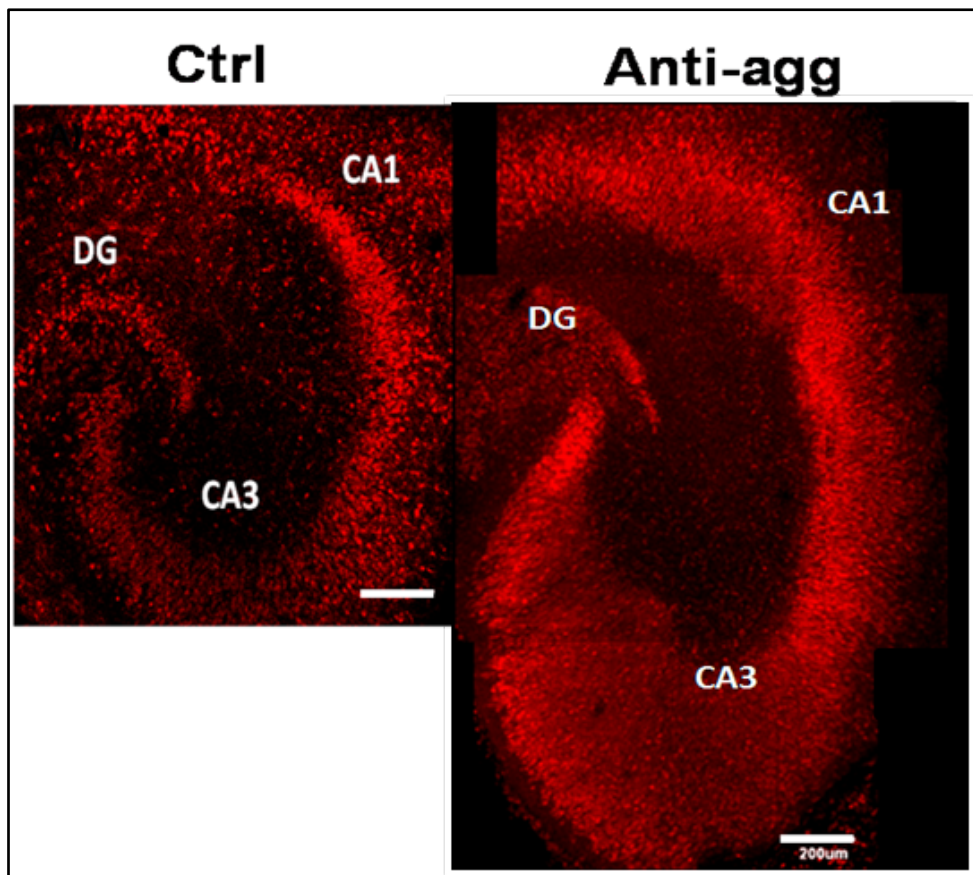


**Figure 17: Larger hippocampus was observed in the anti-aggregant  $\text{Tau}^{\text{RDA-PP}}$  slices at DIV 30.** Overview image of a single organotypic hippocampal slice at DIV 30 immunostained with NeuN antibody: The left image shows a control and the right image shows an anti-aggregant  $\text{Tau}^{\text{RDA-PP}}$  slice stained with NeuN antibody, a marker for mature neurons. The overview image of the hippocampal formation showed a much larger hippocampus with an increased number of neurons. Scale bar: 200µm

Overall there was an impressive increase of the size of the hippocampus as seen in the slices from the anti-aggregant  $\text{Tau}^{\text{RDA-PP}}$  groups compared to the

age-matched controls (Figure 17). The increase was apparent in all regions of the hippocampus like CA1, CA3 and DG.

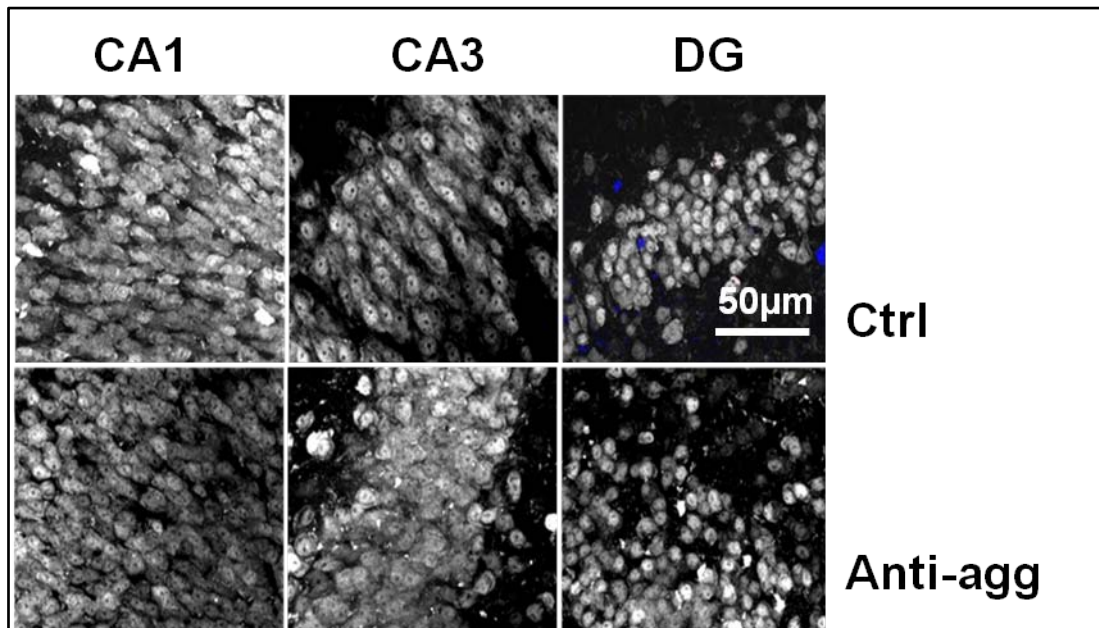
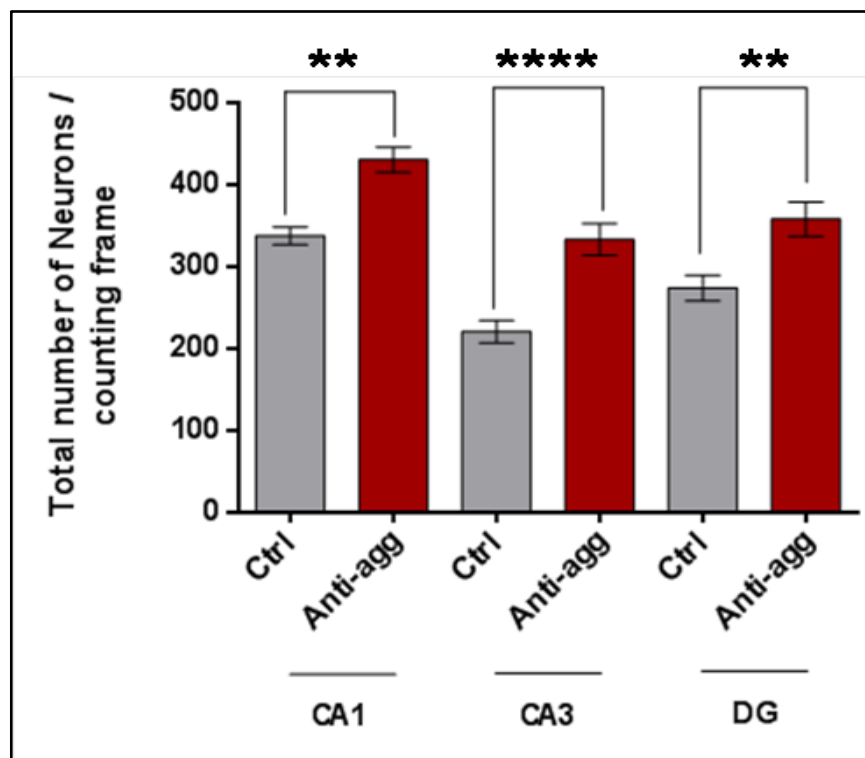


**Figure 18: Individual regions of the hippocampus, the CA1, CA3 and DG.** DIV 30 organotypic hippocampal slices were fixed and immunostained for NeuN antibody (a mature neuronal marker). Slices were imaged with the Olympus Fluoview1000 laser scanning microscope with 60x oil immersion. Z-stacks were taken with a thickness of 1µm. All three regions of the hippocampus, CA1, CA3 and DG were imaged. The Z-stacks were then merged to one single image with the help of ImageJ software. The NeuN<sup>+</sup> cells were counted manually for both the control and anti-aggregant TauRDΔ-PP groups with ImageJ software. Scale bar: 50µm (n=30 slices; 3 slices /animal).

We wanted to verify whether this overall increase in the size of the OHSC's from the anti-aggregant Tau<sup>RDΔ-PP</sup> groups was due to an increase in the total neuronal number. Therefore the total number of neurons in each region of the hippocampus like CA1, CA3 and DG were imaged (Figure 18) and manually counted with the help of the ImageJ software. All cells positive for NeuN were counted. The pyramidal neurons as well as the granular neurons were clearly distinguishable with their morphology. Our previous data from the pro-aggregant Tau<sup>RDΔ</sup> model had extensive pathology in the CA3 and CA1 regions of the hippocampus. This pathology was correlated with neurons showing missorted Tau in the somato-dendritic compartment especially in the

CA3 region (Sydow et al., 2011, Mocanu et al., 2008). This pathology in the adult mice was clearly reproducible in the OHSC's which also showed neuronal loss especially in the CA3 region (Messing et al., 2013). These observations from our pro-aggregant  $\text{Tau}^{\text{R}\Delta\text{A}}$  mice further increased our interest to analyze OHSC's from the anti-aggregant  $\text{Tau}^{\text{R}\Delta\text{A-PP}}$  mice, as they showed an increase in neuronal number specifically in the CA3 region. The CA1, CA3 and DG regions of the hippocampus were individually imaged with a higher magnification (60xoil) and the analysis confirmed that the neuronal number was strongly increased in the anti-aggregant  $\text{Tau}^{\text{R}\Delta\text{A-PP}}$  groups.



It has been reported, that in OHSC's of WT mice, there is an age dependent decrease in neuronal number in the CA1, CA3 and DG regions. We

have also seen a pronounced reduction in neuronal number in the hippocampus of the pro-aggregant  $\text{Tau}^{\text{RDA}}$  transgenic models from our laboratory (Messing et al., 2013). Here in the OHSC's from the anti-aggregant  $\text{Tau}^{\text{RDA-PP}}$  mice we saw a significant increase in the total number of matured neurons in all three regions of the hippocampus with emphasis on the CA3 region. This showed that the anti-aggregant  $\text{Tau}^{\text{RDA-PP}}$ , which cannot aggregate, somehow increased the neuronal number impressively in the CA3 region whereas in the case of the pro-aggregant  $\text{Tau}^{\text{RDA}}$  the aggregation of Tau caused a drastic reduction in the neuronal number in the same CA3 region (Messing et al., 2013). These results suggest that the hippocampus is important for both neurodegeneration as well as neurogenesis. It raises the question whether the increase of hippocampal neurons is due to neurogenesis or decreased neuronal cell death.

#### **6.4. Physiologically active microglia are observed in the anti-aggregant $\text{Tau}^{\text{RDA-PP}}$ slices at DIV 30.**

In order to understand the cause of the increase of neurons in the hippocampus we started to investigate factors and conditions that influence neurogenesis. It was reported that microglia play an important role in neurogenesis. Microglia constitute about 15% of the total glial cells in the adult brain (Lossi et al., 2009). They are abundant in the DG. They mediate inflammation-induced reduction in neurogenesis. However, the role of microglia in neurogenesis under physiological conditions remains poorly understood. The number of microglia in the DG is strongly inversely correlated to the number of stem/progenitor cells in the granular cell layer. In co-culture experiments, microglia but not astrocytes reduced the number of neuronal progenitor/glial cells despite the absence of inflammatory stimuli (Gebara et al., 2013). Experimental activation of microglia by the administration of the

bacterial endotoxin LPS decreases adult neurogenesis by specifically inhibiting the proliferation or survival of the new neuronal cells (Bernardino et al., 2008, Mosher et al., 2012). These effects may be mediated by the release of cytokines such as IL-6, TNF $\alpha$ , IL-1 $\beta$  from microglia, since these molecules show an inhibitory effect on adult neurogenesis *in vitro* or *in vivo*. Normal physiologically active microglia are also needed as they are involved in the regulation of physiological mechanisms such as dendritic spine maintenance or the homeostasis of the neurogenic niche by the removal of newly born cells that die by apoptosis (Gebara et al., 2013). Reduced microglial number is found to be correlating with increased neurogenesis and cell proliferation in C57Bl/6 mice (Sultan et al., 2013). Microglia in their normal physiologically active form may also secrete anti-inflammatory factors like IL10, which in turn might regulate adult neurogenesis in the normal brain (Perez-Asensio et al., 2013).

Therefore we investigated the status of microglial activation and the total number of microglia in our anti-aggregant Tau<sup>RD $\Delta$ -PP</sup> slices at DIV30.

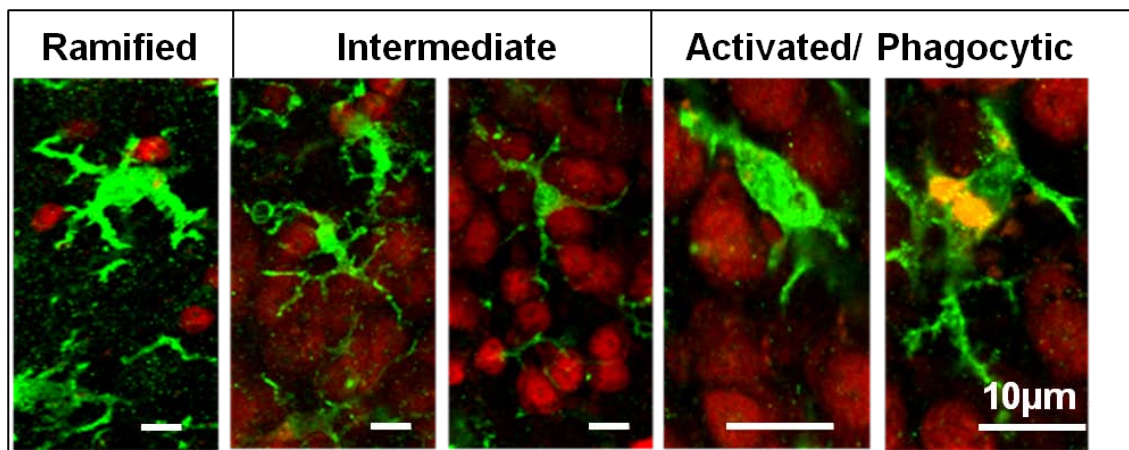


**Figure 20: Different stages of microglial activation as seen in organotypic hippocampal slice cultures.** OHSC at DIV 30 were fixed and immunostained for matured neurons (NeuN, red) and microglia (Iba1, green). The first image shows a ramified microglia which had a cell body with many processes. The next stage in microglial activation is the intermediate form, where the microglia retracts their processes. The third stage is the activated or the phagocytic form of microglia where it retracts all its processes and has a rounded or bigger cell body. The phagocytic form shows a microglia that has engulfed debris, which could be a dead neuron. Scale bar- 10 $\mu$ m.

OHSC's were immunostained with Iba1, for microglia (shown in green) and for matured neurons with NeuN (shown in red) (Figure 20). Initially we saw different morphologies of microglia in the organotypic hippocampal slice cultures at DIV 30 of the WT mice. In young slice cultures we saw more of the ramified form of microglia in both control and anti-aggregant Tau<sup>RDΔ-PP</sup> groups. These ramified forms of microglia have many processes protruding from their cell body and they also have smaller cell bodies. As the cultures age or get matured, there were modifications in the microglial morphology. In the aged cultures the microglia are in their activated or phagocytic forms (Figure 20). This can be due to the chronic inflammation which takes place in the aged brain (Njie et al., 2012). When there is activation of microglia because of inflammation or aging, the microglia take up the phagocytic form or the activated form, which can be seen by retracted processes and enlarged cell bodies.

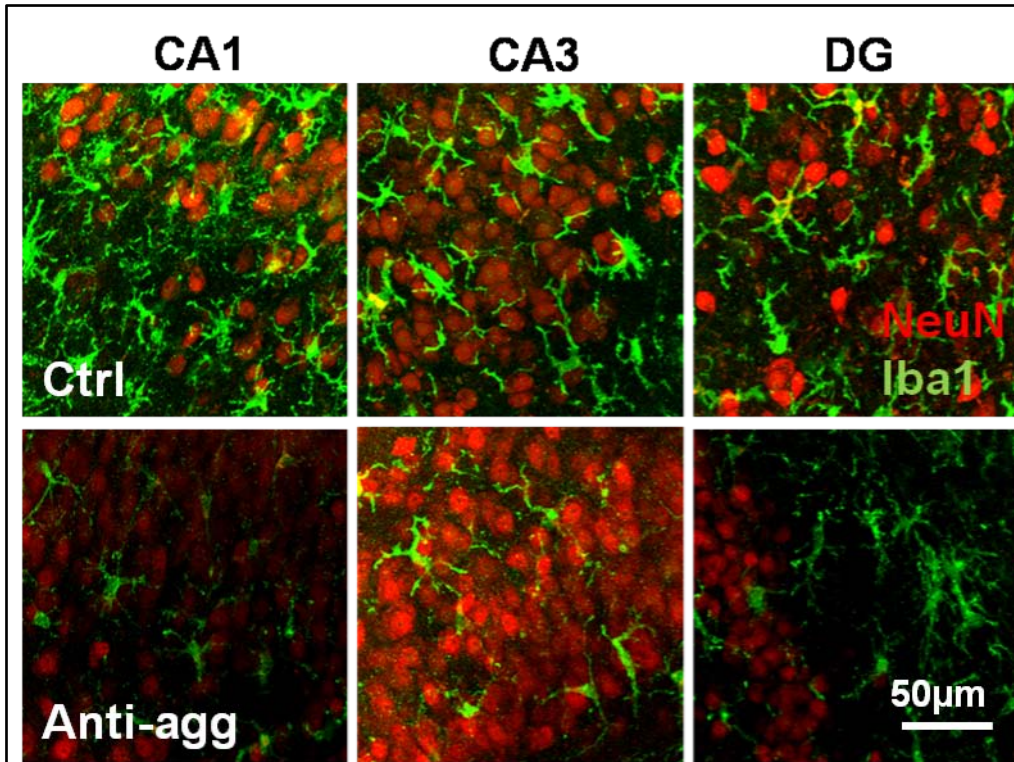


**Figure 21: No activation of microglia was seen in the anti-aggregant  $Tau^{RD\Delta-PP}$  slices at DIV30.** OHSC at DIV 30 were fixed and immunostained for NeuN (matured neurons in red) and Iba1 (microglia in green). Different regions of the hippocampus CA1, CA3 and DG in the control and anti-aggregant  $Tau^{RD\Delta-PP}$  slices were imaged with confocal laser scanning microscopy. The control slices showed the activated form of microglia when compared to the age matched anti-aggregant  $Tau^{RD\Delta-PP}$  slices which showed ramified forms of microglia. The anti-aggregant  $Tau^{RD\Delta-PP}$  slices showed decreased number of microglia in all the three regions of the hippocampus and the microglia were also in their normal physiologically active form. But in the control slices the microglia are in the intermediate or active form which could be related to normal aging. ( $n=30$  slices; 3 slices /animal). Scale bar:  $50\mu m$ ;  $n=30$  slices; 3 slices /animal.

We stained OHSC's with NeuN for matured neurons and Iba1 for total microglia. The total number of Iba1 positive microglia was counted manually with the help of the ImageJ software. We saw a reduction in the total number of microglial cells, all positive for Iba1, in the anti-aggregant  $Tau^{RD\Delta-PP}$  slices when compared to the age-matched control littermates. Along with the reduction of the microglial number there was also a reduced activation of the microglia in the anti-aggregant  $Tau^{RD\Delta-PP}$  slices (Figure 21). The morphological observations showed that the microglia in the anti-aggregant  $Tau^{RD\Delta-PP}$  slices had a

predominantly ramified appearance, even at DIV 30. By contrast, the microglia in the control slices were increased in number and showed more of activated or phagocytic forms. Interestingly in the DG region of the hippocampus the microglia in the anti-aggregant  $\text{Tau}^{\text{RDA-PP}}$  slices did not span the granular cell layer, but stayed in a specific orientation surrounding the granular cell layer of the hippocampus. In contrast, in the control slices the microglia did span the granular cell layer.

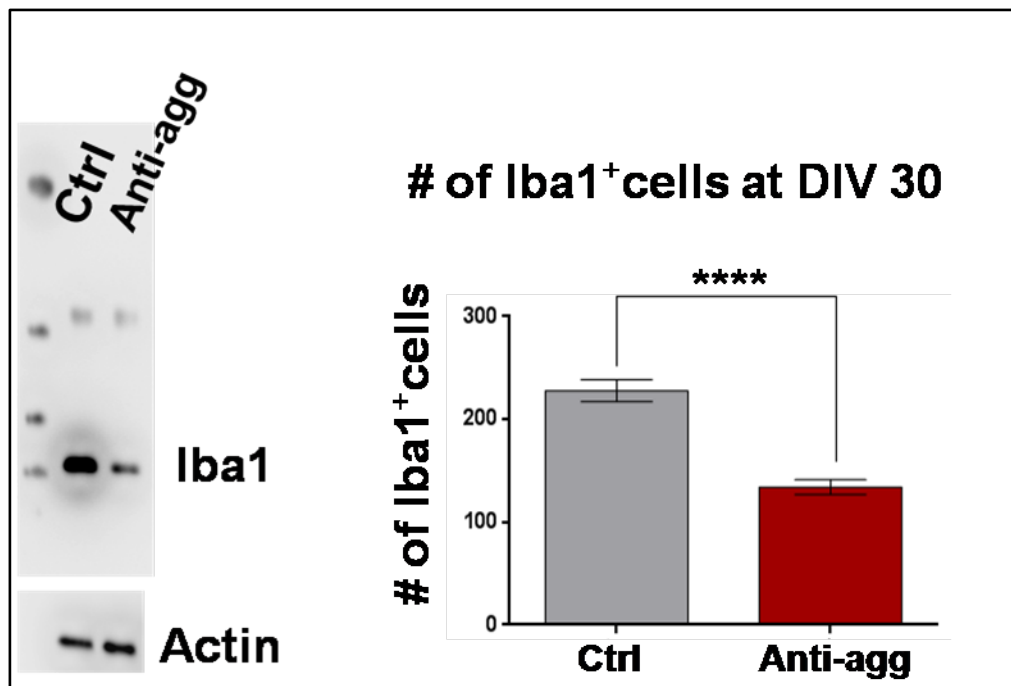


**Figure 22: Decrease of the total number of microglia cells in the anti-aggregant  $\text{Tau}^{\text{RDA-PP}}$  slices at DIV30.** The total number of Iba1 positive cells was manually counted with the help of the ImageJ software. There was a 30% reduction in the total amount of microglia in the anti-aggregant slices at DIV30, when compared to the age matched control littermates ( $n=30$  slices; 3 slices/animal; Unpaired  $t$ -test \*\*\*\*  $p$ -value < 0.0001). The left image shows a western blot using Iba1 antibody against the hippocampal lysates from control and anti-aggregant slices at DIV30.

The organotypic hippocampal slices were collected at DIV30 for further biochemical analysis. Western blot analysis was performed with the hippocampal lysates prepared from control and anti-aggregant  $\text{Tau}^{\text{RDA-PP}}$  slices. There was a reduction in Iba1 protein levels in the anti-aggregant  $\text{Tau}^{\text{RDA-PP}}$



hippocampal lysates (Figure 22) and this correlates with the reduction of Iba1 positive cells as analyzed by ImageJ software.

### **6.5. Physiologically active astrocytes are observed in the anti-aggregant Tau<sup>RDA-PP</sup> slices at DIV 30.**

Astrocytes exert profound effects on neuronal development as they provide support for neuronal survival, axon and dendritic outgrowth and synaptogenesis. These effects are mediated by a variety of factors that are released by the astrocytes. Several studies show that astrocytes cause neuritogenesis and synaptogenesis in neurons (Ullian et al., 2001, Clarke and Barres, 2013). During normal aging, the astrocytes convert to a reactive phenotype and there is also an increased rate of proliferation of the astrocytes. During normal aging there is no further differentiation of astrocytes, when compared to young (2 month) mouse brain (Capilla-Gonzalez et al., 2014).

We wanted to see the status of the astrocytes in the anti-aggregant Tau<sup>RDA-PP</sup> and the control slices at DIV30. We first observed that the astrocytes like the microglia are also of different morphology in the slice cultures (Figure 23). They were of the radial form with long elongated processes, the intermediate form with shorter processes and then the activated star shaped form.

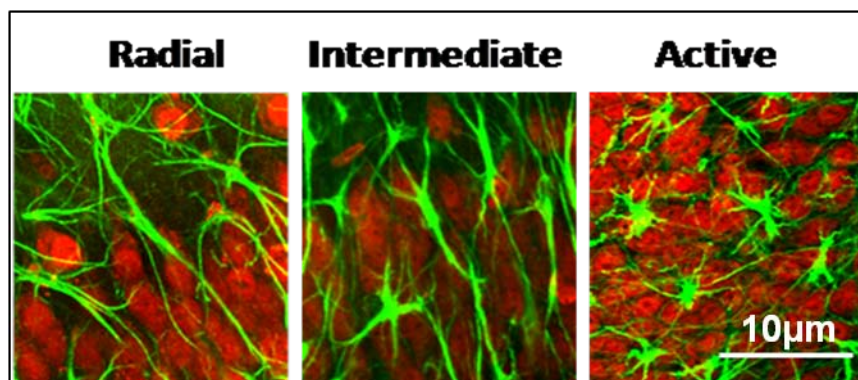


**Figure 23: Different forms of astrocytes seen in organotypic hippocampal slice cultures at DIV30.** Organotypic hippocampal slice cultures from the WT mice are fixed at DIV30 and immunostained for mature neurons (NeuN, red) and astrocytes (GFAP, green). The above image depicts different stages of astrocytes as seen in organotypic hippocampal slice cultures. The astrocytes can be differentiated into three different forms based on their morphology, the radial, intermediate and the active form. Scale bar- 10µm

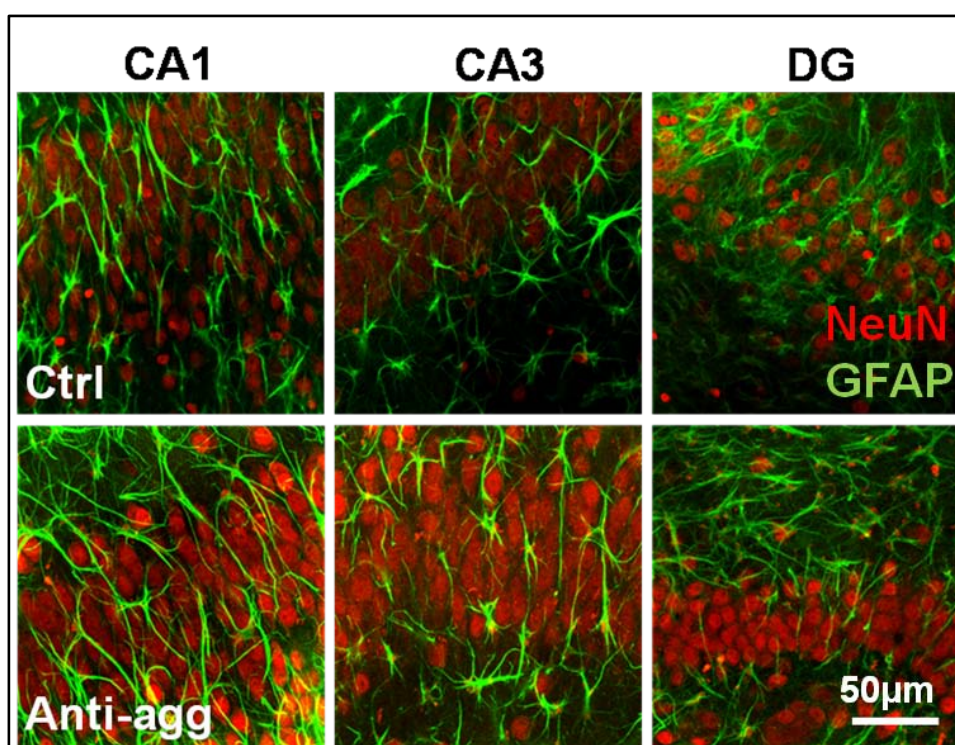


**Figure 24: Activated astrocytes were not present at DIV30 in the anti-aggregant  $Tau^{RD\Delta-PP}$  slices.** Slices from the control and anti-aggregant  $Tau^{RD\Delta-PP}$  groups were fixed at DIV30 and immunostained for mature neurons (NeuN in red) and astrocytes (GFAP in green). More star shaped astrocytes were seen in the control slices and more radial astrocytes were seen in the anti-aggregant  $Tau^{RD\Delta-PP}$  slices, in the CA1, CA3 and DG regions of the hippocampus. Scale bar-50µm n=30 slices; 3 slices/animal.

We observed different forms of astrocytes in different regions of the hippocampus. The control slices had more star-shaped astrocytes in the CA1, CA3 and DG regions (Figure 24). The anti-aggregant Tau<sup>RDΔ-PP</sup> slices had radial type of astrocytes in the CA1 region and more of the intermediate forms in the CA3 and DG region. Unlike microglia, the astrocytes were more difficult to be counted manually, because of their extended long processes which move through all the cell layers of the slices. By the morphological analysis we conclude that the astrocytes in the anti-aggregant Tau<sup>RDΔ-PP</sup> slices were more in the RGL form than the more star-shaped astrocytes in the controls at DIV30.

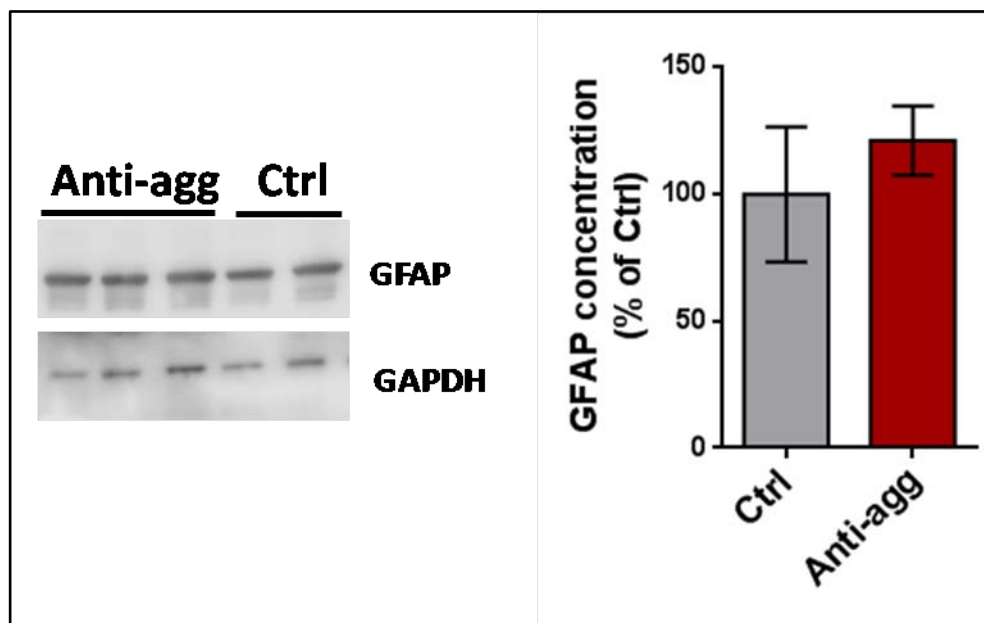


**Figure 25: Astrocytic GFAP protein levels in western blots show no significant increase in the anti-aggregant Tau<sup>RDΔ-PP</sup> slices at DIV30.** Hippocampal lysates were prepared from the control and the anti-aggregant Tau<sup>RDΔ-PP</sup> slices and used for western blot analysis against GFAP antibody for total astrocytes. The figure shows the western blot for total GFAP levels in the hippocampal lysates from the control and the anti-aggregant Tau<sup>RDΔ-PP</sup> slices. The graph represents the quantification of the western blot for the total amount of astrocytes in the control and the anti-aggregant Tau<sup>RDΔ-PP</sup> groups. There was a slight increase in the total amount of astrocytes in the anti-aggregant Tau<sup>RDΔ-PP</sup> groups, compared to the age matched control littermates. The western blot analysis was done from three different animals of the anti-aggregant Tau<sup>RDΔ-PP</sup> group and two animals of the control group.

The hippocampal slices were collected at DIV 30 from the control and the anti-aggregant Tau<sup>RDΔ-PP</sup> groups and used for further biochemical analysis.

Total protein levels of astrocytes were detected by blotting against GFAP antibody (Figure 25). The total amount of astrocytes in the anti-aggregant Tau<sup>RDΔ-PP</sup> group was not significantly increased compared to the controls.

### 6.6. No change in spine density.

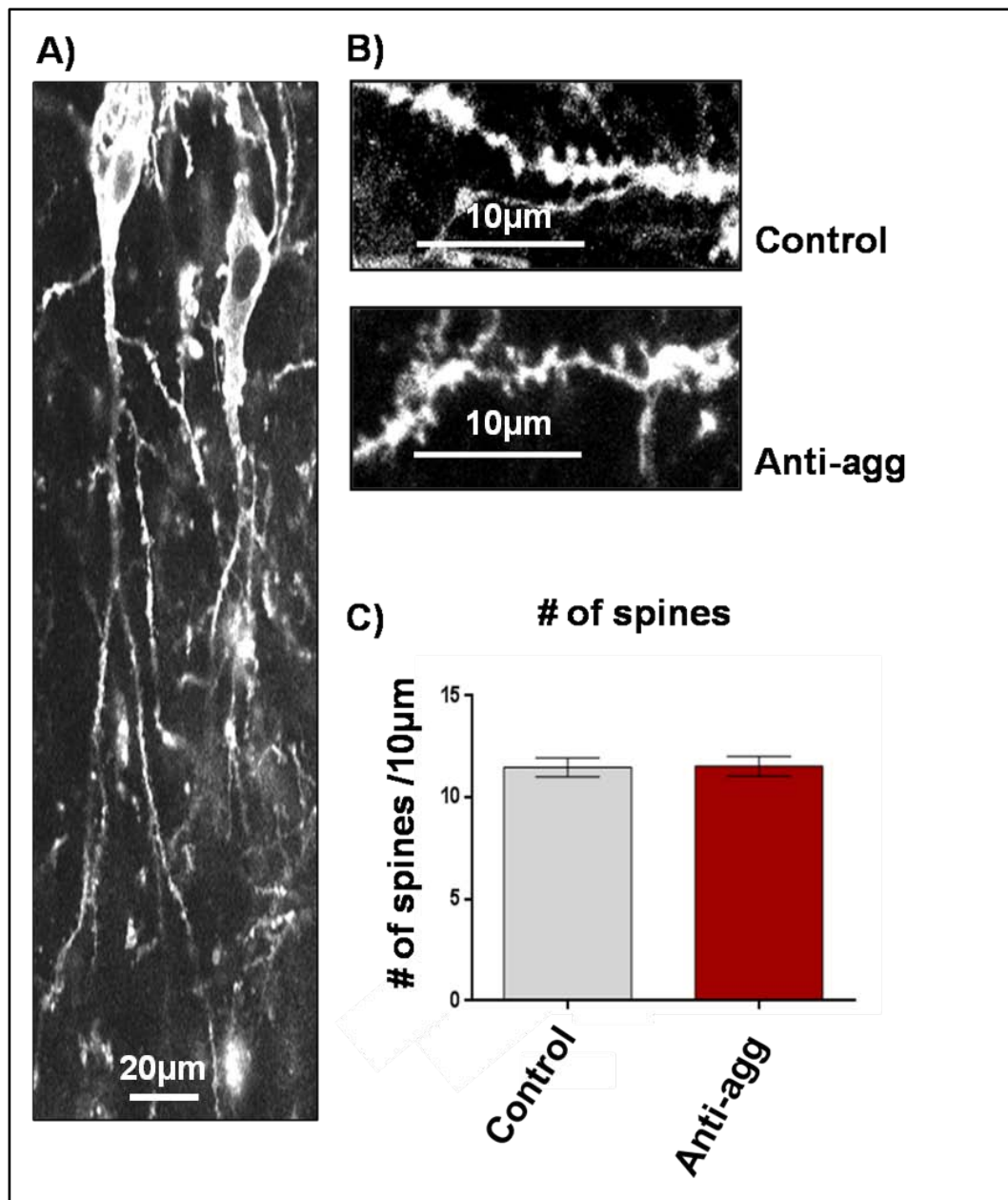


**Figure 26: No change in spine density in the apical and basal dendrites of the CA1 pyramidal neurons.** DIV30 Organotypic hippocampal slice cultures were labeled with DiI with the help of a gene gun. (A) CA1 pyramidal neurons labeled with DiI. The cell body and the apical dendrites of the CA1 pyramidal neurons were clearly visible. (B) Higher magnification images of one dendrite from the control and the anti-aggregant TauRD $\Delta$ -PP group. Scale bar 10µm. These higher magnification images were used for counting the total number of spines per 10µm length of the dendrite. (C) Quantification of the total number of spines per 10µm length of the dendrite in the control and the anti-aggregant TauRD $\Delta$ -PP groups. There was no difference in the total number of spines per 10µm dendrite length between the groups.  $n=30$  neurons taken from 15 slices prepared from 5 different animals /group.

We wanted to see whether an increase in the neuronal number causes some change in the spine density. Therefore the organotypic hippocampal slice cultures at DIV 30 were labeled with Dil with the help of the gene-gun. The CA1 pyramidal neurons that were randomly shot by the gene gun were used for spine counting (Figure 26). Spines in both the apical and basal dendrite of the pyramidal neurons were imaged and counted manually with the help of the ImageJ software. There was no change in the spine density in the anti-aggregant Tau<sup>RDΔ-PP</sup> slices compared to the age matched control slices.

## **6.7. Increase in the total number of proliferating BrdU positive cells.**

### **6.7.1. The BrdU incorporation assay.**

5'Bromo-2'-deoxyuridine (BrdU) is a thymidine analogue that is used in cell proliferation studies. BrdU is incorporated into the DNA during DNA synthesis. The molecular weight of BrdU is 307.1. BrdU labeling can be done either in-vitro for cell culture or tissue culture experiments or in-vivo in experimental animals.

For in-vivo studies 50 µg/ml BrdU in saline was injected intraperitoneally in the anti-aggregant Tau<sup>RDΔ-PP</sup> mice at post-natal day 8 (Figure 13). The animals were kept alive for 2 hours because 2 hours post injection is a short time for the new born cells to migrate from the region of birth or die by apoptosis and thus the rate of proliferating and the niche of the dividing cells can be studied.

BrdU positive cells are seen even after 30 min post injection in animals (Namba et al., 2005). At post-natal day 5, the hilar region of the hippocampus contains many proliferating cells. At post-natal day 5 the hilar region has many BrdU positive cells, which are later found in the inner half of the granular cell layer at P12 and P19 animals. Similarly in rats a dense population of Ki67

(proliferation marker) positive cells are found in the hilus and partly in the SGZ, from P5-P8. This distribution gradually changes with age. At P19, the Ki67 positive cells are mostly seen in the SGZ and no more at the hilus region of the hippocampus (Namba et al., 2005). The process of neurogenesis seen in P19 animals is nearly identical to that of adult neurogenesis (Altman and Das, 1965, Seki and Arai, 1993, Kuhn et al., 1996, Gould and Gross, 2002). The total number of BrdU positive cells increase from P5-P8, but does not change between P8 and P19 (Namba et al., 2005). This is the main reason why we selected P8 animals for the preparation of OHSC's, so that we can analyze the post-natal and early adult hippocampal neurogenesis and also analyze adult hippocampal neurogenesis at later time points of slice culturing. The length of the cell-cycle of the granule cells is estimated to be 16-25 hours in live rats (Cameron and McKay, 2001, Nowakowski et al., 1989). Experiments done by transfecting EGFP into DIV14 slice cultures have shown that the slice cultures intrinsically retain a neurogenic potential quantitatively similar to the hippocampus in the living animal. 25% of retrovirus (EGFP) transfected cells were also positive for NeuN. This stands as a proof that small, but not all populations of the dividing cells become mature neurons in the slice cultures after a period of 2-3 weeks (Kamada et al., 2004)

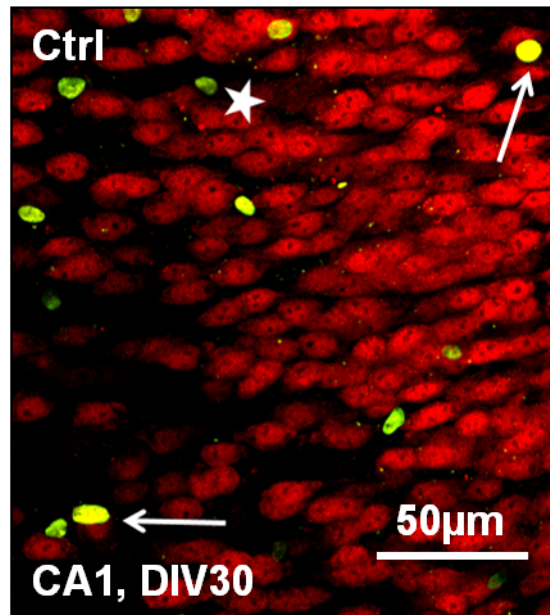


*Figure 27: BrdU gets incorporated into the proliferating cells which can be detected by immunostaining with Anti-BrdU antibody as seen in OHSC's at DIV30. The above image is a representation of the CA1 region that is immunostained with both NeuN (red) and BrdU (green). The arrows show a single cell that is immunostained for both NeuN and BrdU (Merge). The star shows a single cell that is immunostained only for BrdU.*

BrdU labeling in OHSC's was done by adding 50 mM BrdU (freshly prepared) in 1 ml of slice culture media and used for in-vitro slice culture studies. Since BrdU is incorporated into DNA during mitosis, its density diminishes during the following cell divisions (Dayer et al., 2003). Because of this reason we added 50µM BrdU into the slice culture media, every second day after media change, thereby preventing the disappearance of highly proliferating cells by BrdU immunoreactivity. The application of BrdU in the slice cultures began at DIV15 so that the dividing cells from DIV15 onwards take up the BrdU label. DIV15 of the culturing period in OHSC's can be compared to the adult life of the animal. Therefore the BrdU positive proliferating cells in OHSC's from DIV15 indicate the rate of proliferation in the adult live animal. Organotypic hippocampal slice cultures are believed to become matured from DIV14 onwards comparable to the adult life of the animal.



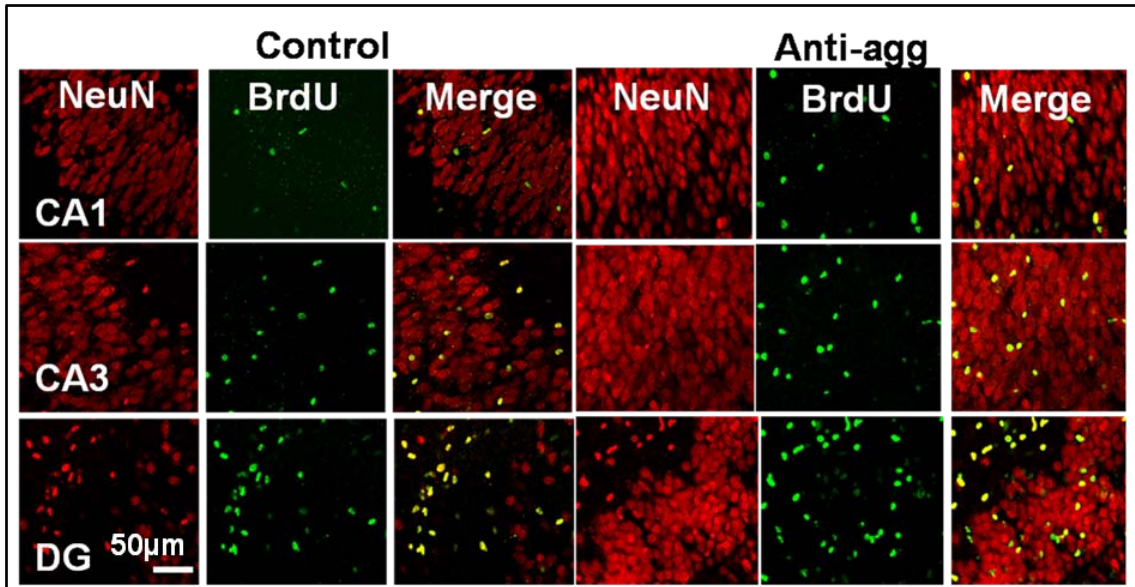


**Figure 28: Control and anti-aggregant  $Tau^{RD\Delta-PP}$  slices treated with BrdU from DIV 15 to DIV 30.**  $50\mu\text{M}$  BrdU was dissolved in the culture media of the anti-aggregant  $Tau^{RD\Delta-PP}$  and control slices. BrdU was applied from DIV 15 until DIV 30. The media containing BrdU was refreshed during every media change. Finally the slices were fixed with 4% FA and then used for further immunohistochemical analysis. The slices were immunostained with NeuN and BrdU antibodies. BrdU positive cells were found in the CA1, CA3 and DG regions of the hippocampus. Scale bar:  $50\mu\text{m}$ .

OHSC's were immunostained for NeuN and BrdU at DIV30. The CA1, CA3 and the DG regions showed BrdU positive cells (Figure 28). In the hippocampus only the DG region was considered to be neurogenic, but BrdU positive cells were also seen in the CA1 and CA3 regions. These cells were seen in the control and also in the anti-aggregant  $Tau^{RD\Delta-PP}$  slices. It is believed that in OHSC's generated by the interface method the three dimensional structure of the neurogenic niche is somewhat reorganized in the slice culture system (Kamada et al., 2004). So we speculate that the reason behind the presence of BrdU positive cells in the CA1 and CA3 regions can develop because of some architectural rearrangements in the slice culture technique. But the interesting observation was, these BrdU positive cells were seen even at the later stages of the slice cultivation (DIV30). The DG region of the hippocampus, which is the niche of neurogenesis showed increased number of BrdU positive cells in the

anti-aggregant  $\text{Tau}^{\text{RD}\Delta\text{-PP}}$  slices when compared to the age-matched control slices. Next we wanted to quantify the total number of BrdU positive cells in both groups in all three distinct regions of the hippocampus (Figure 29).

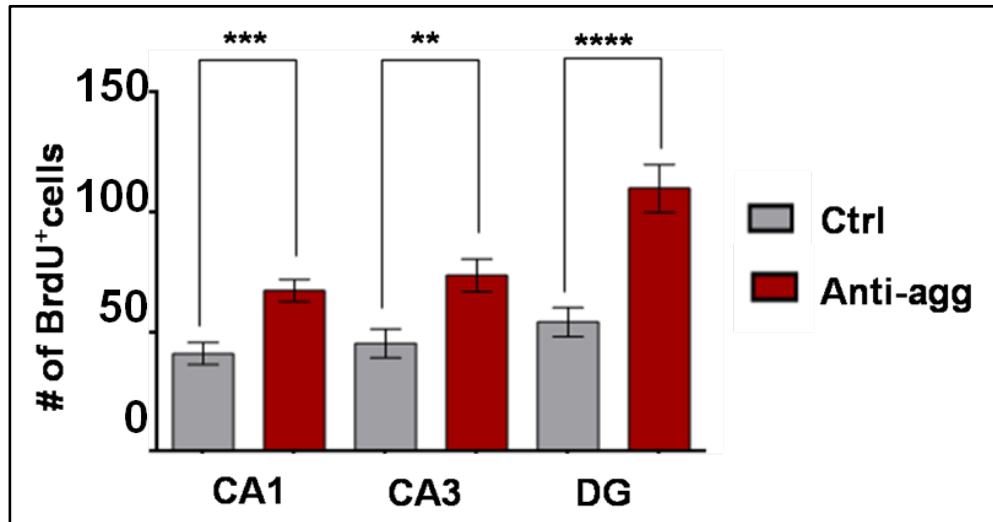


**Figure 29: Rate of proliferation: Number of BrdU positive cells in the control and the anti-aggregant  $\text{Tau}^{\text{RD}\Delta\text{-PP}}$  slices at DIV 30.** The concentration of BrdU in the culture media of the anti-aggregant  $\text{Tau}^{\text{RD}\Delta\text{-PP}}$  and control slices was  $50\mu\text{M}$ . BrdU was applied from DIV 15 until DIV 30. The media containing BrdU was refreshed during every media change. Finally the slices were fixed with 4% FA and immunostained with NeuN and BrdU antibodies. All the BrdU positive cells (all green) were counted manually with the ImageJ software. BrdU positive cells were found in the CA1, CA3 and DG region. The anti-aggregant  $\text{Tau}^{\text{RD}\Delta\text{-PP}}$  slices had increased number of BrdU positive cells than in the controls. This indicates that more of the proliferation of the progenitor cells was taking place in the anti-aggregant  $\text{Tau}^{\text{RD}\Delta\text{-PP}}$  slices when compared to the controls. Even though a significant increase was seen in the DG region, the CA1 and the CA3 regions also showed prominent increase in the total number of BrdU positive, proliferating progenitor cells in the anti-aggregant  $\text{Tau}^{\text{RD}\Delta\text{-PP}}$  slices. This indicates that the anti-aggregant  $\text{Tau}^{\text{RD}\Delta\text{-PP}}$  protein causes an increase of proliferation of the progenitor cells. Data was analyzed by Student t-test;  $n=30$  slices; 3 slices per animal/group; \*\* $p<0.01$ ; \*\*\* $p<0.001$ ; \*\*\*\* $p<0.0001$ .

All the NeuN positive cells (shown in red) and all the BrdU positive cells (shown in green) (Figure 28) were counted manually by ImageJ software. There was a 30-40% increase in the total number of BrdU positive cells in the anti-aggregant  $\text{Tau}^{\text{RD}\Delta\text{-PP}}$  slices when compared to the age matched control littermates (Figure 29), especially in DG, CA1 and CA3 regions. Thus the rate of proliferation was enhanced in the anti-aggregant  $\text{Tau}^{\text{RD}\Delta\text{-PP}}$  slices.

Next the percentage of BrdU positive cells were calculated between the control and the anti-aggregant  $\text{Tau}^{\text{RD}\Delta\text{-PP}}$  slices (Figure 30). Compared to the control slices the fraction of BrdU positive cells were almost 50% higher in the anti-aggregant  $\text{Tau}^{\text{RD}\Delta\text{-PP}}$  slices in the CA1 and CA3 regions whereas in the DG region there were twice as many BrdU positive cells (+100%).

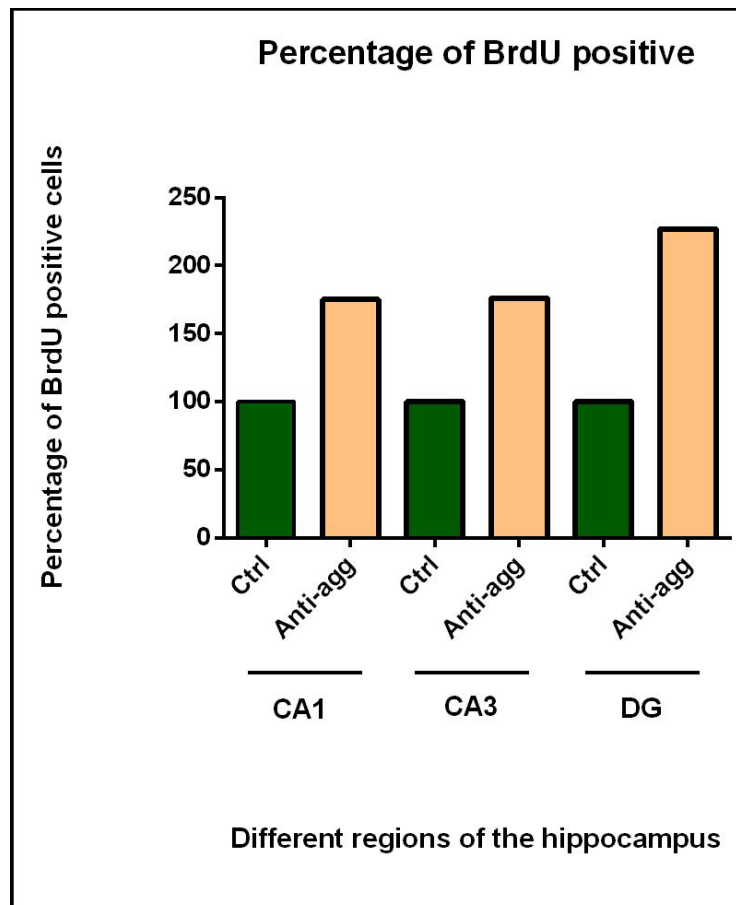


**Figure 30: Percentage of the cells that are BrdU positive are almost doubled in the anti-aggregant  $\text{Tau}^{\text{RD}\Delta\text{-PP}}$  slices when compared to the controls. Compared to the controls the anti-aggregant  $\text{Tau}^{\text{RD}\Delta\text{-PP}}$  slices had twice as many BrdU positive proliferating cells.**

These data indicate that the expression of the anti-aggregant  $\text{Tau}^{\text{RD}\Delta\text{-PP}}$  increases the rate of proliferation, as analyzed by the BrdU incorporation assay.

We also wanted to analyze the rate of differentiation in the anti-aggregant  $\text{Tau}^{\text{RD}\Delta\text{-PP}}$  and control OHSC's. When the slice cultures were immunostained for NeuN and BrdU at DIV30, certain amounts of cells showed

double labeling of BrdU with NeuN and these cells are represented in yellow (Figure 27; Figure 28). Previous reports (Kamada et al., 2004) have shown that there is neuronal differentiation in the slice cultures which needs a minimum of 2 weeks to take place. The rate in slices is faster than the neuronal stem cell differentiation in the live mice/rats. In our slices not all of the BrdU positive cells were co-labeled for NeuN. But small populations of BrdU positive, proliferating cells were also positive for the mature neuronal marker NeuN. Therefore we were interested to see whether the expression of the anti-aggregant Tau<sup>RDA-PP</sup> had an effect on the rate of differentiation into neurons. All the cells with BrdU and NeuN staining (yellow bars in Figure 28) were counted manually with the help of the ImageJ software. Statistical analysis revealed an interesting observation that the total number of cells that were positive for both NeuN and BrdU were significantly increased in the anti-aggregant Tau<sup>RDA-PP</sup> slices, when compared to the control littermates (Figure 31).

Next we checked the rate of differentiation in a larger group of control and anti-aggregant Tau<sup>RDΔ-PP</sup> slices. Almost all of the BrdU positive cells in the control groups were also positive for NeuN. This means that the rate of differentiation into mature neurons in control groups was equal to the rate of proliferation and this rate of differentiation was seen in all regions of the hippocampus. Similarly we checked the rate of differentiation in the anti-aggregant Tau<sup>RDΔ-PP</sup> slices. In the CA1 region there was a significant reduction in the total number of BrdU and NeuN double-positive cells, simply indicating that even though the rate of proliferation was high in the CA1 region in the anti-aggregant Tau<sup>RDΔ-PP</sup> slices, the rate of differentiation is significantly less in this region. But in the CA3 and the DG, almost all of the BrdU positive cells were also positive for NeuN. This indicates that in the CA3 and the DG the rate of proliferation was equal to the rate of differentiation in the anti-aggregant Tau<sup>RDΔ-PP</sup> groups. Therefore in the anti-aggregant Tau<sup>RDΔ-PP</sup> groups, there is enhanced proliferation followed by enhanced differentiation of the neural progenitor cells in the CA3 and the DG regions of the hippocampus.

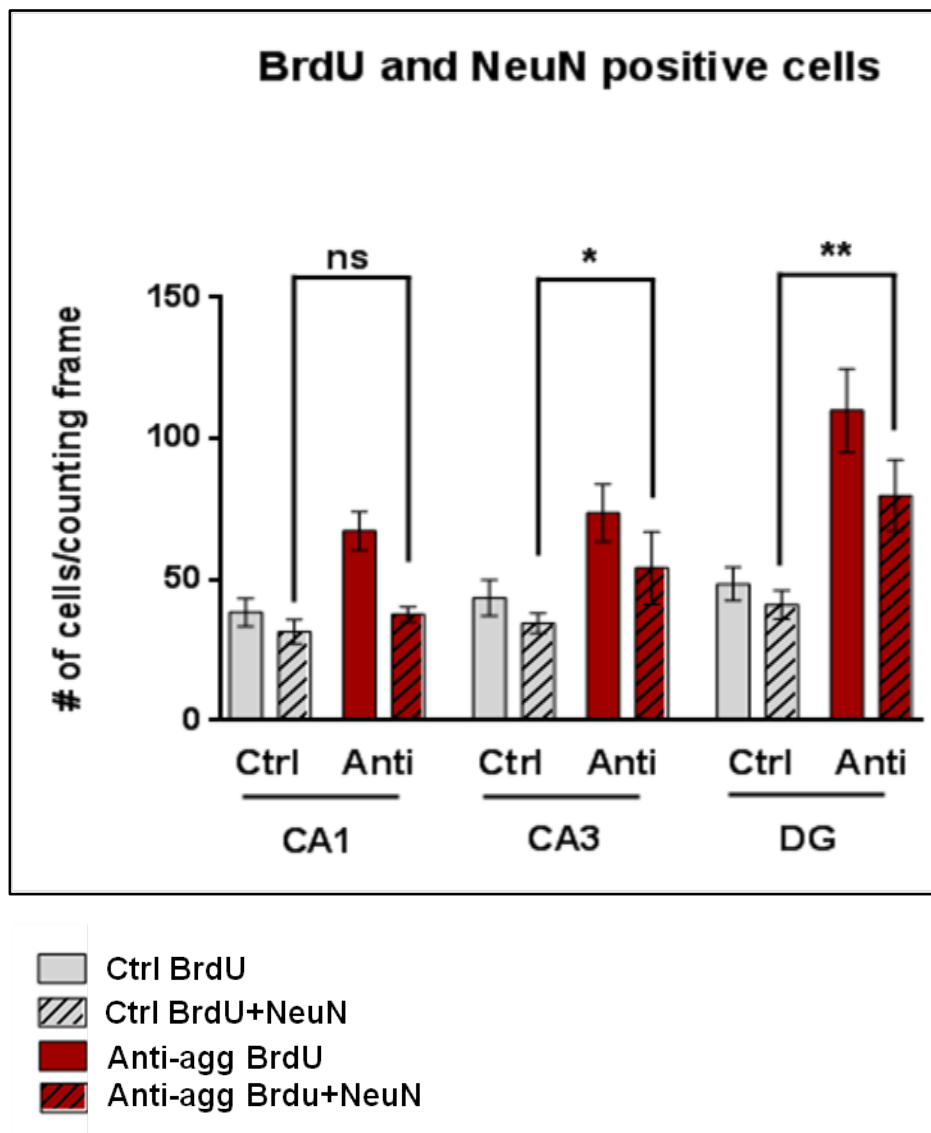


**Figure 31: Rate of differentiation: Number of BrdU positive cells that were co-labeled with NeuN, a marker of mature neurons.** The concentration of BrdU in the culture media of the anti-aggregant  $TauRD\Delta$ -PP and control slices was  $50\mu M$ . BrdU was applied from DIV 15 until DIV 30. The media containing BrdU was refreshed during media change. Finally the slices were fixed with 4% FA and immunostained with NeuN and BrdU antibodies. All the BrdU positive cells (all green), and the BrdU and NeuN positive cells (yellow) were counted manually with the ImageJ software. Both types of cells were found in the CA1, CA3 and DG region of the hippocampus. The anti-aggregant  $TauRD\Delta$ -PP slices had more of the BrdU positive cells than the control littermates. This indicates that more of the progenitor cell proliferation takes place in the anti-aggregant  $TauRD\Delta$ -PP slices when compared to the control littermates. Even though a significant increase was seen in the DG region, the CA1 and the CA3 regions also showed prominent increase in the total number of BrdU positive, proliferating progenitor cells. This indicates that the anti-aggregant  $TauRD\Delta$ -PP causes an increase in the proliferation of the progenitor cells and also an increase in the number of differentiated cells, which was not seen in the control littermates. Data was analyzed by Student *t*-test;  $n=30$  slices; 3 slices per animal/group; \* $p<0.05$ ; \*\* $p<0.01$ .

We also performed immunostaining on OHSC's for different markers and different cell types like the astrocytes and microglia, to see whether the newly generated cells with BrdU staining were also differentiated into other non-neuronal cell types. In both the control and the anti-aggregant Tau<sup>RDΔ-PP</sup> groups, there was no differentiation of BrdU positive proliferating cells into astrocytes or microglia (data not shown). Moreover we did not observe a significant increase in astrocytes (Figure 25) and in fact the microglia were significantly decreased in the anti-aggregant Tau<sup>RDΔ-PP</sup> slices (Figure 22).

## **6.8. Neuronal stem cells at different proliferating stages are seen in aged anti-aggregant Tau<sup>RDΔ-PP</sup> slices (DIV30) but are absent in the age matched control littermates.**

### **6.8.1. Ki67 positive cells are observed in the anti-aggregant Tau<sup>RDΔ-PP</sup> slices but are absent in the control slices at DIV 30.**

Ki67 is a nuclear protein and is expressed during all phases of the cell cycle except G<sub>1</sub> (Kee et al., 2002). It is the most important marker of stem cell proliferation.

With advanced age the level of proliferation measured by the Ki67 is lower in the controls than in the age matched anti-aggregant Tau<sup>RDΔ-PP</sup> slices. This decrease is also seen in human brain samples, where Ki67 immunoreactivity was not seen after 38 years of age and DCX immunoreactivity was not seen beyond 65 years of age in control as well as AD/Tauopathy brain samples (Knoth et al., 2010).

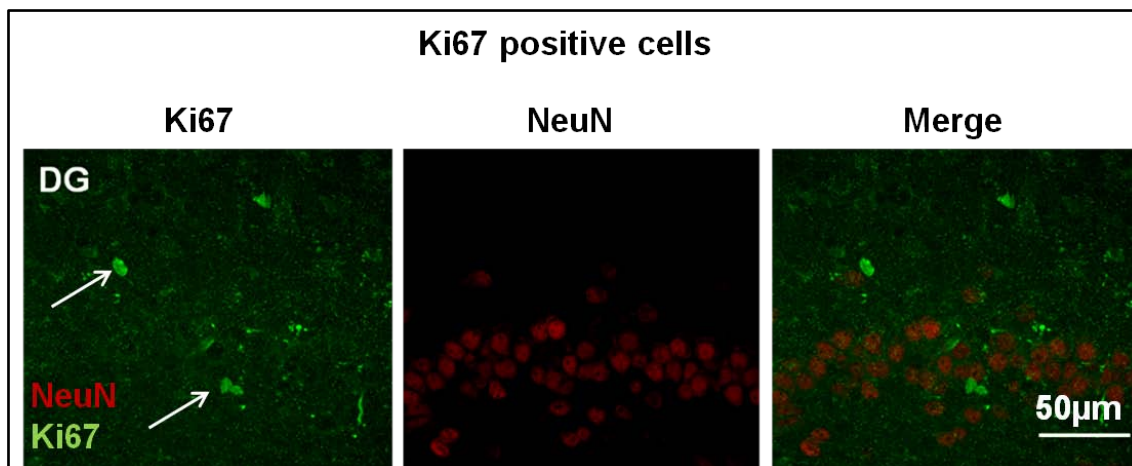


**Figure 32: Ki67 positive neuroblast cells from the neuronal stem cell lineage were seen in the anti-aggregant  $Tau^{RDA-PP}$  slices at DIV 30.** Organotypic hippocampal slice cultures were prepared from the control and the anti-aggregant  $Tau^{RDA-PP}$  groups. The slices were cultured until DIV 30 after which they were fixed with 4% FA, followed by antigen retrieval and immunostaining with NeuN (red) and Ki67 (green) antibody. Ki67 positive neuroblasts were seen in the anti-aggregant  $Tau^{RDA-PP}$  slices (as indicated by arrows) even at DIV 30 but were not seen in the age matched control slices. This shows that the anti-aggregant slices still have the capacity to proliferate and also to differentiate the neuronal progenitors, which is reduced in the controls.

We were interested to see the distribution of Ki67 positive cells in control and anti-aggregant  $Tau^{RDA-PP}$  slices at DIV30. Ki67 positive cells were not visible in the control slices but were visible in the anti-aggregant  $Tau^{RDA-PP}$  slices (Figure 32) in the DG region of the hippocampus, even at later time points of culturing. The Ki67 positive cells enter later into the maturation and differentiation phase and similar results were also reported for human samples (Reif et al., 2006). Ki67 labeling does not differentiate between neural and glial cells, as the marker is expressed before the cells undergo terminal differentiation. Thus Ki67 labeling can only provide a marker for neural progenitor cells.



**6.8.2. Doublecortin (DCX) positive cells are observed in the anti-aggregant Tau<sup>RDΔ-PP</sup> slices at DIV 30 but are absent in the control slices.**

Radial glia-like (RGL) precursor cells exhibit functional GABA(A) receptors and tonic responses to ambient GABA (Song et al., 2012). The first functional synaptic inputs on proliferating neuroblasts appear within four days after birth (Song et al., 2013). Initial GABAergic synaptic inputs are not sufficient to elicit action potentials and are therefore unlikely to be directly involved in information processing. Outputs of new neurons are controlled by glutamatergic synaptic inputs. The glutamatergic synaptic response emerges in 11-14 days old newborn neurons. These glutamatergic synaptic responses mature over the next several weeks, accompanied by increased density of dendritic spines (Chancey et al., 2014, Esposito et al., 2005).

DCX is a brain specific MT associated protein whose exact function is not yet known. It could be a MT stabilizer that is particularly pertinent to migration (Gleeson et al., 1999, Weimer and Anton, 2006, Knoth et al., 2010). DCX positive cells in the DG receive GABAergic inputs into the inner third layer of the granular cell layer (Couillard-Despres et al., 2005, Wang et al., 2005, Filippov et al., 2003). The DCX positive stage of adult hippocampal neurogenesis is considered as the central phase during hippocampal neurogenesis. This phase ranges from a progenitor cell stage to the calretinin positive period which is the maturation period of the neuron. It is in this phase that the cell begins to develop dendrites and axons and establish functional connections (Brandt et al., 2003). New born granular cells in young adult mice develop a single primary dendrite with multiple branches that reaches the molecular layer of the DG within 7 days and exhibits rapid growth between 7 and 17 days, followed by modest growth for at least two months (Sun et al., 2013). Experiments done

with human brain samples, showed that the expression level of DCX is very high in the fetal brain compared to the juvenile healthy tissue and the adult epileptic hippocampus (Knoth et al., 2010).

We were interested to see the distribution of DCX positive cells in the control and the anti-aggregant  $\text{Tau}^{\text{RD}\Delta\text{-PP}}$  slices (Figure 33) at DIV30. Different morphology of DCX positive cells were seen in the CA1 and CA3 regions compared to the DCX positive cells in the DG in the anti-aggregant  $\text{Tau}^{\text{RD}\Delta\text{-PP}}$  slices and no DCX positive cells were seen in the control slices.

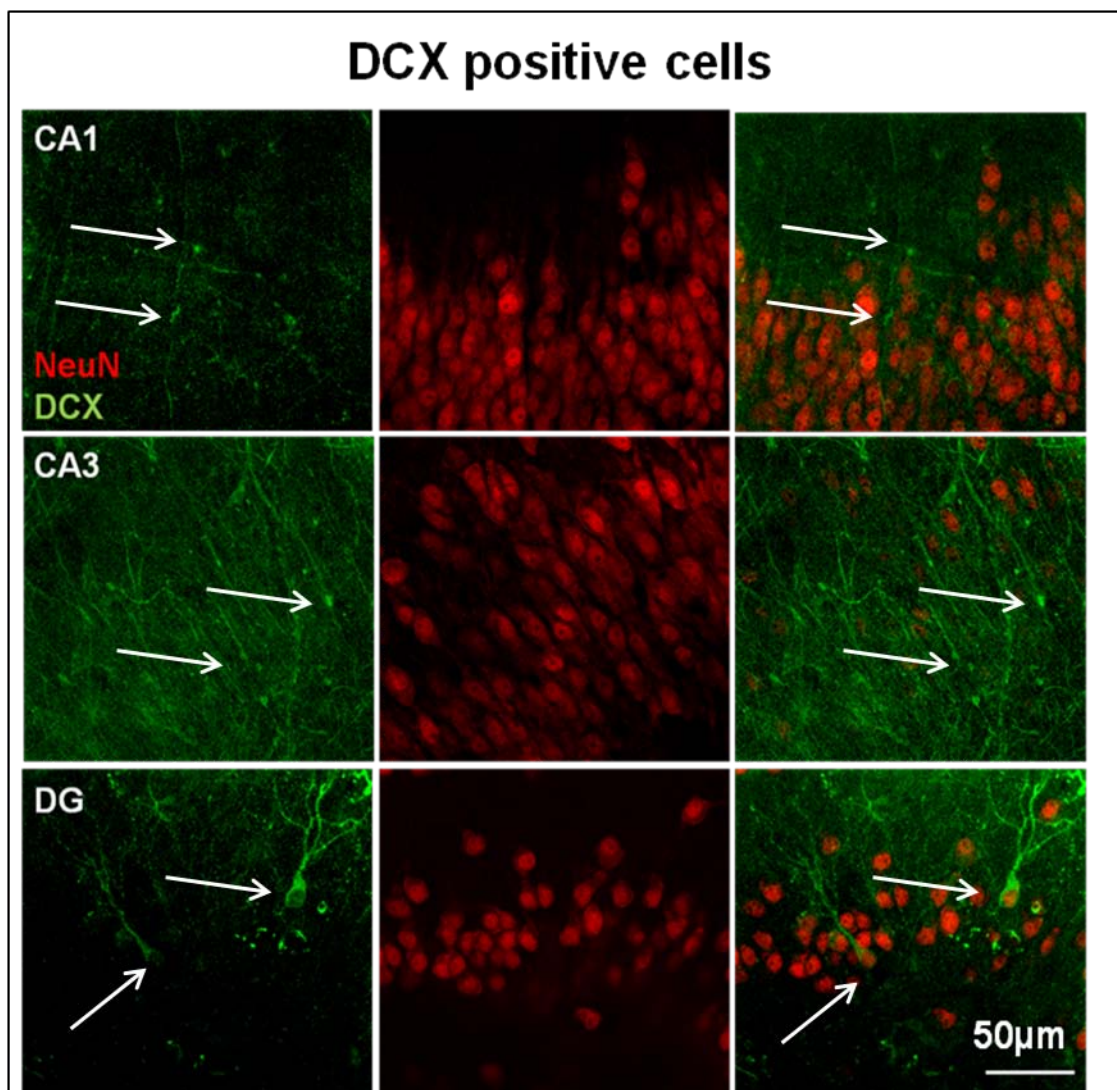


**Figure 33: DCX positive neuroblast cells from the neuronal stem cell lineage were seen in the anti-aggregant  $Tau^{RD\Delta-PP}$  slices at DIV 30.** Organotypic hippocampal slice cultures were prepared from the control and the anti-aggregant  $Tau^{RD\Delta-PP}$  groups. The slices were cultured till DIV 30 after which they were fixed with 4% FA, followed by antigen retrieval and immunostaining with NeuN (red) and DCX (green) antibody. DCX positive neuroblasts were seen in the anti-aggregant  $Tau^{RD\Delta-PP}$  slices even at DIV 30 but were not seen in the age matched control slices. This shows that the anti-aggregant  $Tau^{RD\Delta-PP}$  slices still have the capacity to proliferate and also to differentiate, which is reduced in the control (see also preceding figure).

Morphologically, the type of DCX positive cells in the CA1 and CA3 regions of the hippocampus, is similar to the DCX positive cells seen in the 5 month old human brain sample (Knoth et al., 2010). Similar types of cells are also seen in the DG and hilus region of the hippocampus, in P8 and P19 rats injected with BrdU. The elongated cells have an appearance of migrating

immature neurons with branched leading and single trailing processes (Namba et al., 2005). The morphology depicts a small cell body with a thin long extended process. These cells could be in the middle phase of their maturation before they develop prominent dendrites and axons. Such cells are not seen in the age matched control littermates. Klempin et al (2011) reported that DCX-positive post mitotic cells in the piriform cortex of the adult (2 months old) mice showed enhanced LTP. This could be correlated with enhanced synaptic plasticity (Klempin et al., 2011). We see an enhanced number of DCX positive cells in the CA1 and CA3 region of the hippocampus and speculate that this increase may cause the increase in the LTP of CA1 in anti-aggregant Tau<sup>RDA-PP</sup> mice at 10 month of age (Sydow et al., 2011). It has been reported that DCX positive cells (which were also shown to be non-dividing neurons) signify transient neuronal lineage commitment together with migration and neuronal structural plasticity in the adult hippocampal niche. They indicate synaptic plasticity in the adult piriform cortex layer II that is necessary for rapid adaptations to environmental changes (Klempin et al., 2011). During the first years of life the human DG shows an expression pattern of DCX in numerous combinations with markers of proliferation, maturation and differentiation like in the hippocampal neurogenesis in rodents (Knoth et al., 2010).

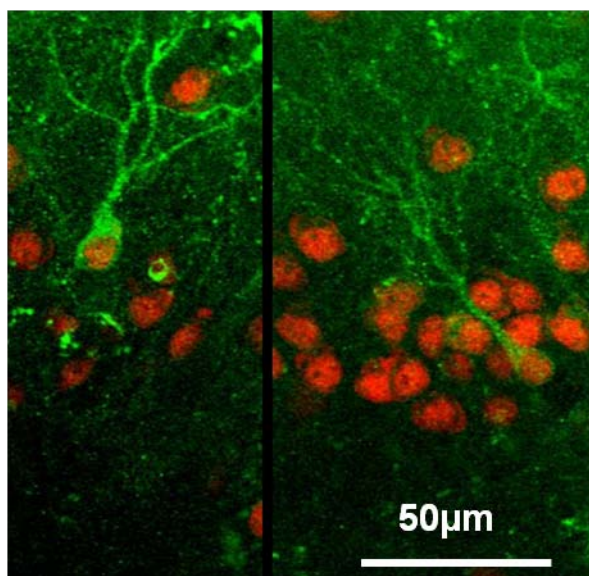


**Figure 34: DCX positive cells co-stained with NeuN in the DG of the anti-aggregant  $Tau^{RD\Delta-PP}$  groups at DIV30.** Organotypic hippocampal slice cultures were prepared from the control and the anti-aggregant  $Tau^{RD\Delta-PP}$  groups. The slices were cultured till DIV 30 after which they are fixed with 4% FA, followed by antigen retrieval and immunostaining with NeuN (red) and DCX (green) antibody. DCX positive neuroblasts were seen in the anti-aggregant  $Tau^{RD\Delta-PP}$  slices even at DIV 30 but were not seen in the age matched control slices. The figure represents the matured neurons in red stained with NeuN and the DCX positive cells stained in green in the DG region of the anti-aggregant  $Tau^{RD\Delta-PP}$  slice. The DCX positive cells were seen with extended dendritic branches. Scale bar indicate 50 $\mu$ m.

DCX positive cells in the DG region of the hippocampus (Figure 34) showed dendritic features of matured neurons even at old age in the anti-aggregant  $Tau^{RD\Delta-PP}$  slices. The phase of DCX expression in rodents is also the phase during which cells are eliminated by cell death (Biebl et al., 2000, Kuhn et al., 2005, Plumpe et al., 2006). In the anti-aggregant  $Tau^{RD\Delta-PP}$  slices there were more DCX positive cells that were also positive for NeuN in the DG region. This clearly indicates that the DCX positive cells get properly matured and integrated into the existing hippocampal circuit.

### 6.9. Tau distribution in organotypic hippocampal slice cultures.

Tau is an axonal protein and it is mainly present in the neurons. Some studies show that the Tau protein is also present in some glial cells like

astrocytes and oligodendrocytes (Tashiro et al., 1997). In mice only the 4 Repeat Tau (4RTau) is expressed in adult neurons, but is not present in the fetal brain which contains only the smallest 3R isoform (0N3R). By contrast, the adult human brain has all the six isoforms of Tau. Full-length Tau is needed for adult neurogenesis and also for neuronal migration (Fuster-Matanzo et al., 2012).

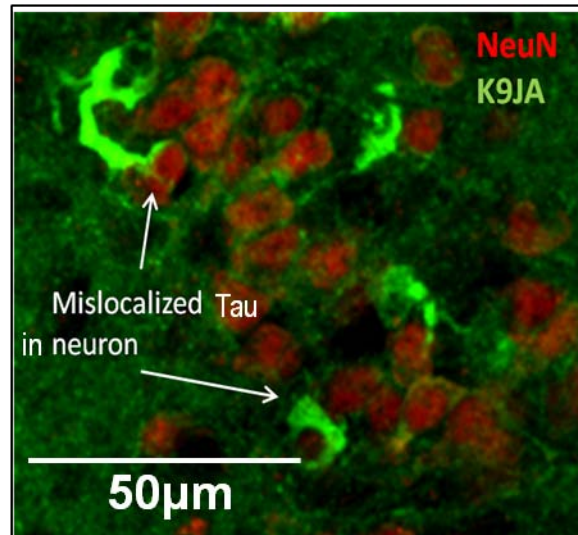


**Figure 35: Mislocalization of Tau into the somato dendritic compartment in slice cultures.** The CA3 region of the hippocampus is depicted here. The matured pyramidal neurons in the CA3 regions are stained with the NeuN antibody in red and Tau is stained green with the polyclonal antibody K9JA, which detects both the endogenous as well as the exogenous human Tau. The arrows indicate some pyramidal neurons which are heavily loaded with Tau in the somato-dendritic compartment.

In the Tau over-expression model, like the pro-aggregant Tau<sup>RDΔ-PP</sup> mouse model, there is a clear mislocalization of Tau into the somato-dendritic compartment of the pyramidal cells. The mislocalization of Tau can also be monitored in the organotypic hippocampal slice cultures prepared from these mice (Figure 35; Figure 36) (Messing et al., 2013).

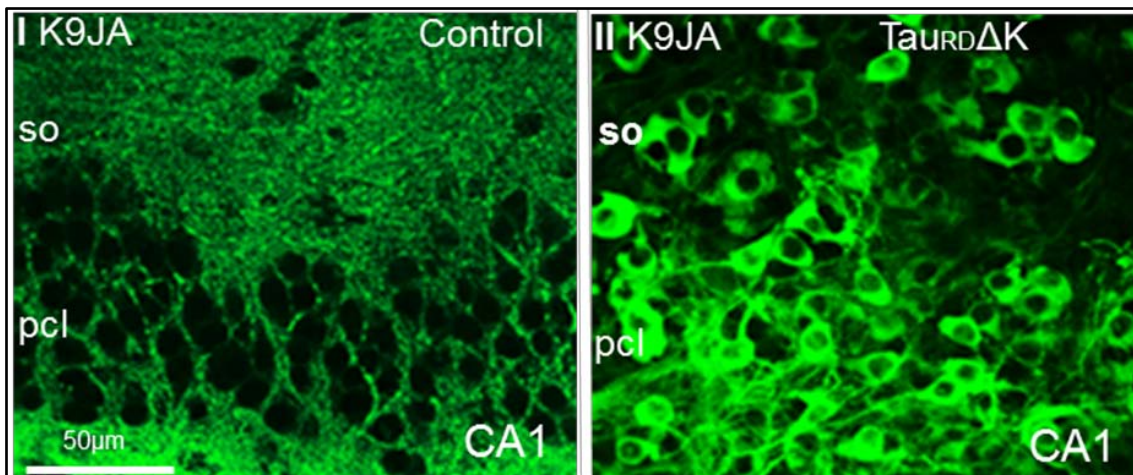


*Figure 36: Mislocalization of Tau in the somato-dendritic compartment of the CA1 pyramidal neurons of pro-aggregant  $\text{Tau}^{\text{RD}\Delta}$  mice as seen in organotypic hippocampal slice cultures. Figure from (Messing et al., 2013)*

In the anti-aggregant  $\text{Tau}^{\text{RD}\Delta\text{-PP}}$  mice, by analogy the pro-aggregant  $\text{Tau}^{\text{RD}\Delta}$  mice, there was over-expression of the human  $\text{Tau}^{\text{RD}\Delta\text{-PP}}$  construct. Therefore we were interested to see whether there was mislocalization of Tau in the anti-aggregant  $\text{Tau}^{\text{RD}\Delta\text{-PP}}$  slices similar to the pro-aggregant  $\text{Tau}^{\text{RD}\Delta}$  slices. It was published earlier from our laboratory that in the anti-aggregant  $\text{Tau}^{\text{RD}\Delta\text{-PP}}$  mice, there was only little mislocalization of Tau in the somato-dendritic compartment starting at 10-12 months of age (Sydow et al., 2011, Mocanu et al., 2008). We therefore wanted to see whether the same results were achieved in the slices prepared from the anti-aggregant  $\text{Tau}^{\text{RD}\Delta\text{-PP}}$  mice.

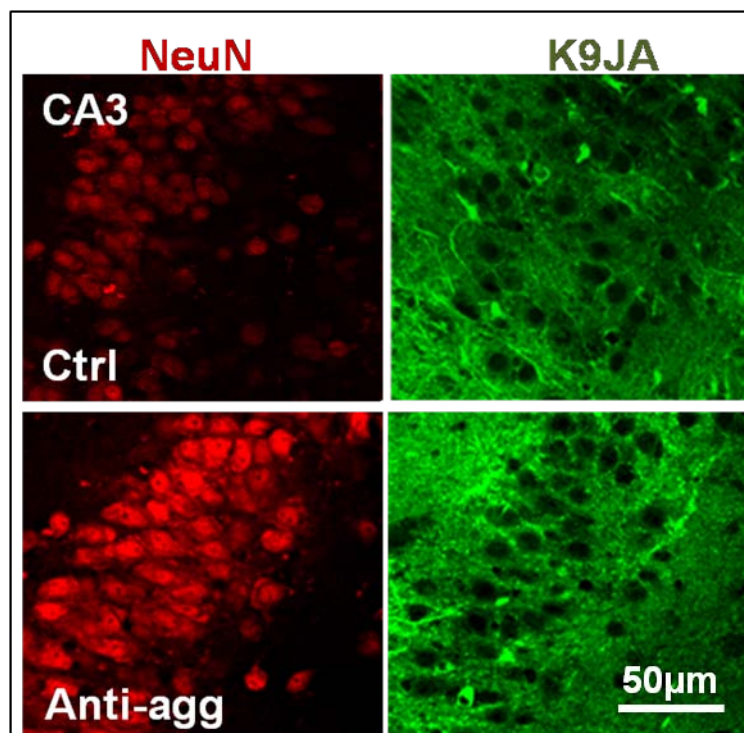


**Figure 37: Distribution of Tau in control and anti-aggregant  $Tau^{RDA-PP}$  slices at DIV 30.** OHSC were stained for total Tau with K9JA antibody and for matured neurons with NeuN antibody at DIV 30. Tau staining is seen in the axons in both the control and the anti-aggregant  $Tau^{RDA-PP}$  slices. The figure shows the CA3 region of the hippocampus with the NeuN staining in red and K9JA staining in green. There was no mislocalization of Tau into the somato-dendritic compartment in controls and anti-aggregant  $Tau^{RDA-PP}$  slices but there was an intense staining of Tau with the polyclonal K9JA antibody, in the anti-aggregant  $Tau^{RDA-PP}$  slices.

There was no mislocalization of Tau in the CA1, CA3 and DG regions of the hippocampus in the anti-aggregant  $Tau^{RDA-PP}$  slices as well as in the control slices even at DIV 30 (Figure 37). Tau was stained only in the axonal compartment. There was an increase in the intensity of the Tau immunostaining in the anti-aggregant  $Tau^{RDA-PP}$  slices, compared to the age-matched control slices. This prompted us to investigate the total Tau levels in the anti-aggregant  $Tau^{RDA-PP}$  and control groups.



### 6.10. Increased endogenous mouse Tau levels are seen in the anti-aggregant Tau<sup>RDA-PP</sup> slices.

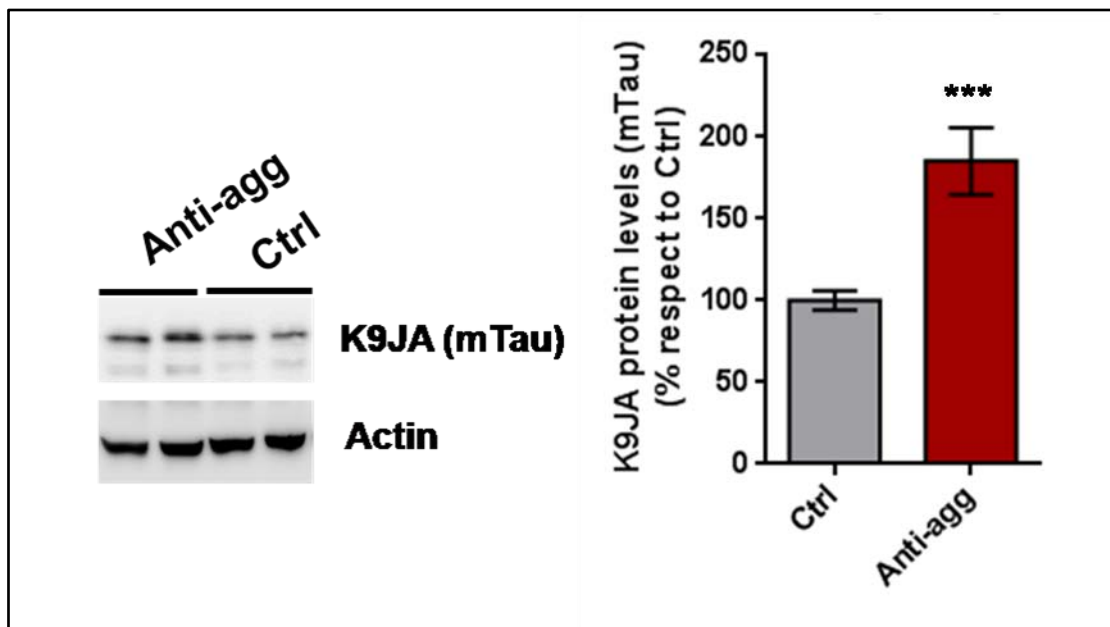


**Figure 38: Levels of the endogenous mouse Tau was increased in the anti-aggregant Tau<sup>RDA-PP</sup> slices at DIV 30.** Organotypic hippocampal slices were cultured until DIV30 and then collected for biochemical analysis. The hippocampal lysates from control and anti-aggregant Tau<sup>RDA-PP</sup> slices were used for western blot analysis. The level of endogenous mouse Tau was analyzed by western blotting against Tau polyclonal K9JA antibody. (A) Western blots of the anti-aggregant Tau<sup>RDA-PP</sup> and control hippocampal lysates against K9JA antibody. (B) Quantification of the western blot of K9JA antibody against the total amount of endogenous mouse Tau levels. There was a significant increase in the endogenous mouse Tau levels ~50% in the anti-aggregant Tau<sup>RDA-PP</sup> groups when compared to the age-matched control groups ( $n=5-6$  slices/animal; 4-5 animals/group Data was analyzed by Student t-test; \*\*\* $p<0.001$ ).

The levels of total mouse Tau (as detected by pan Tau polyclonal antibody K9JA) was analyzed by western blot analysis. The mouse Tau runs approximately 45KDa and the exogenous human Tau<sup>RDA-PP</sup> runs approximately at 12-14KDa (Figure 38). To our surprise there was approximately 50% increase in the endogenous mouse Tau levels in the anti-aggregant Tau<sup>RDA-PP</sup> groups. The expression of the anti-aggregant Tau<sup>RDA-PP</sup> causes an increased expression of the endogenous mouse Tau.

### 6.11. Switch-off experiments with doxycycline.

The expression of the anti-aggregant Tau<sup>RDΔ-PP</sup> in our mouse model is under the control of the tetracycline regulatory system controlled by the administration of DOX (Tet off system). Without DOX the anti-aggregant Tau<sup>RDΔ-PP</sup> gets expressed, with DOX the Tau expression is switched-off. By applying DOX from DIV 15 to DIV30 in our slice model, we were able to switch-off the expression of the anti-aggregant Tau<sup>RDΔ-PP</sup>. This time point (DIV15) in the organotypic hippocampal slice cultures can be compared to the adult period in a living mouse, because it is considered that from DIV15 onwards the slices can be considered to be mature.

Doxycycline has been found to reduce the injury of CNS after reperfusion (Clark et al., 1997). It is also neuroprotective against dopaminergic neuron degradation in the substantia nigra, by suppressing the expression of metalloproteinase (MMP)-3, thereby reducing cell stress. Furthermore, DOX also suppresses the microglial activation through the down regulation of metalloproteinase in the microglia, and also suppression of the production of nitric oxide and TNF $\alpha$ , which are mainly produced by activated microglia (Cho et al., 2009). DOX also inhibits the production of the pro-inflammatory cytokines (Jantzie and Todd, 2010). Interestingly it was shown that DOX also increases neurogenesis in C57Bl/6 mice, by increasing the proliferation of neuronal stem cells, but there was no effect on neuronal differentiation (Sultan et al., 2013).

After switching-off the expression of the anti-aggregant Tau<sup>RDΔ-PP</sup> in organotypic hippocampal slice cultures by DOX, we were interested to see whether there are changes in neurogenesis, the total neuronal number, the rate of proliferation and also in the level of endogenous mouse Tau.

**6.11.1. Switch-off of the anti-aggregant Tau<sup>RDA-PP</sup> by doxycycline causes a reduction of endogenous mouse Tau level in the anti-aggregant Tau<sup>RDA-PP</sup> slices.**

Organotypic hippocampal slice cultures were treated with DOX from DIV15 to DIV30. To check whether the expression of the anti-aggregant Tau<sup>RDA-PP</sup> was switched off during the required time, the organotypic hippocampal slice cultures were checked by their bioluminescence signal. The anti-aggregant Tau<sup>RDA-PP</sup> slices did not show bioluminescence signal after 6-8 hours of DOX application, indicating that the expression of the anti-aggregant Tau<sup>RDA-PP</sup> was switched-off.

The anti aggregant Tau<sup>RDA-PP</sup> slices had 50% more endogenous mouse Tau compared to the age matched control slices (Figure 38). When the expression of the anti-aggregant Tau<sup>RDA-PP</sup> was switched off by DOX, the endogenous mouse Tau was significantly reduced comparable to controls (Figure 39).

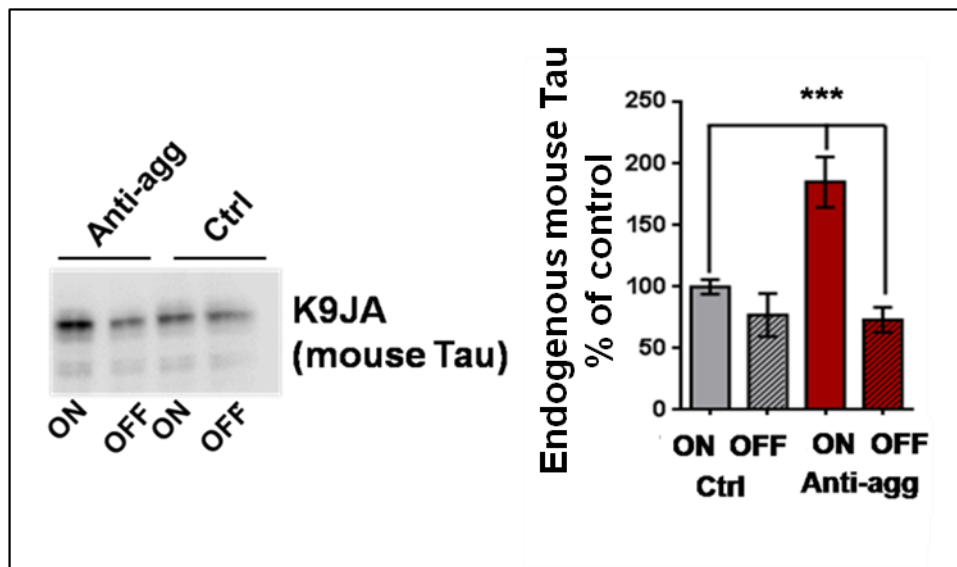


**Figure 39: Endogenous mouse Tau was decreased after application of doxycycline to the anti-aggregant  $Tau^{RD\Delta-PP}$  slices.** Organotypic hippocampal slice cultures were cultured till DIV15. At DIV15, both the control and the anti-aggregant  $Tau^{RD\Delta-PP}$  slices were treated with DOX, to switch-off the expression of the exogenous human  $Tau^{RD\Delta-PP}$ . The hippocampal lysates from the control and the anti-aggregant  $Tau^{RD\Delta-PP}$  slices, with and without DOX treatment were collected at DIV30 and then used for western blot analysis. The total Tau levels for both the endogenous mouse Tau and the exogenous human Tau were analyzed by western blotting against the polyclonal K9JA antibody. (A) Western blot of the anti-aggregant  $Tau^{RD\Delta-PP}$  and control hippocampal lysates, with and without DOX treatment, against K9JA antibody. (B) Quantification of the western blot of K9JA antibody against the total amount of endogenous mouse Tau levels. There was a significant increase in the endogenous mouse Tau levels ~50% in the anti-aggregant  $Tau^{RD\Delta-PP}$  slices when compared to the age-matched control slices. Data was analyzed by Student t-test;  $n=5-6$  slices/animal; 4-5 animals/group; \*\*\* $p<0.001$ .

By contrast there was no such reduction of Tau in the control slices treated with DOX (Figure 39). This clearly shows that the expression of the anti-aggregant  $Tau^{RD\Delta-PP}$  either directly or indirectly has an effect on the expression of the endogenous mouse Tau.

### 6.11.2. Switch-off of the anti-aggregant $\text{Tau}^{\text{RD}\Delta\text{-PP}}$ decreases the total number of neurons in the anti-aggregant $\text{Tau}^{\text{RD}\Delta\text{-PP}}$ slices.

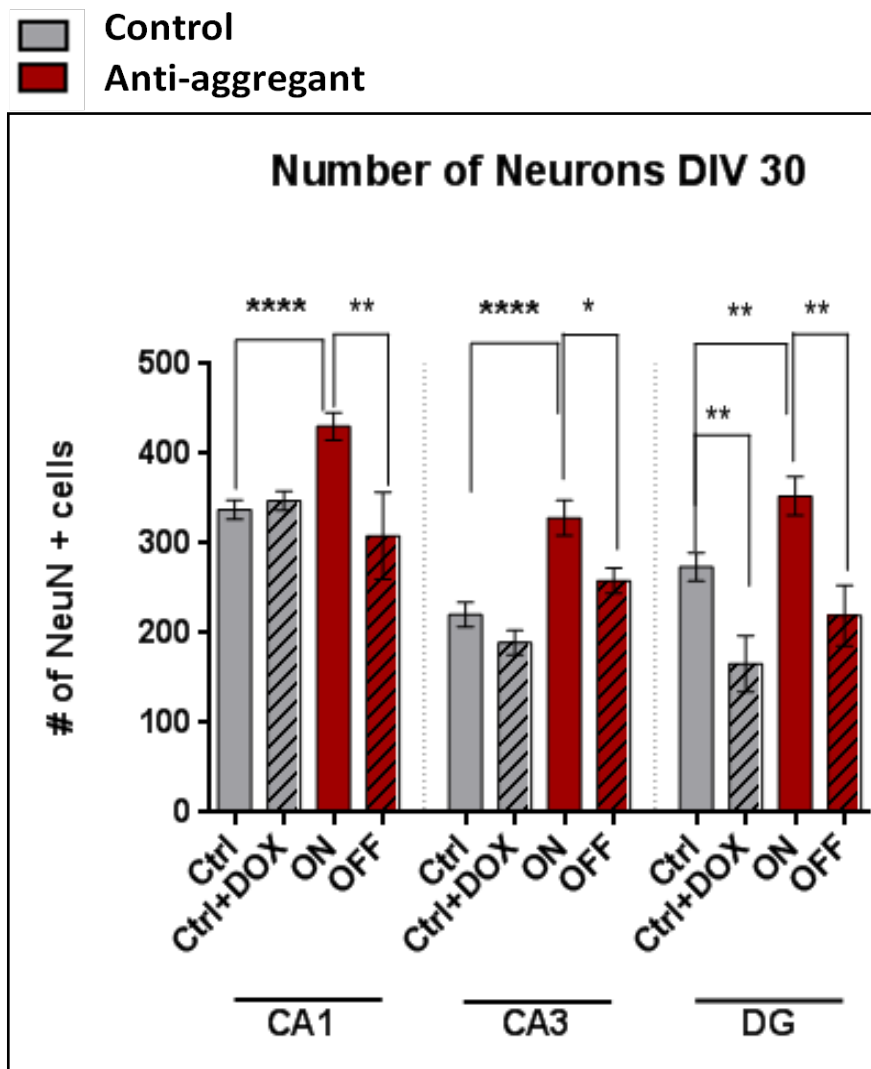


**Figure 40: Doxycycline treatment decreases the total number of neurons in the anti-aggregant  $\text{Tau}^{\text{RD}\Delta\text{-PP}}$  slices.**  $2\mu\text{M}$  DOX was applied to the culture media. Both the control and the anti-aggregant  $\text{Tau}^{\text{RD}\Delta\text{-PP}}$  slices are treated with DOX from DIV 15 to DIV 30 and refreshed during every media change. There was a reduction in the number of NeuN positive mature neurons in the DOX treated anti-aggregant  $\text{Tau}^{\text{RD}\Delta\text{-PP}}$  slices when compared to the untreated anti-aggregant  $\text{Tau}^{\text{RD}\Delta\text{-PP}}$  slices. This increase in the neuronal number observed in the anti-aggregant  $\text{Tau}^{\text{RD}\Delta\text{-PP}}$  slices was caused by the expression of anti-aggregant  $\text{Tau}^{\text{RD}\Delta\text{-PP}}$  protein. Data was analyzed by Student t-test;  $n=30$  slices; 3 slices per animal/group; \* $p<0.05$ ; \*\* $p<0.01$ ; \*\*\*\* $p<0.0001$ .

Next we also investigated whether the switch-off of the anti-aggregant  $\text{Tau}^{\text{RD}\Delta\text{-PP}}$  also causes some changes in the total neuronal number of neurons

(Figure 40). When the expression of the anti-aggregant  $\text{Tau}^{\text{RDA-PP}}$  was switched off from DIV15 to DIV30 of the culturing period, there was a significant reduction in the total number of neurons in the CA1, CA3 and DG regions down to the level of the control groups. There was a partial reduction in the neuronal number in the control groups that were treated with DOX. The combined application of BrdU and DOX was started from DIV15 onwards. With such an experimental set up we were able to analyze the rate of differentiation after switching-off the expression of the anti-aggregant  $\text{Tau}^{\text{RDA-PP}}$ . We speculate that the expression of the anti-aggregant  $\text{Tau}^{\text{RDA-PP}}$  is needed for the differentiation of new born neurons and since the new-born neurons need Tau for their migration and differentiation, there is enhancement in the expression level of the endogenous mouse Tau.

Next we analyzed whether switching-off the expression of the anti-aggregant  $\text{Tau}^{\text{RDA-PP}}$  has an influence on the rate of proliferation (Figure 41) in the anti-aggregant  $\text{Tau}^{\text{RDA-PP}}$  groups.

### **6.11.3. Switch-off of the anti-aggregant $\text{Tau}^{\text{RDA-PP}}$ decreases the total number of BrdU positive cells in the anti-aggregant $\text{Tau}^{\text{RDA-PP}}$ groups.**

When the expression of the anti-aggregant  $\text{Tau}^{\text{RDA-PP}}$  was switched-off from DIV15 to DIV30, there was a reduction in the total number of proliferating cells in the anti-aggregant  $\text{Tau}^{\text{RDA-PP}}$  slices (Figure 41). There was no change in the total number of BrdU positive proliferating cells in the control groups, with the application of DOX.

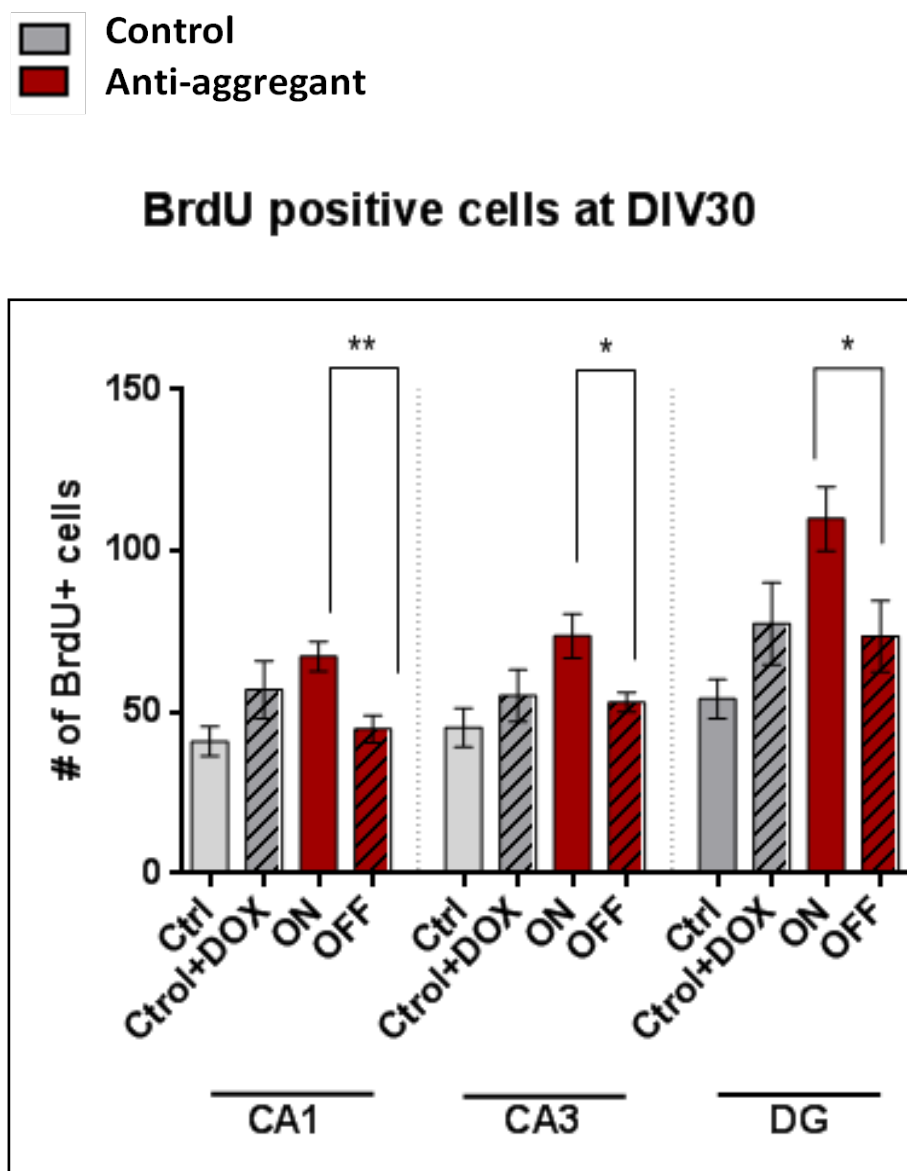


**Figure 41: Doxycycline treatment decreases the total number of BrdU positive cells in the anti-aggregant  $Tau^{RD\Delta-PP}$  slices.**  $2\mu M$  DOX was applied to the culture media. Both the control and the anti-aggregant  $Tau^{RD\Delta-PP}$  slices were treated with DOX from DIV 15 to DIV 30. DOX was refreshed during every media change. There was a reduction in the BrdU positive proliferating cells in the DOX treated anti-aggregant  $Tau^{RD}$  slices when compared to the untreated anti-aggregant  $Tau^{RD\Delta-PP}$  slices. This clearly shows that the increase in proliferation observed in the anti-aggregant  $Tau^{RD\Delta-PP}$  slices was caused by the expression of anti-aggregant  $Tau^{RD\Delta-PP}$  protein. Data was analyzed by Student t-test;  $n=30$  slices; 3 slices per animal/group; \* $p<0.05$ ; \*\* $p<0.01$ .

## 6.12. The rate of proliferation (BrdU positive cells) was increased in the anti-aggregant $\text{Tau}^{\text{RDA-PP}}$ animals at P8.

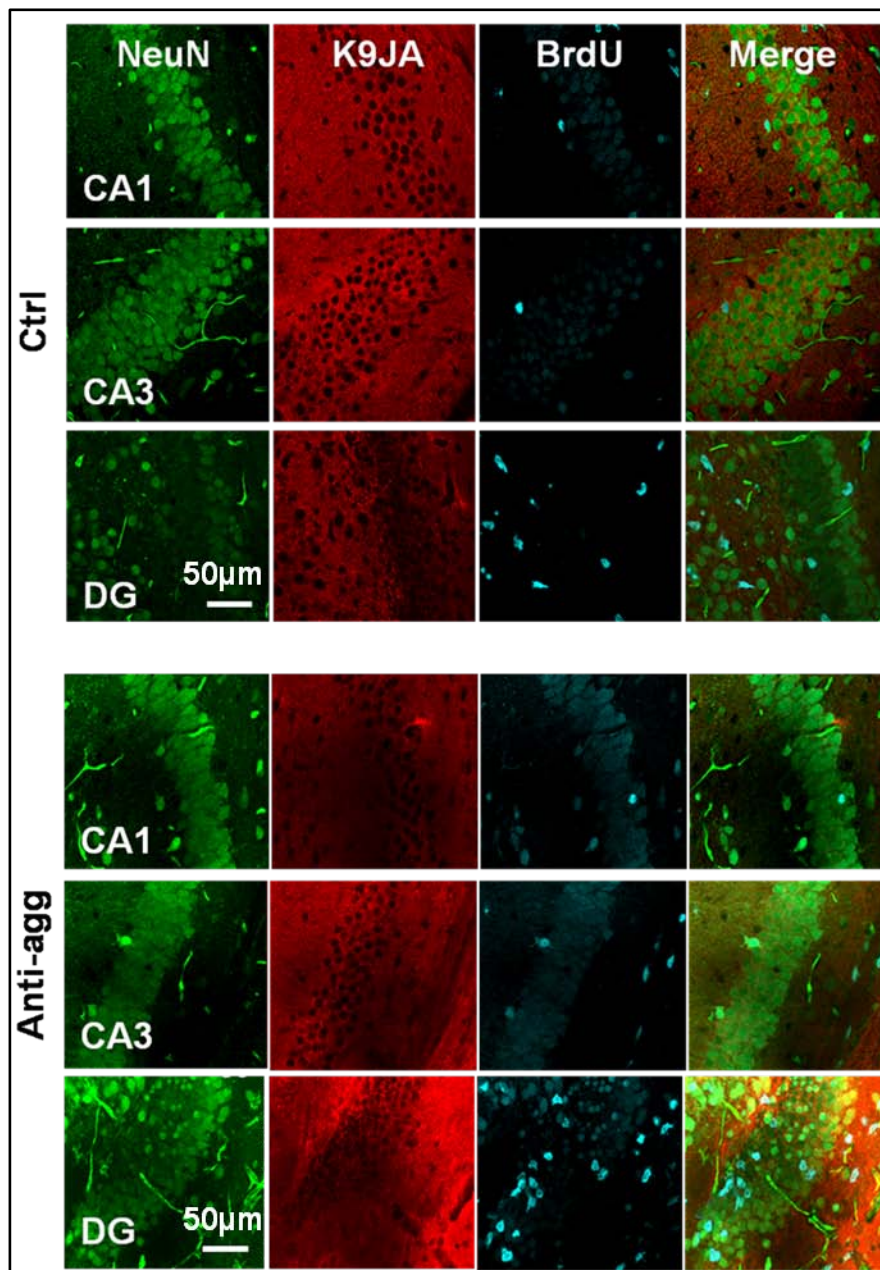
No	Sex	Age	Genotype	Body wt in g	Brain Wt in g	Expression level IVIS
1	F	P8	Anti-agg	5.53	0.284	0.5*10(6)
2	M	P8	Anti-agg	4.33	0.286	6.0*10(8)
3	M	P8	Anti-agg	4.47	0.285	4.0*10(8)
4	F	P8	Anti-agg	5.21	0.315	2.0*10(6)
5	F	P8	Anti-agg	4.36	0.284	5.0*10(8)
6	F	P8	Control	3.91	0.266	-
7	F	P8	Control	5.029	0.299	-
8	F	P8	Control	5.614	0.310	-
9	M	P8	Control	4.260	0.285	

Table 1: List of anti-aggregant  $\text{Tau}^{\text{RDA-PP}}$  and control animals that were used for BrdU injection experiments. The body weights of the animals were taken. Two hours after the BrdU injection animals were killed by cervical decapitation and brains removed. The brain weight was also measured. The expression levels of the anti-aggregant  $\text{Tau}^{\text{RDA-PP}}$  protein in mice were measured by IVIS. Anti-aggregant  $\text{Tau}^{\text{RDA-PP}}$  animal brains that showed bioluminescence signal of more than 10(7) was take for further analysis.

The expression of the anti-aggregant  $\text{Tau}^{\text{RDA-PP}}$  starts from the embryonic stage onwards. Post-natal day 8 animals were used for the preparation of organotypic hippocampal slice cultures. We wanted to see whether the rate of proliferation and post-natal neurogenesis are increased at this age of the animal. The above table (Table 1) shows the list of the control and the anti-aggregant  $\text{Tau}^{\text{RDA-PP}}$  animals that were used for the following experiments. The P8 animals were injected with BrdU and sacrificed after two hours. In the two hour time period BrdU gets incorporated into the proliferating cells and the proliferating cells would not have migrated from the niche/region of proliferation. This way we can analyze the total number of proliferating cells in each group and their localization inside the hippocampus. The brain slices from P8 animals were



immunostained for matured neurons (NeuN in green), BrdU (in blue) and for K9JA (pan Tau) (in red) (Figure 42).



**Figure 42: BrdU incorporation in the hippocampus of P8 control and anti-aggregant *TauRDΔ-PP* animals.** 40µm thick vibratome sections of the brains from the control and the anti-aggregant *TauRDΔ-PP* animals at postnatal day 8 were cut and immunostained with NeuN, K9JA and Anti-BrdU antibodies. BrdU positive cells were also seen in the CA1 and CA3 regions of the hippocampus along with the expected BrdU population in the DG region of the hippocampus. The BrdU positive cells were not co-localized with the pan-Tau antibody K9JA.

BrdU positive cells were seen in all the three regions of the hippocampus, the CA1, CA3 and DG. The presence of BrdU positive cells were not only restricted to the DG region of the hippocampus in this post-natal period of the animals. The importance was that there was an increase in the total number of BrdU positive proliferating cells in the anti-aggregant Tau<sup>RDA-PP</sup> groups, significantly in the CA3 region, compared to the age matched control groups (Figure 42).

### **6.13. Increased proliferation in the anti-aggregant Tau<sup>RDA-PP</sup> animals at P8 in the CA3 region of the hippocampus.**

In the literature it is described that BrdU positive proliferating cells are present only in the DG region of the adult hippocampus and the DG is considered as the niche for neurogenesis. In the case of postnatal hippocampal neurogenesis, the neurogenic niche is present in all three regions the CA1, CA3 and the DG. Studies in the mouse brain, following hypoxic-ischemic injury in fetal and neonatal brain, have shown that there is increased proliferation assessed by BrdU labeling in the CA1, CA3 and the DG regions (Bartley et al., 2005).

To analyze post-natal neurogenesis in the anti-aggregant Tau<sup>RDA-PP</sup> P8 mice (Figure 47) we counted BrdU positive cells by stereology in the different regions of the hippocampus BrdU positive cells were present in CA1, CA3 and DG regions in both the control and the anti-aggregant Tau<sup>RDA-PP</sup> groups. Interestingly (Figure 43) the total number of BrdU positive cells were significantly increased only in the CA3 region of the anti-aggregant Tau<sup>RDA-PP</sup> groups. There was no change in the total number of BrdU positive cells in the DG region of the hippocampus. Apart from the DG the CA1 and CA3 regions of the hippocampus also have the stem cell niche and we speculate that, with

proper intrinsic and extrinsic cues, the stem cell niche in these regions of the hippocampus will also be maintained into adulthood.

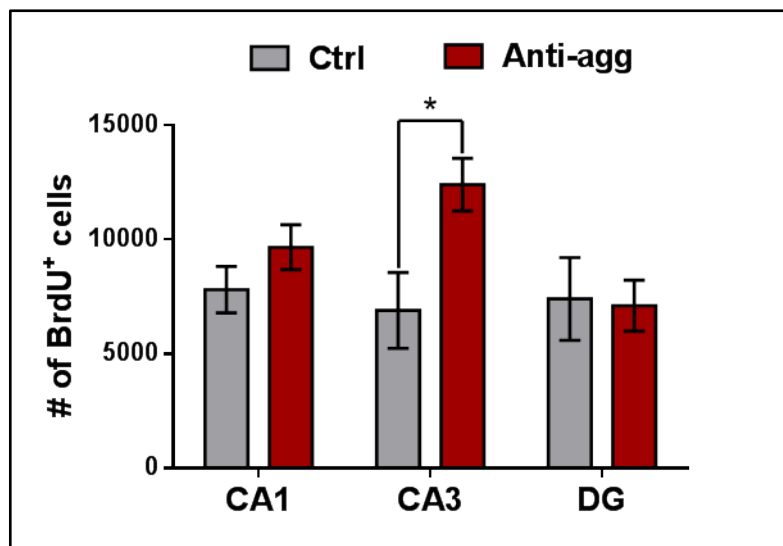


**Figure 43: Increased number of BrdU positive proliferating cells in the CA3 region in the anti-aggregant  $Tau^{RD\Delta-PP}$  groups.** Pups were injected with BrdU and 2 hours later brains were removed. The graph represents total number of BrdU positive cells analyzed by stereology. There was a significant increase in the number of BrdU positive proliferating cells in the CA3 region of the hippocampus of the anti-aggregant  $Tau^{RD\Delta-PP}$  P8 animals. There was no change in the total number of BrdU positive proliferating cells in the CA1 and DG region of the hippocampus, between the control and the anti-aggregant  $Tau^{RD\Delta-PP}$  groups. The graph shows mean  $\pm$  sem ( $n= 3-6$  animals/group). Data was analyzed by student's  $t$ -test. \*  $p<0.05$  compared to the control. Increase in BrdU positive cells was observed in the CA3 region of the anti-aggregant  $Tau^{RD\Delta-PP}$  groups.

The anti-aggregant  $Tau^{RD\Delta-PP}$  apparently stimulates neurogenesis especially in the CA3 region. We also were curious to see whether these new-born cells have Tau in their cell bodies as reports from the literature claim that 3R Tau is needed for the development of new-born neurons. We co-labeled the brain sections with K9JA, a pan-Tau antibody (Figure 42) but did not see any BrdU positive cells, co-labeled with K9JA in their cell bodies.

#### 6.14. Increased hippocampal volume in the anti-aggregant $\text{Tau}^{\text{RD}\Delta\text{-PP}}$ animals at post-natal day 8.

To answer the question whether the increase in proliferation and thus neurogenesis in the CA3 region of the hippocampus of the anti-aggregant  $\text{Tau}^{\text{RD}\Delta\text{-PP}}$  mice had an effect on the total volume of the hippocampus we analyzed the total hippocampal volume by stereology. The volume of individual regions, the CA1, CA3 and DG was measured and the total volume was calculated from these data (Figure 44).

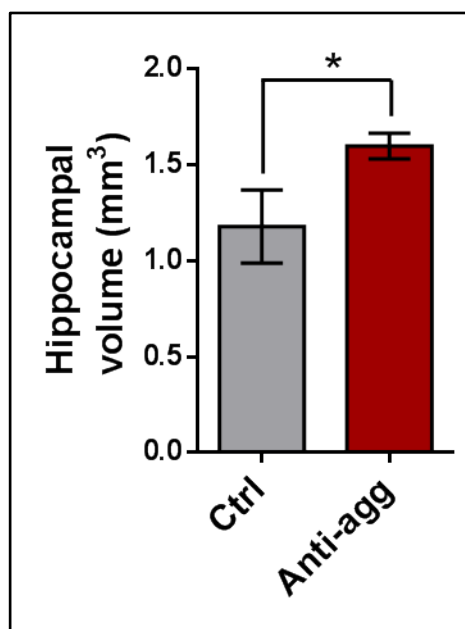


**Figure 44: Total hippocampal volume is increased in the anti-aggregant  $\text{Tau}^{\text{RD}\Delta\text{-PP}}$  pups at P8 as measured by stereology.** The brains of P8 pups were removed and cut into 40 $\mu\text{m}$  thick coronal sections. The sections were stained with NeuN antibody. Hippocampal volume of controls and anti-aggregant  $\text{Tau}^{\text{RD}\Delta\text{-PP}}$  sections were stereologically measured. Data was analyzed by student's *t*-test ( $n=3-6$  animals/group). \* $p < 0.05$ , as compared to control P8 pups. Increased hippocampal volume was observed in the anti-aggregant  $\text{Tau}^{\text{RD}\Delta\text{-PP}}$  mice.

As expected there was a significant increase in the total volume of the hippocampus in the anti-aggregant  $\text{Tau}^{\text{RD}\Delta\text{-PP}}$  groups, compared to the age-matched control littermates at post-natal day 8.

### 6.15. No change in hippocampal volume in the anti-aggregant $\text{Tau}^{\text{RD}\Delta\text{-PP}}$ animals at 17-22 months of age.

Following the experiments done in post-natal day 8 animals, we wanted to analyze whether the increase in the hippocampal volume we see at post-natal day 8, was also persistent in older mice. We selected animals between 17 and 22 months of age from control and anti-aggregant  $\text{Tau}^{\text{RD}\Delta\text{-PP}}$  groups. The brains from these animals were sectioned and stained for NeuN antibody. The volume of the individual regions the CA1, CA3 and DG was analyzed stereologically. The total sum of all these regions of the hippocampus was measured to give the total volume of the hippocampus (Figure 45). The outcome of these experiments was that there was no significant difference in the hippocampal volume between anti-aggregant  $\text{Tau}^{\text{RD}\Delta\text{-PP}}$  and control mice at older age.

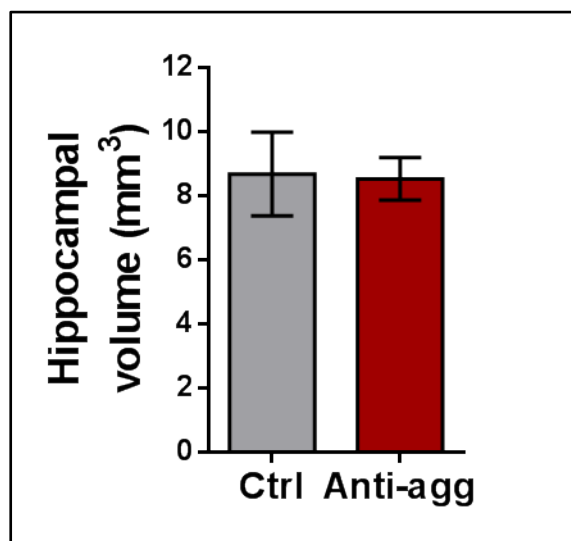


**Figure 45: No difference in the total hippocampal volume at 17-22 months of age.** Brains of 17-22 month control and anti-aggregant  $\text{Tau}^{\text{RD}\Delta\text{-PP}}$  animals were removed. The sections were stained with NeuN antibody. Hippocampal volume of controls and anti-aggregant  $\text{Tau}^{\text{RD}\Delta\text{-PP}}$  sections were stereologically measured. Data was analyzed by student's *t*-test (*n*= 3-6 animals/group).

Next we analyzed whether there was any change in the neuronal number in the anti-aggregant  $\text{Tau}^{\text{RD}\Delta\text{-PP}}$  and control groups at 17-22 months of age. We

speculated that the density of the neurons in the hippocampus was increased in the anti-aggregant  $\text{Tau}^{\text{RDA-PP}}$  groups. This could have been the reason for no change in the hippocampal volume. By stereological analysis we calculated the density of neurons in the CA1, CA3 and the DG regions of the hippocampus (Figure 46). There was a slight increase in the neuronal density in the CA3 region of the hippocampus of the anti-aggregant  $\text{Tau}^{\text{RDA-PP}}$  groups, but there was no significant difference between the groups.

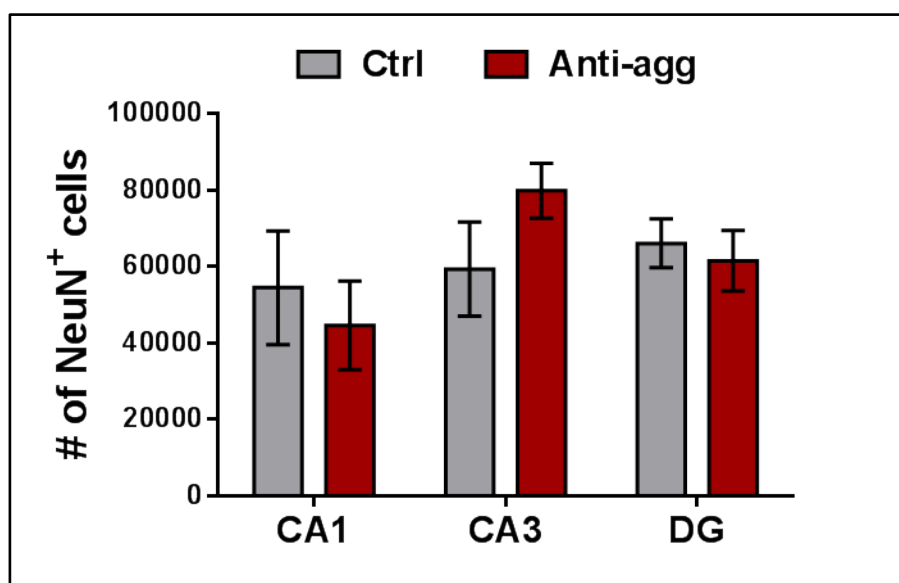


**Figure 46: No significant difference in the density of hippocampal neurons at 17-22 months of age.** Coronal sections of 17-22 month old WT and anti-aggregant  $\text{Tau}^{\text{RDA-PP}}$  mice were stained with NeuN and the total number of neurons was stereologically counted in the CA1, CA3 and DG regions. Results are expressed as a mean  $\pm$  sem  $n=3-4$  animals/group.

### 6.16. Expression of the endogenous mouse Tau was high in the anti-aggregant $\text{Tau}^{\text{RDA-PP}}$ animals at 17-22 months of age.

As the volume and the density of cells in the hippocampus of 17-22 month old mice showed no difference between the anti-aggregant  $\text{Tau}^{\text{RDA-PP}}$  and control mice, we checked for the Tau levels in these animals (Figure 47). Surprisingly, the endogenous mouse Tau levels are 50% higher in the anti-

aggregant  $\text{Tau}^{\text{RD}\Delta\text{-PP}}$  groups compared to the age-matched control littermates. This indicates that the level of Tau is not correlated to the number of neurons.

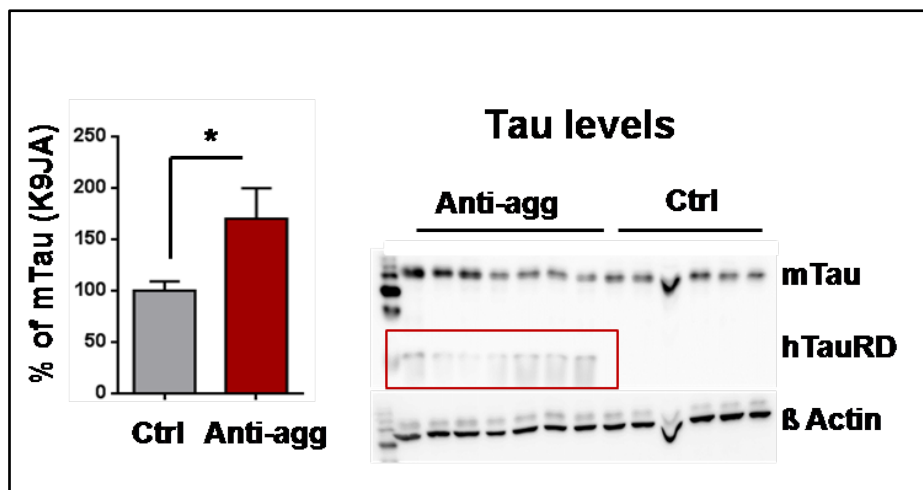


**Figure 47: Increase in the endogenous mouse Tau levels in the anti-aggregant  $\text{Tau}^{\text{RD}\Delta\text{-PP}}$  groups at 17-22 months of age.** 17 month old control and anti-aggregant  $\text{Tau}^{\text{RD}\Delta\text{-PP}}$  animals were sacrificed and brains removed. The hippocampus and cortex were separated. The hippocampal lysates prepared from the control and the anti-aggregant  $\text{Tau}^{\text{RD}\Delta\text{-PP}}$  groups and the total amount of endogenous mouse Tau and exogenous human Tau were determined by western blotting. The expression of the exogenous human Tau protein is clearly visible around 12-14 KDa in the anti-aggregant  $\text{Tau}^{\text{RD}\Delta\text{-PP}}$  groups. The endogenous mouse Tau level was analyzed in the control and the anti-aggregant  $\text{Tau}^{\text{RD}\Delta\text{-PP}}$  groups with K9JA pan-Tau antibody and the levels were normalized against  $\beta$ -actin. There was a significant increase in the level of endogenous mouse Tau in the anti-aggregant  $\text{Tau}^{\text{RD}\Delta\text{-PP}}$  groups compared to the age matched control littermates. Data represents mean  $\pm$  sem ( $n=6-7$  animals/group) and are expressed as a % of control. Data was analyzed by student's  $t$ -test. \* $p<0.05$ , as compared to the control.

### 6.17. GSK3 $\beta$ and its role in neurogenesis.

GSK3 $\beta$  plays an important role in the pathogenesis of AD and it is also actively involved in neurogenesis. GSK3 $\beta$  is an important regulator during proliferation and differentiation of neural progenitor cells (NPC's). Inhibition of GSK3 $\beta$  and also down-regulation of GSK3 $\beta$  increase the number of Tuj1 positive immature neurons. In contrast knocking-out GSK3 $\alpha$ , did not have any effect on neurogenesis. Experiments done by stably expressing the GSK3's by viral vectors, inhibited neural differentiation and helped the NPC to maintain their progenitor activity. Thus GSK3 $\beta$  negatively controls neuronal

differentiation of the progenitor cells (Ahn et al., 2014). Mice expressing constitutively active GSK3 $\beta$ (S9A) showed a reduced number of differentiating cells that are positive for DCX. Constitutively active GSK3 $\beta$ (S9A) mice as well as neuron-specific GSK3 $\beta$  knockout mice (GSK3 $\beta$   $-/-$ ) showed reduced size of the DG and also impaired hippocampal dependent behavioral tasks (Kondratiuk et al., 2013). Increasing activity of GSK3 $\beta$  causes an increase in the proliferation of the new born cells but not the survival or differentiation of the new-born neurons (Hong et al., 2010). Another report says the opposite that activation of GSK3 $\beta$  promotes neuronal differentiation and inactivation of GSK3 $\beta$  promotes neuronal proliferation (Hur and Zhou, 2010).



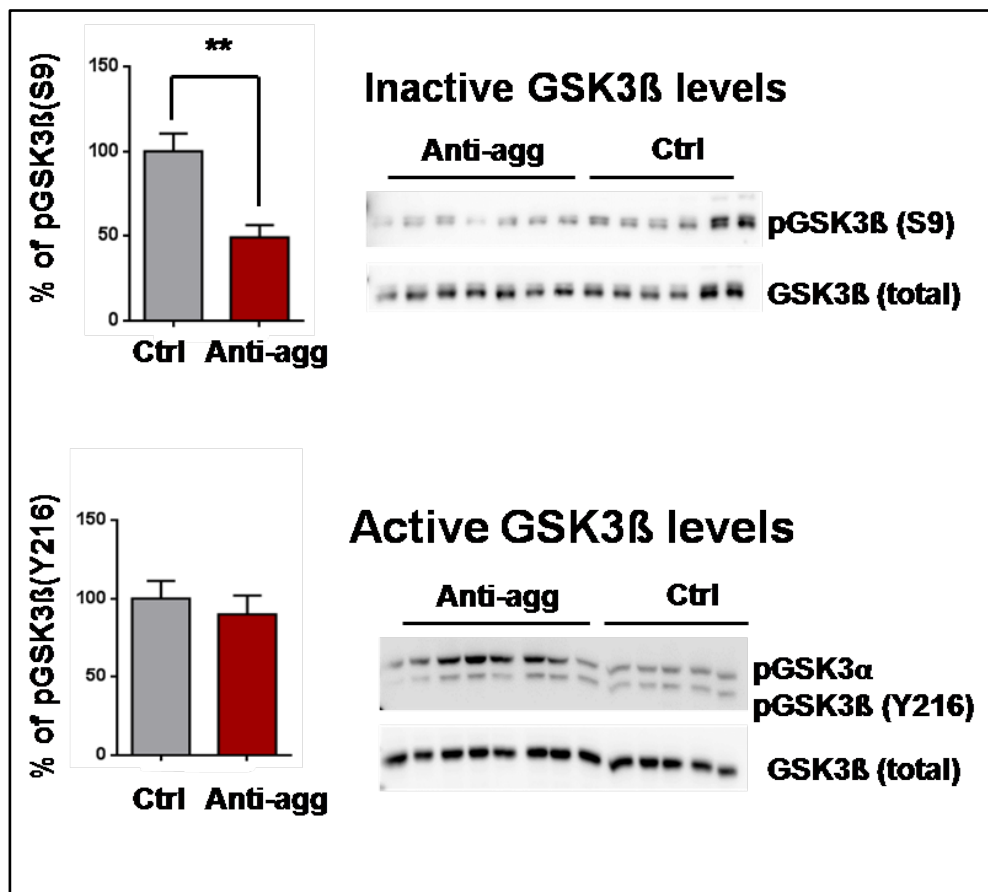


**Figure 48: Decrease in the inactive form of GSK3β levels in the anti-aggregant  $Tau^{RD\Delta-PP}$  groups at 17 month of age.** 17 month old control and anti-aggregant  $Tau^{RD\Delta-PP}$  animals were sacrificed and brains removed. The hippocampus and cortex were separated. Hippocampal lysates were prepared from the control and the anti-aggregant  $Tau^{RD\Delta-PP}$  groups. The total level of GSK3β(S9) (inactive form) was significantly less in the anti-aggregant  $Tau^{RD\Delta-PP}$  slices compared to the age matched control littermates. The total amount of activated form of GSK3β was analyzed with the pGSK3β(Y216) antibody. The levels of the active form of GSK3β remained unchanged between the anti-aggregant  $Tau^{RD\Delta-PP}$  and the control groups. Results are expressed as mean  $\pm$  sem ( $n=6-7$  animals/group) and represent the ratio between each protein and GSK3β (total) obtained by the densitometric analysis of the WB. Data are expressed as % and was analyzed by student's  $t$ -test.  $**p<0.01$  as compared to the controls.

The increase in the total levels of endogenous mouse Tau in the anti-aggregant  $Tau^{RD\Delta-PP}$  groups was seen in OHSC's (Figure 38) and also in 17-22 month old animals (Figure 47). Since GSK3β is an important kinase in regard to Tau, we analyzed the total levels of GSK3β and its active and inactive forms in the control and the anti-aggregant  $Tau^{RD\Delta-PP}$  hippocampal lysates collected from 17-22 months old animals (Figure 48). The total amount of GSK3β in the control

and the anti-aggregant  $\text{Tau}^{\text{RDA-PP}}$  groups was equal, irrespective of the fact that the anti-aggregant  $\text{Tau}^{\text{RDA-PP}}$  group had almost 50% more endogenous mouse Tau. Next we checked for the levels of the active and inactive forms of GSK3 $\beta$  in the control and the anti-aggregant  $\text{Tau}^{\text{RDA-PP}}$  groups (Figure 48). The active form of GSK3 $\beta$  was recognised by its phosphorylation at Y216 site. The levels of the active form of GSK3 $\beta$  were the same between the control and the anti-aggregant  $\text{Tau}^{\text{RDA-PP}}$  groups. The levels of activation of GSK3 $\beta$  was not changed with the over-expression of the anti-aggregant  $\text{Tau}^{\text{RDA-PP}}$  or the high expression levels of the endogenous mouse Tau levels in the anti-aggregant  $\text{Tau}^{\text{RDA-PP}}$  groups. This could support the fact that the active form of GSK3 $\beta$  is needed for the normal differentiation of the newborn neurons because the active GSK3 $\beta$  level was the same between the control and the anti-aggregant  $\text{Tau}^{\text{RDA-PP}}$  groups and also the rate of differentiation. The inactive form of GSK3 $\beta$ , seen by an antibody against S9 phosphorylation, was significantly reduced in the anti-aggregant  $\text{Tau}^{\text{RDA-PP}}$  groups compared to the age matched controls. Surprisingly the active form of GSK3 $\alpha$  was significantly increased in the anti-aggregant  $\text{Tau}^{\text{RDA-PP}}$  groups when analyzed at 17-22 months of age. The cause of this is not known.

### **6.18. Decreased Wnt5a levels in the anti-aggregant $\text{Tau}^{\text{RDA-PP}}$ slices.**

The Wnt signaling pathway is actively involved in neurogenesis and also in neuroinflammation. During pathological conditions like PD and AD there is deregulation of the glial cells which thereby influence the glial-neuron interactions and this can be linked to the deregulation of the Wnt signaling pathway. Approaches to restore the Wnt signaling pathway has shown to be promising in the field of neurodegeneration as well as aging (L'Episcopo et al., 2014). Wnt5a can activate the canonical pathway or inhibit it (Inestrosa et al., 2012). Wnt5a acts via the  $\beta$ -catenin independent pathway comprising the Ror2

receptors. This tyrosine kinase receptor contains a CRD domain and it responds to Wnt5a (Cerpa et al., 2011, Cuitino et al., 2010, Xu et al., 1998, Varela-Nallar et al., 2009). Electrophysiological studies in hippocampal slices of postnatal adult rats (p30) showed that Wnt-7a but not Wnt-5a increases the neurotransmitter release in CA3-CA1 synapses suggesting that Wnt-7a regulates presynaptic function. On the other hand Wnt-5a increases the amplitude but not the frequency of endplate postsynaptic currents (EPSPc) (Cerpa et al., 2008, Cerpa et al., 2010)

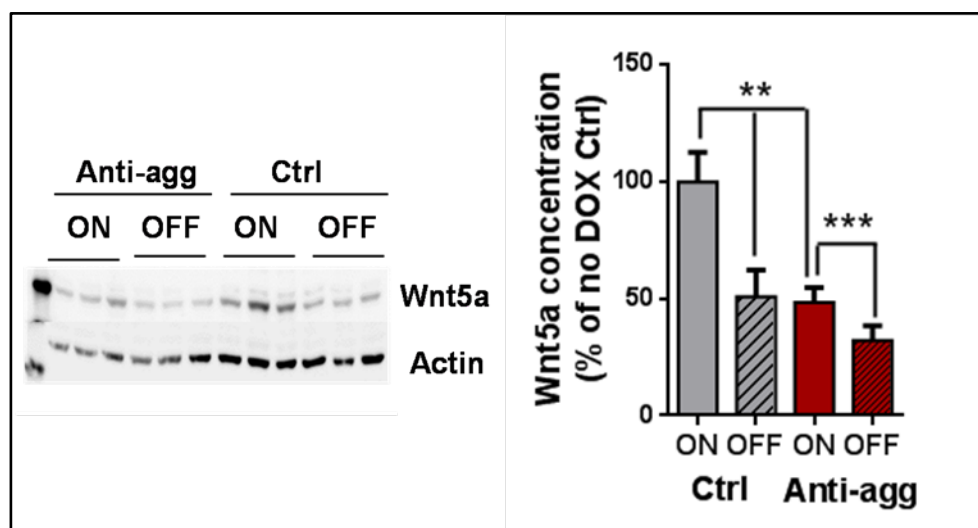


**Figure 49:** The Wnt5a levels were significantly reduced in the anti-aggregant  $Tau^{RD\Delta-PP}$  slices. These levels were further significantly reduced when the expression of anti-aggregant  $Tau^{RD\Delta-PP}$  was switched off by the application of doxycycline. Organotypic hippocampal slice cultures were cultured until DIV15. At DIV15, both control and anti-aggregant  $Tau^{RD\Delta-PP}$  slices were treated with DOX, to switch-off the expression of the exogenous human Tau. The hippocampal lysates from the control and the anti-aggregant  $Tau^{RD\Delta-PP}$  slices, with and without DOX treatment were collected at DIV30 and used for western blot analysis. The total level of Wnt5a in the controls and the anti-aggregant  $Tau^{RD\Delta-PP}$  slices were normalized against actin. The anti-aggregant  $Tau^{RD\Delta-PP}$  groups had almost 50% less amounts of Wnt5a compared to the age matched controls. With the application of DOX there was a further reduction in the Wnt5a levels in the anti-aggregant  $Tau^{RD\Delta-PP}$  slices. There was a significant reduction in the Wnt5a level in the control groups to the level in anti-aggregant  $Tau^{RD\Delta-PP}$  slices with the application of DOX. . Data represents mean  $\pm$  sem ( $n=6-7$  animals/group) and are expressed as a % of control. Data was analyzed by student's  $t$ -test. \*\* $p<0.01$  and \*\*\* $p<0.001$  , as compared to the control.

Because of the relationships of Wnt5a signaling and neurogenesis we checked the level of Wnt5a in control and anti-aggregant Tau<sup>RDΔ-PP</sup> slice cultures at DIV 30 (Figure 49). The slices were cultured as usual till DIV15. From DIV 15 half of the slices from both control and anti-aggregant Tau<sup>RDΔ-PP</sup> groups were treated with DOX to switch off the expression of the human tau and the other half was left as such. Surprisingly there was a 50% reduction in the total amount of Wnt5a protein in the anti-aggregant Tau<sup>RDΔ-PP</sup> slices when compared to the age matched control littermate, in the normal switch-ON conditions. When the expression of the anti-aggregant Tau<sup>RDΔ-PP</sup> was switched off by DOX the level of Wnt5a in the anti-aggregant Tau<sup>RDΔ-PP</sup> groups was further reduced. Treatment of the control slices with DOX reduced the level of Wnt5a to the levels in the anti-aggregant Tau<sup>RDΔ-PP</sup> groups. The effect of DOX on Wnt5a levels in the normal control conditions still remains to be answered. A very interesting finding in our experiments is that the application of DOX to the control slices from middle age (DIV15) to older age of the slice cultures (DIV30) drastically reduces the levels of Wnt5a protein to that of the levels in the anti-aggregant Tau<sup>RDΔ-PP</sup> slices.

## 7. DISCUSSION

The aim of this work was to characterize the organotypic hippocampal slice cultures derived from anti-aggregant  $\text{Tau}^{\text{RD}\Delta\text{-PP}}$  mouse model expressing the mutant  $\text{Tau}^{\text{RD}\Delta\text{K280PP}}$ . Previous histopathological and biochemical analysis had revealed the following (Mocanu et al., 2008, Sydow et al., 2011):

- (1) The anti-aggregant  $\text{Tau}^{\text{RD}\Delta\text{-PP}}$  mice showed no aggregated Tau in the sarkosyl insoluble pellet at 3 and 12 months of age.
- (2) No phosphorylation at the KXGS motifs in the anti-aggregation  $\text{Tau}^{\text{RD}\Delta\text{-PP}}$  mutant at 3 months of age, but low levels at 12 months of age.
- (3) No NFT's were observed in the anti-aggregant  $\text{Tau}^{\text{RD}\Delta\text{-PP}}$  mice at 3 months and 22 months of age.
- (4) No learning and memory deficits were observed in the anti-aggregant  $\text{Tau}^{\text{RD}\Delta\text{-PP}}$  mice.
- (5) In acute slices from 10 month old anti-aggregant  $\text{Tau}^{\text{RD}\Delta\text{-PP}}$  mice, posttetanic potentiation (PTP) was significantly reduced, but LTP was unaltered in the mossy fiber pathway (CA3 LTP).
- (6) Increase in theta burst induced LTP in CA1 pyramidal neurons was observed in the anti-aggregant  $\text{Tau}^{\text{RD}\Delta\text{-PP}}$  acute slices prepared from 10 month old mice.

### **7.1. Expression of the anti-aggregant $\text{Tau}^{\text{RD}\Delta\text{-PP}}$ in organotypic hippocampal slice cultures causes enhanced proliferation and differentiation of neuronal stem cells into neurons.**

Active adult neurogenesis has been shown in almost all mammalian species examined so far (Lledo et al., 2006, Lledo and Gheusi, 2006, Ming and

Song, 2005). Adult neurogenesis in the sub ventricular zone (SVZ) results in the formation of newborn neurons that migrate to the olfactory bulb or striatum (Ernst et al., 2014) and differentiate mostly into interneurons. The adult neurogenesis in the sub granular zone (SGZ) of the hippocampal DG results in newborn granule cells that integrate locally (Ming and Song, 2011, Kempermann and Gage, 1998). We investigated adult hippocampal neurogenesis in the anti-aggregant Tau<sup>RDA-PP</sup> slices by examining the rate of neuronal stem cells (NSC's) proliferation in OHSC's from DIV15 to DIV30. There was a 50% increase in the rate of proliferation, as assessed by BrdU incorporation assay (Figure 29) in the anti-aggregant Tau<sup>RDA-PP</sup> slices compared to controls. The enhanced proliferation was followed by enhanced neuronal differentiation (Figure 31). Almost 80% of the proliferating cells were positive for NeuN, a marker for matured neurons. This clearly indicates that the expression of the anti-aggregant Tau<sup>RDA-PP</sup> enhances the rate of proliferation and differentiation in the hippocampus. To pin down the exact role of the anti-aggregant Tau<sup>RDA-PP</sup> in NSC's proliferation and differentiation, we switched off the expression of the exogenous anti-aggregant Tau<sup>RDA-PP</sup> by the application of DOX. Interestingly when the expression was switched off from DIV15 to DIV30, there was a reduction in the rate of proliferation (Figure 41) as well as a reduction in the total number of matured neurons (Figure 40) comparable to levels in the control slices. This suggests that the effects on proliferation and differentiation in the anti-aggregant Tau<sup>RDA-PP</sup> slices are caused directly by the expression of the mutant protein.

We further investigated the differentiation of NSC's into non-neuronal cell types like astrocytes and microglia in the anti-aggregant Tau<sup>RDA-PP</sup> slices and found, that there were no cells positive for GFAP or Iba1, indicating that there was no differentiation of the proliferating cells into astrocytes or microglia (data

not shown). Additionally there was a decrease in total number of microglia (Figure 22) and no significant change in the total amount of astrocytes (Figure 25). All this data indicates that the adult hippocampal proliferation leads mainly to the generation of neurons. Previous studies have reported a decrease in adult hippocampal neurogenesis with increased age in rodents (Klempin and Kempermann, 2007, Kuhn et al., 1996) and also in humans (Knoth et al., 2010). We observed in OHSC's at DIV30, still cells positive for the proliferation marker Ki67 (Figure 32) and the neuronal differentiation marker DCX (Figure 33) in the anti-aggregant  $\text{Tau}^{\text{RD}\Delta\text{-PP}}$  slices, but the occurrence of such cells were greatly reduced in the age-matched control slices.

Thus the expression of the anti-aggregant  $\text{Tau}^{\text{RD}\Delta\text{-PP}}$  enhances adult hippocampal neurogenesis and counteracts the decrease of neurogenesis in old age.

## **7.2. Expression of anti-aggregant $\text{Tau}^{\text{RD}\Delta\text{-PP}}$ decreases microglia number, but not astrocytes.**

Brain microglia come from both infiltrating blood monocytes and resident progenitor cells. In OHSC's there is evidence for endogenous proliferation of microglia. When challenged with specific stimuli mimicking inflammation, microglia in hippocampal slice cultures respond with a pronounced proliferation (Bernardino et al., 2008, Lossi et al., 2009). Microglia are abundant in the dentate gyrus (DG) and probably mediate the inflammation-induced reduction in neurogenesis. Interestingly, with the expression of the anti-aggregant  $\text{Tau}^{\text{RD}\Delta\text{-PP}}$  there was a dramatic reduction in the total number of microglia (Figure 22). Apart from this there were morphological differences between microglia from control and anti-aggregant  $\text{Tau}^{\text{RD}\Delta\text{-PP}}$  slices (Figure 21). They were mostly found in the resting form in the anti-aggregant  $\text{Tau}^{\text{RD}\Delta\text{-PP}}$  slices (Figure 21), compared to the controls where they were in the

phagocytic form. Co-cultures of decreasing neural progenitor/glia ratio showed that microglia but not astroglia reduced the number of progenitor cells. Microglia inhibits the proliferation of neural stem/progenitor cells despite the absence of inflammatory stimuli (Paolicelli et al., 2011, Paolicelli and Gross, 2011). Our results show that the reduction of microglia and the resting state morphology support hippocampal neurogenesis in the anti-aggregant Tau<sup>RDA-PP</sup> slices. It has been demonstrated that the NPCs regulate microglia function in vitro by the secretion of growth factors (Mosher et al., 2012) and in turn resting microglia may be involved in the regulation of physiological mechanisms such as dendritic spine maintenance (Paolicelli et al., 2011, Paolicelli and Gross, 2011). Microglia may modulate the pre- and postsynaptic structure of synapses on adult born neurons including synaptic transmission (Ekdahl, 2012). The expression of the anti-aggregant Tau<sup>RDA-PP</sup> reduces the total number of microglia and this is inversely correlated with the number of stem/progenitor cells in the hippocampus.

Next we studied the level of astrocytes in the anti-aggregant Tau<sup>RDA-PP</sup> slices. It has been shown that stem cells in the neurogenic zone have astroglial properties and are mostly destined to be astrocytes (Morrens et al., 2012). In both neurogenic and non-neurogenic regions of the brain there are astrocytes and there are non-neurogenic astrocytes in the neurogenic niche (Wang and Bordey, 2008). The radial-glia like (RGL) cells in the hilus and the granular layer of the DG generates neurons in the early post-natal stages (P5-P12) (Namba et al., 2005). Studies with nestin-GFP mice have revealed that proliferating progenitors are converted from astrocytic to neuronal cells (Filippov et al., 2003, Kronenberg et al., 2003, Fukuda et al., 2003). We first looked for the morphology of astrocytes in the OHSC's at DIV30 from the control and the anti-aggregant Tau<sup>RDA-PP</sup> slices (Figure 23; Figure 24). In the anti-aggregant Tau<sup>RDA-PP</sup>



slices the astrocytes are more of the RGL morphology in the DG, CA1 and CA3 regions, whilst in the control slices the astrocytes are star shaped. This indicates that in the anti-aggregant Tau<sup>RDA-PP</sup> slices the stem cell pool is still maintained even though there is pronounced proliferation and differentiation of the hippocampal stem cells. Since all of these observations have been made on DIV30 slices we conclude, that the residing astrocytes in the anti-aggregant Tau<sup>RDA-PP</sup> slices still maintain their RGL property. This holds even at late stages of the slice cultures where the control groups have star shaped astrocytes. The GFAP level determined by western blotting in the hippocampal lysates from the control and the anti-aggregant Tau<sup>RDA-PP</sup> slices showed no significant changes (Figure 25). These results support the view that the amount of microglia but not of astroglia is inversely correlated with neurogenesis (Gebara et al., 2013).

### **7.3. Expression of the anti-aggregant Tau<sup>RDA-PP</sup> increases the rate of hippocampal stem cell proliferation and the total hippocampal volume in young mice.**

Considering the increase in proliferation and also in the total number of neurons in the anti-aggregant Tau<sup>RDA-PP</sup> slices, we were interested to analyze, whether the changes in proliferation and differentiation we observed in DIV30 slices, are restricted to the adult stages of slices or whether they are also seen in post natal animals. Therefore the anti-aggregant Tau<sup>RDA-PP</sup> mice were analyzed for postnatal hippocampal neurogenesis at day 8 after birth. The post-natal neurogenesis, a transition state between embryonic and adult neurogenesis in the hippocampus, is an important issue because it provides information about how neurogenesis continues in the hippocampus (Namba et al., 2005). There was an increase in the total number of BrdU positive cells at P8 in the anti-aggregant Tau<sup>RDA-PP</sup> pups (Figure 43) particularly in the CA3 region of the

hippocampus but not in DG and CA1 region. Previous reports have shown, that during post-natal stages of brain development the hilus region of the hippocampus shows more neurogenesis (Altman and Bayer, 1990) and more than half of the granule cells are born post-natally (P5-P14) (Angevine, 1965, Schlessinger et al., 1975, Bayer, 1980). One of our striking findings was, that with the expression of the anti-aggregant Tau<sup>RDA-PP</sup> there was an enhanced proliferation in the CA3 region, which has not been reported earlier. Thus it is interesting to note, that the total hippocampal volume in the anti-aggregant Tau<sup>RDA-PP</sup> groups was also significantly increased (Figure 44). This is a surprising finding, that the anti-aggregant Tau<sup>RDA-PP</sup> can enhance hippocampal neurogenesis especially in the CA3 region and also increase the total volume of the hippocampus even at earlier stages of development.

#### **7.4. Anti-aggregant Tau<sup>RDA-PP</sup> enhances the expression of the endogenous mouse Tau.**

Absence of Tau results in retarded neurogenesis and neuronal differentiation. On the contrary overexpression of Tau which can undergo pathological modifications that provoke lysosomal aberrations may cause neurodegeneration (Lim et al., 2001). The expression of the anti-aggregant Tau<sup>RDA-PP</sup> caused a 50% increase of endogenous mouse Tau in OHSC's (Figure 38). When the expression of the exogenous anti-aggregant Tau<sup>RDA-PP</sup> was switched-off in OHSC's by the application of DOX, the levels of the endogenous mouse Tau also got reduced (Figure 39) to that of the control groups. Additionally there was a reduction in the total number of BrdU positive proliferating cells (Figure 41) and a reduction in the total number of neurons (Figure 40). From the switch-off experiments it became clear that the expression of the anti-aggregant Tau<sup>RDA-PP</sup> influences either directly or indirectly the levels

of the endogenous mouse Tau. So the question arises whether having more Tau is beneficial?

It has been reported previously, that in mice overexpression of the full length human Tau with P301L mutation (under the neuron specific Thy1 promoter) at 2-3 months of age (before the occurrence of pathology), showed an increase of endogenous mouse Tau. These mice had enhanced LTP in the DG region of the hippocampus which correlates to improved memory formation without affecting hippocampal neurogenesis (Boekhoorn et al., 2006). This study suggests that increased concentration of endogenous Tau protein improves the cognitive performance in these young mice. In another study, transgenic mice expressing the p25 fragment of calpain-cleaved p35 (activator of CDK5), which is found in the brain of AD patients, showed no signs of neurodegeneration. Instead there was an increased expression of the endogenous mouse Tau, which improved reversal learning and altered fear conditioning in mice (Angelo et al., 2003). These studies can be compared to our anti-aggregant Tau<sup>RDΔ-PP</sup> mice that also showed elevated endogenous mouse Tau, slight hyper-phosphorylation of Tau or mislocalization and no motor neuron deficits or learning impairments (Mocanu et al., 2008, Sydow et al., 2011). Surprisingly in our mice there was a positive effect on hippocampal neurogenesis and the hippocampal CA1 LTP was greatly enhanced (Mocanu et al., 2008). What is the significance of the enhanced expression of the mouse Tau in the anti-aggregant Tau<sup>RDΔ-PP</sup> mice? Does the increase of the endogenous mouse Tau modulate the differentiation and maturation of the newly born neurons?

Does the expression of the anti-aggregant Tau<sup>RDΔ-PP</sup> causes an increase in proliferation of hippocampal stem cells? Do these new-born cells require more endogenous mouse Tau for their differentiation into mature neurons? Is this the

reason for the elevation of the endogenous mouse Tau? Further support for this hypothesis comes from studies which have emphasized the importance of Tau protein in this context. Increased microtubule mass and enhanced microtubule stability were seen when rat fibroblasts were microinjected with Tau (Drubin and Kirschner, 1986) or when the fibroblasts were engineered to over-express Tau (Kanai et al., 1989). Similar Tau-overexpression experiments were done in Sf9 cells (Knops et al., 1991, Biernat and Mandelkow, 1999), PC12 cells (Esmaeli-Azad et al., 1994) and also primary neurons (Caceres and Kosik, 1990), all emphasizing the role of Tau in axogenesis and neurite outgrowth. Previous studies have shown that embryonic hippocampal cultures from Tau-KO mice show a significant delay in maturation in respect to axonal and neuronal outgrowth (Dawson et al., 2001) emphasizing the important role of Tau. This delay was rescued and showed normal axonal growth and neuronal maturation when the TKO mice were crossed with transgenic mice expressing all the six isoforms of human Tau so that the expression of the total human Tau was five times higher than the endogenous mouse Tau in WT mice (Dawson et al., 2001). This data argues that Tau is needed for the normal differentiation and maturation of neurons.

Apart from studies done on TKO mice, an increased proliferation of neural precursor cells has also been reported in the hippocampus of AD patient (Jin et al., 2004, Nagy et al., 1997). However these immature neurons are not able to mature as shown by the absence of markers such as NeuN and MAP2 was not observed (Jin et al., 2004, Li et al., 2008). There was a lower number of HuC/D positive post mitotic neurons (matured neurons) in the DG of AD patients above 80 years of age in Braak stages V-VI (Ekonomou et al., 2014). Could this phenomenon in AD be reverted when the expression of Tau is modulated without inducing some toxic effects? In advanced AD,

corresponding to late Braak stages there is hippocampal degeneration (Braak and Braak, 1991) and functional deficits in the DG (Ohm, 2007).

A contrary view has emerged from Tau reduction studies in different hAPP transgenic mice (Roberson et al., 2007, Roberson et al., 2011, Ittner et al., 2010), showing that lowering of Tau protein is beneficial and prevents the progression of pathology in these animal models. Imbalance in the different Tau isoforms and an increase in the total Tau levels were seen in cortex and striatum lysates from Huntington's disease patients (Fernandez-Nogales et al., 2014). We therefore checked for level of endogenous mouse Tau in 17-22 month old adult mice from control and anti-aggregant Tau<sup>RDA-PP</sup> groups. In anti-aggregant Tau<sup>RDA-PP</sup> mice, even though there was overexpression of a mutated human Tau<sup>RDA-PP</sup>, there was no sign of neurodegeneration or neuroinflammation. Surprisingly we saw an increase in endogenous mouse Tau level of about 50% (Figure 47) but no significant change in neuronal number (Figure 46) in the hippocampus and total hippocampal volume (Figure 45).

## 7.5. GSK3 $\beta$ and its role in neurogenesis.

Since we observed an increase in the endogenous mouse Tau level in anti-aggregant Tau<sup>RDA-PP</sup> slices and in adult animals, we further investigated the level of GSK3 $\beta$  in anti-aggregant Tau<sup>RDA-PP</sup> and control adult animals. GSK3 $\beta$  is a well known Tau kinase (Hong et al., 2010) and an important regulator during proliferation and differentiation of neural progenitor cells (NPC's) (Ahn et al., 2014). GSK3 $\beta$  has a high basal activity in resting cells and is inactivated by phosphorylation by upstream kinases.

Increased activation of GSK3 $\beta$  is a common feature in Familial Alzheimer disease (FAD) as well as Sporadic Alzheimer disease (SAD) (Avila et al., 2010) and also in other Tauopathies (Engel et al., 2006). Active GSK3 $\beta$  is a prominent Tau kinase in newborn neurons (Hong et al., 2010). Activation of GSK3 $\beta$

promotes neuronal differentiation and inactivation of GSK3 $\beta$  promotes neuronal proliferation (Hur and Zhou, 2010). Thus the level of GSK3 $\beta$  (active and inactive) has to be closely regulated. To investigate the molecular mechanism mediated by the expression of the anti-aggregant Tau<sup>RDA-PP</sup>, we checked for active and inactive levels of GSK3 $\beta$  in the hippocampal lysates. Active GSK3 $\beta$  was similar in the control and the anti-aggregant Tau<sup>RDA-PP</sup> groups (Figure 48) and the same was true for total GSK3 $\beta$ .

Interestingly there was a significant decrease in the level of the inactive form of GSK3 $\beta$  (Figure 48). It has been reported that inhibition of GSK3 $\beta$  and also down-regulation of GSK3 $\beta$  increased the number of Tuj1 positive immature neurons. This could be the reason for the enhanced neuronal differentiation seen in the anti-aggregant Tau<sup>RDA-PP</sup> animals. GSK3 $\beta$  regulates the activity of several MAPs and may therefore be involved in the overall microtubule dynamics (Zhou and Snider, 2005). Mice expressing constitutively active GSK3 $\beta$ (S9A) showed reduced number of differentiating cells that are positive for DCX. Constitutively active GSK3 $\beta$ (S9A) mice as well as neuron-specific GSK3 $\beta$  knockout mice (GSK3 $\beta$  -/-) showed a reduced size of the DG and also impaired hippocampal dependent behavioral tasks (Kondratiuk et al., 2013). Thus the level of active and inactive forms of GSK3 $\beta$  should be tightly regulated to enhance neuronal differentiation and proliferation. The active level of GSK3 $\beta$  may be required for the physiological phosphorylation of Tau, even though there was a 50% increase in endogenous mouse Tau.

Surprisingly there was an increase in GSK3 $\alpha$  expression in anti-aggregant Tau<sup>RDA-PP</sup> animals at 17-22 month of age. Knock-out of GSK3 $\alpha$  did not have any effect, when tested on NPC's (Ahn et al., 2014). However there are not many studies dealing with the overexpression of GSK3 $\alpha$ .

## 7.6. Anti-aggregant Tau<sup>RDA-PP</sup> suppresses Wnt5a levels.

The decreased level of the inactive form of GSK3 $\beta$  was another hint to study the upstream factors that could be involved in the regulation of GSK3 $\beta$  and neurogenesis. GSK3 $\beta$  has been shown to mediate various signaling pathways, among which the growth factors and the Wnt signaling pathways are the most studied ones (Woodgett, 2001). Wnt signaling is the principal regulator of adult hippocampal neurogenesis and has a role in adult hippocampal function (Lie et al., 2005). Increased LTP in the CA1 region of the hippocampus of the anti-aggregant Tau<sup>RDA-PP</sup> groups (Sydow et al., 2011) further supported the possible involvement of the Wnt signaling pathway, as it is assumed that it has a predominant role in hippocampal LTP (Chen et al., 2006), neurogenesis and neuroinflammation. Wnt5a is up-regulated in AD brains (Li et al., 2011) and increased Wnt5a is considered as a direct inhibitor of the canonical Wnt signaling pathway (Florian et al., 2013). The Increased level of Wnt5a is a marker of aging (Florian et al., 2013). We therefore analyzed whether changes in the Wnt5a level was due to the expression of anti-aggregant Tau<sup>RDA-PP</sup>. The level of Wnt5a in anti-aggregant Tau<sup>RDA-PP</sup> slices was reduced to 50% when compared to age matched control slices (Figure 49). When the expression of anti-aggregant Tau was switched-off by DOX, the level of Wnt5a in the anti-aggregant Tau<sup>RDA-PP</sup> slices were further reduced significantly. The level of Wnt5a in the controls was also reduced with the administration of DOX. With all this data we conclude that the expression of anti-aggregant Tau suppresses Wnt5a levels and thereby enhances neurogenesis and reduces neuroinflammation in this mouse model.

## 8) CONCLUSIONS

The expression of the anti-aggregant Tau enhances neurogenesis by directly influencing the proliferation and differentiation of hippocampal stem cells. It also increases the endogenous mouse Tau and thereby supporting neuronal differentiation and maturation in this mouse model. There is a reduced number of microglia and thus reduced neuroinflammation. The anti-aggregant Tau enhances hippocampal neurogenesis via the Wnt signaling pathway by suppressing the non-canonical Wnt signaling molecule Wnt5a.



## 9. REFERENCE

- AHN, J., JANG, J., CHOI, J., LEE, J., OH, S. H., YOON, K. & KIM, S. 2014. GSK3beta, but not GSK3alpha, inhibits the neuronal differentiation of neural progenitor cells as a downstream target of mammalian target of rapamycin complex1. *Stem Cells Dev*, 23, 1121-33.
- AIMONE, J. B., DENG, W. & GAGE, F. H. 2010. Adult neurogenesis: integrating theories and separating functions. *Trends Cogn Sci*, 14, 325-37.
- ALBUS, K., WAHAB, A. & HEINEMANN, U. 2008. Standard antiepileptic drugs fail to block epileptiform activity in rat organotypic hippocampal slice cultures. *Br J Pharmacol*, 154, 709-24.
- ALTMAN, J. & BAYER, S. A. 1990. Migration and distribution of two populations of hippocampal granule cell precursors during the perinatal and postnatal periods. *J Comp Neurol*, 301, 365-81.
- ALTMAN, J. & DAS, G. D. 1965. Autoradiographic and histological evidence of postnatal hippocampal neurogenesis in rats. *J Comp Neurol*, 124, 319-35.
- ALVAREZ-BUYLLA, A., SERI, B. & DOETSCH, F. 2002. Identification of neural stem cells in the adult vertebrate brain. *Brain Res Bull*, 57, 751-8.
- ANDREADIS, A., BROWN, W. M. & KOSIK, K. S. 1992. Structure and novel exons of the human tau gene. *Biochemistry*, 31, 10626-33.
- ANGELO, M., PLATTNER, F., IRVINE, E. E. & GIESE, K. P. 2003. Improved reversal learning and altered fear conditioning in transgenic mice with regionally restricted p25 expression. *Eur J Neurosci*, 18, 423-31.
- ANGEVINE, J. B., JR. 1965. Time of neuron origin in the hippocampal region. An autoradiographic study in the mouse. *Exp Neurol Suppl*, Suppl 2:1-70.
- AVILA, J., INSAUSTI, R. & DEL RIO, J. 2010. Memory and neurogenesis in aging and Alzheimer's disease. *Aging Dis*, 1, 30-6.
- BALLATORE, C., LEE, V. M. & TROJANOWSKI, J. Q. 2007. Tau-mediated neurodegeneration in Alzheimer's disease and related disorders. *Nat Rev Neurosci*, 8, 663-72.
- BARGHORN, S., ZHENG-FISCHHOFER, Q., ACKMANN, M., BIERNAT, J., VON BERGEN, M., MANDELKOW, E. M. & MANDELKOW, E. 2000. Structure, microtubule interactions, and paired helical filament aggregation by tau mutants of frontotemporal dementias. *Biochemistry*, 39, 11714-21.
- BARON, U. & BUJARD, H. 2000. Tet repressor-based system for regulated gene expression in eukaryotic cells: principles and advances. *Methods Enzymol*, 327, 401-21.
- BARON, U., GOSSSEN, M. & BUJARD, H. 1997. Tetracycline-controlled transcription in eukaryotes: novel transactivators with graded transactivation potential. *Nucleic Acids Res*, 25, 2723-9.

- BARTLEY, J., SOLTAU, T., WIMBORNE, H., KIM, S., MARTIN-STUDDARD, A., HESS, D., HILL, W., WALLER, J. & CARROLL, J. 2005. BrdU-positive cells in the neonatal mouse hippocampus following hypoxic-ischemic brain injury. *BMC Neurosci*, 6, 15.
- BAYER, S. A. 1980. Development of the hippocampal region in the rat. I. Neurogenesis examined with 3H-thymidine autoradiography. *J Comp Neurol*, 190, 87-114.
- BERGOLD, P. J. & CASACCIA-BONNEFIL, P. 1997. Preparation of organotypic hippocampal slice cultures using the membrane filter method. *Methods Mol Biol*, 72, 15-22.
- BERNARDINO, L., BALOSSO, S., RAVIZZA, T., MARCHI, N., KU, G., RANDLE, J. C., MALVA, J. O. & VEZZANI, A. 2008. Inflammatory events in hippocampal slice cultures prime neuronal susceptibility to excitotoxic injury: a crucial role of P2X7 receptor-mediated IL-1beta release. *J Neurochem*, 106, 271-80.
- BIEBL, M., COOPER, C. M., WINKLER, J. & KUHN, H. G. 2000. Analysis of neurogenesis and programmed cell death reveals a self-renewing capacity in the adult rat brain. *Neurosci Lett*, 291, 17-20.
- BIERNAT, J. & MANDELKOW, E. M. 1999. The development of cell processes induced by tau protein requires phosphorylation of serine 262 and 356 in the repeat domain and is inhibited by phosphorylation in the proline-rich domains. *Mol Biol Cell*, 10, 727-40.
- BINDER, L. I., FRANKFURTER, A. & REBHUN, L. I. 1985. The distribution of tau in the mammalian central nervous system. *J Cell Biol*, 101, 1371-8.
- BLISS, T. V. & COLLINGRIDGE, G. L. 1993. A synaptic model of memory: long-term potentiation in the hippocampus. *Nature*, 361, 31-9.
- BOEKHOORN, K., TERWEL, D., BIEMANS, B., BORGHGRAEF, P., WIEGERT, O., RAMAKERS, G. J., DE VOS, K., KRUGERS, H., TOMIYAMA, T., MORI, H., JOELS, M., VAN LEUVEN, F. & LUCASSEN, P. J. 2006. Improved long-term potentiation and memory in young tau-P301L transgenic mice before onset of hyperphosphorylation and tauopathy. *J Neurosci*, 26, 3514-23.
- BRAAK, H. & BRAAK, E. 1991. Neuropathological staging of Alzheimer-related changes. *Acta Neuropathol*, 82, 239-59.
- BRANDT, M. D., JESSBERGER, S., STEINER, B., KRONENBERG, G., REUTER, K., BICKSANDER, A., VON DER BEHRENS, W. & KEMPERMANN, G. 2003. Transient calretinin expression defines early postmitotic step of neuronal differentiation in adult hippocampal neurogenesis of mice. *Mol Cell Neurosci*, 24, 603-13.
- BRANDT, R., LEGER, J. & LEE, G. 1995. Interaction of tau with the neural plasma membrane mediated by tau's amino-terminal projection domain. *J Cell Biol*, 131, 1327-40.
- BRION, J. P., COUCK, A. M., PASSAREIRO, E. & FLAMENT-DURAND, J. 1985. Neurofibrillary tangles of Alzheimer's disease: an immunohistochemical study. *J Submicrosc Cytol*, 17, 89-96.
- BRION, J. P., GUILLEMINOT, J., COUCHIE, D., FLAMENT-DURAND, J. & NUNEZ, J. 1988a. Both adult and juvenile tau microtubule-associated proteins are axon specific in the developing and adult rat cerebellum. *Neuroscience*, 25, 139-46.

- BRION, J. P., GUILLEMINOT, J. & NUNEZ, J. 1988b. Dendritic and axonal distribution of the microtubule-associated proteins MAP2 and tau in the cerebellum of the nervous mutant mouse. *Brain Res Dev Brain Res*, 44, 221-32.
- BRION, J. P., SMITH, C., COUCK, A. M., GALLO, J. M. & ANDERTON, B. H. 1993. Developmental changes in tau phosphorylation: fetal tau is transiently phosphorylated in a manner similar to paired helical filament-tau characteristic of Alzheimer's disease. *J Neurochem*, 61, 2071-80.
- BULLMANN, T., DE SILVA, R., HOLZER, M., MORI, H. & ARENDT, T. 2007. Expression of embryonic tau protein isoforms persist during adult neurogenesis in the hippocampus. *Hippocampus*, 17, 98-102.
- BULLMANN, T., HARTIG, W., HOLZER, M. & ARENDT, T. 2010. Expression of the embryonal isoform (ON/3R) of the microtubule-associated protein tau in the adult rat central nervous system. *J Comp Neurol*, 518, 2538-53.
- BULLMANN, T., HOLZER, M., MORI, H. & ARENDT, T. 2009. Pattern of tau isoforms expression during development in vivo. *Int J Dev Neurosci*, 27, 591-7.
- CACERES, A. & KOSIK, K. S. 1990. Inhibition of neurite polarity by tau antisense oligonucleotides in primary cerebellar neurons. *Nature*, 343, 461-3.
- CACERES, A., POTREBIC, S. & KOSIK, K. S. 1991. The effect of tau antisense oligonucleotides on neurite formation of cultured cerebellar macroneurons. *J Neurosci*, 11, 1515-23.
- CAMERON, H. A. & MCKAY, R. D. 2001. Adult neurogenesis produces a large pool of new granule cells in the dentate gyrus. *J Comp Neurol*, 435, 406-17.
- CAMPBELL, S. & MACQUEEN, G. 2004. The role of the hippocampus in the pathophysiology of major depression. *J Psychiatry Neurosci*, 29, 417-26.
- CAMPION, D., DUMANCHIN, C., HANNEQUIN, D., DUBOIS, B., BELLARD, S., PUEL, M., THOMAS-ANTERION, C., MICHON, A., MARTIN, C., CHARBONNIER, F., RAUX, G., CAMUZAT, A., PENET, C., MESNAGE, V., MARTINEZ, M., CLERGET-DARPOUX, F., BRICE, A. & FREBOURG, T. 1999. Early-onset autosomal dominant Alzheimer disease: prevalence, genetic heterogeneity, and mutation spectrum. *Am J Hum Genet*, 65, 664-70.
- CAPILLA-GONZALEZ, V., CEBRIAN-SILLA, A., GUERRERO-CAZARES, H., GARCIA-VERDUGO, J. M. & QUINONES-HINOJOSA, A. 2014. Age-related changes in astrocytic and ependymal cells of the subventricular zone. *Glia*, 62, 790-803.
- CERPA, W., FARIAS, G. G., GODOY, J. A., FUENZALIDA, M., BONANSCO, C. & INESTROSA, N. C. 2010. Wnt-5a occludes Abeta oligomer-induced depression of glutamatergic transmission in hippocampal neurons. *Mol Neurodegener*, 5, 3.
- CERPA, W., GAMBRILL, A., INESTROSA, N. C. & BARRIA, A. 2011. Regulation of NMDA-receptor synaptic transmission by Wnt signaling. *J Neurosci*, 31, 9466-71.
- CERPA, W., GODOY, J. A., ALFARO, I., FARIAS, G. G., METCALFE, M. J., FUENTEALBA, R., BONANSCO, C. & INESTROSA, N. C. 2008. Wnt-7a modulates the synaptic vesicle cycle and synaptic transmission in hippocampal neurons. *J Biol Chem*, 283, 5918-27.
- CHANCEY, J. H., POULSEN, D. J., WADICHE, J. I. & OVERSTREET-WADICHE, L. 2014. Hilar mossy cells provide the first glutamatergic synapses to adult-born dentate granule cells. *J Neurosci*, 34, 2349-54.

- CHAPIN, S. J. & BULINSKI, J. C. 1991. Non-neuronal 210 x 10(3) Mr microtubule-associated protein (MAP4) contains a domain homologous to the microtubule-binding domains of neuronal MAP2 and tau. *J Cell Sci*, 98 ( Pt 1), 27-36.
- CHARTIER-HARLIN, M. C., CRAWFORD, F., HOULDEN, H., WARREN, A., HUGHES, D., FIDANI, L., GOATE, A., ROSSOR, M., ROQUES, P., HARDY, J. & ET AL. 1991. Early-onset Alzheimer's disease caused by mutations at codon 717 of the beta-amyloid precursor protein gene. *Nature*, 353, 844-6.
- CHEN, J., PARK, C. S. & TANG, S. J. 2006. Activity-dependent synaptic Wnt release regulates hippocampal long term potentiation. *J Biol Chem*, 281, 11910-6.
- CHESSER, A. S., PRITCHARD, S. M. & JOHNSON, G. V. 2013. Tau clearance mechanisms and their possible role in the pathogenesis of Alzheimer disease. *Front Neurol*, 4, 122.
- CHO, S., LIU, D., FAIRMAN, D., LI, P., JENKINS, L., MCGONIGLE, P. & WOOD, A. 2004. Spatiotemporal evidence of apoptosis-mediated ischemic injury in organotypic hippocampal slice cultures. *Neurochem Int*, 45, 117-27.
- CHO, Y., SON, H. J., KIM, E. M., CHOI, J. H., KIM, S. T., JI, I. J., CHOI, D. H., JOH, T. H., KIM, Y. S. & HWANG, O. 2009. Doxycycline is neuroprotective against nigral dopaminergic degeneration by a dual mechanism involving MMP-3. *Neurotox Res*, 16, 361-71.
- CHOW, K. M., GUAN, H. & HERSH, L. B. 2010. Aminopeptidases do not directly degrade tau protein. *Mol Neurodegener*, 5, 48.
- CLARK, W. M., LESSOV, N., LAUTEN, J. D. & HAZEL, K. 1997. Doxycycline treatment reduces ischemic brain damage in transient middle cerebral artery occlusion in the rat. *J Mol Neurosci*, 9, 103-8.
- CLARKE, L. E. & BARRES, B. A. 2013. Emerging roles of astrocytes in neural circuit development. *Nat Rev Neurosci*, 14, 311-21.
- COUILLARD-DESPRES, S., WINNER, B., SCHAUBECK, S., AIGNER, R., VROEMEN, M., WEIDNER, N., BOGDAHN, U., WINKLER, J., KUHN, H. G. & AIGNER, L. 2005. Doublecortin expression levels in adult brain reflect neurogenesis. *Eur J Neurosci*, 21, 1-14.
- CUITINO, L., GODOY, J. A., FARIAS, G. G., COUVE, A., BONANSCO, C., FUENZALIDA, M. & INESTROSA, N. C. 2010. Wnt-5a modulates recycling of functional GABAA receptors on hippocampal neurons. *J Neurosci*, 30, 8411-20.
- DAWSON, H. N., FERREIRA, A., EYSTER, M. V., GHOSHAL, N., BINDER, L. I. & VITEK, M. P. 2001. Inhibition of neuronal maturation in primary hippocampal neurons from tau deficient mice. *J Cell Sci*, 114, 1179-87.
- DAYER, A. G., FORD, A. A., CLEAVER, K. M., YASSAEE, M. & CAMERON, H. A. 2003. Short-term and long-term survival of new neurons in the rat dentate gyrus. *J Comp Neurol*, 460, 563-72.
- DE SIMONI, A. & YU, L. M. 2006. Preparation of organotypic hippocampal slice cultures: interface method. *Nat Protoc*, 1, 1439-45.
- DOETSCH, F. & HEN, R. 2005. Young and excitable: the function of new neurons in the adult mammalian brain. *Curr Opin Neurobiol*, 15, 121-8.
- DRUBIN, D. G. & KIRSCHNER, M. W. 1986. Tau protein function in living cells. *J Cell Biol*, 103, 2739-46.

- ECKERMANN, K., MOCANU, M. M., KHLISTUNOVA, I., BIERNAT, J., NISSEN, A., HOFMANN, A., SCHONIG, K., BUJARD, H., HAEMISCH, A., MANDELKOW, E., ZHOU, L., RUNE, G. & MANDELKOW, E. M. 2007. The beta-propensity of Tau determines aggregation and synaptic loss in inducible mouse models of tauopathy. *J Biol Chem*, 282, 31755-65.
- EICHENBAUM, H. 2000a. A cortical-hippocampal system for declarative memory. *Nat Rev Neurosci*, 1, 41-50.
- EICHENBAUM, H. 2000b. Hippocampus: mapping or memory? *Curr Biol*, 10, R785-7.
- EKDAHL, C. T. 2012. Microglial activation - tuning and pruning adult neurogenesis. *Front Pharmacol*, 3, 41.
- EKONOMOU, A., SAVVA, G. M., BRAYNE, C., FORSTER, G., FRANCIS, P. T., JOHNSON, M., PERRY, E. K., ATTEMS, J., SOMANI, A., MINGER, S. L. & BALLARD, C. G. 2014. Stage-Specific Changes in Neurogenic and Glial Markers in Alzheimer's Disease. *Biol Psychiatry*.
- ENGEL, T., LUCAS, J. J., GOMEZ-RAMOS, P., MORAN, M. A., AVILA, J. & HERNANDEZ, F. 2006. Coexpression of FTDP-17 tau and GSK-3beta in transgenic mice induce tau polymerization and neurodegeneration. *Neurobiol Aging*, 27, 1258-68.
- ERNST, A., ALKASS, K., BERNARD, S., SALEHPOUR, M., PERL, S., TISDALE, J., POSSNERT, G., DRUID, H. & FRISEN, J. 2014. Neurogenesis in the striatum of the adult human brain. *Cell*, 156, 1072-83.
- ESMAELI-AZAD, B., MCCARTY, J. H. & FEINSTEIN, S. C. 1994. Sense and antisense transfection analysis of tau function: tau influences net microtubule assembly, neurite outgrowth and neuritic stability. *J Cell Sci*, 107 ( Pt 4), 869-79.
- ESPOSITO, M. S., PIATTI, V. C., LAPLAGNE, D. A., MORGENSTERN, N. A., FERRARI, C. C., PITOSI, F. J. & SCHINDER, A. F. 2005. Neuronal differentiation in the adult hippocampus recapitulates embryonic development. *J Neurosci*, 25, 10074-86.
- FAULKNER, R. L., JANG, M. H., LIU, X. B., DUAN, X., SAILOR, K. A., KIM, J. Y., GE, S., JONES, E. G., MING, G. L., SONG, H. & CHENG, H. J. 2008. Development of hippocampal mossy fiber synaptic outputs by new neurons in the adult brain. *Proc Natl Acad Sci U S A*, 105, 14157-62.
- FERNANDEZ-NOGALES, M., CABRERA, J. R., SANTOS-GALINDO, M., HOOZEMANS, J. J., FERRER, I., ROZEMULLER, A. J., HERNANDEZ, F., AVILA, J. & LUCAS, J. J. 2014. Huntington's disease is a four-repeat tauopathy with tau nuclear rods. *Nat Med*.
- FILIPPOV, V., KRONENBERG, G., PIVNEVA, T., REUTER, K., STEINER, B., WANG, L. P., YAMAGUCHI, M., KETTENMANN, H. & KEMPERMANN, G. 2003. Subpopulation of nestin-expressing progenitor cells in the adult murine hippocampus shows electrophysiological and morphological characteristics of astrocytes. *Mol Cell Neurosci*, 23, 373-82.
- FLORIAN, M. C., NATTAMAI, K. J., DORR, K., MARKA, G., UBERLE, B., VAS, V., ECKL, C., ANDRA, I., SCHIEMANN, M., OOSTENDORP, R. A., SCHARFFETTER-KOCHANNEK, K., KESTLER, H. A., ZHENG, Y. & GEIGER, H. 2013. A canonical to non-canonical Wnt signalling switch in haematopoietic stem-cell ageing. *Nature*, 503, 392-6.
- FORTIN, N. J., AGSTER, K. L. & EICHENBAUM, H. B. 2002. Critical role of the hippocampus in memory for sequences of events. *Nat Neurosci*, 5, 458-62.

- FOSTER, N. L., WILHELMSSEN, K., SIMA, A. A., JONES, M. Z., D'AMATO, C. J. & GILMAN, S. 1997. Frontotemporal dementia and parkinsonism linked to chromosome 17: a consensus conference. Conference Participants. *Ann Neurol*, 41, 706-15.
- FRENCH, J. A., WILLIAMSON, P. D., THADANI, V. M., DARCEY, T. M., MATTSON, R. H., SPENCER, S. S. & SPENCER, D. D. 1993. Characteristics of medial temporal lobe epilepsy: I. Results of history and physical examination. *Ann Neurol*, 34, 774-80.
- FRIEDHOFF, P., VON BERGEN, M., MANDELKOW, E. M., DAVIES, P. & MANDELKOW, E. 1998. A nucleated assembly mechanism of Alzheimer paired helical filaments. *Proc Natl Acad Sci U S A*, 95, 15712-7.
- FUKUDA, S., KATO, F., TOZUKA, Y., YAMAGUCHI, M., MIYAMOTO, Y. & HISATSUNE, T. 2003. Two distinct subpopulations of nestin-positive cells in adult mouse dentate gyrus. *J Neurosci*, 23, 9357-66.
- FURTH, P. A., ST ONGE, L., BOGER, H., GRUSS, P., GOSSSEN, M., KISTNER, A., BUJARD, H. & HENNIGHAUSEN, L. 1994. Temporal control of gene expression in transgenic mice by a tetracycline-responsive promoter. *Proc Natl Acad Sci U S A*, 91, 9302-6.
- FUSTER-MATANZO, A., DE BARREDA, E. G., DAWSON, H. N., VITEK, M. P., AVILA, J. & HERNANDEZ, F. 2009. Function of tau protein in adult newborn neurons. *FEBS Lett*, 583, 3063-8.
- FUSTER-MATANZO, A., LLORENS-MARTIN, M., JURADO-ARJONA, J., AVILA, J. & HERNANDEZ, F. 2012. Tau protein and adult hippocampal neurogenesis. *Front Neurosci*, 6, 104.
- GAGE, F. H. 2004. Structural plasticity of the adult brain. *Dialogues Clin Neurosci*, 6, 135-41.
- GAHWILER, B. H. 1981. Organotypic monolayer cultures of nervous tissue. *J Neurosci Methods*, 4, 329-42.
- GAHWILER, B. H., CAPOGNA, M., DEBANNE, D., MCKINNEY, R. A. & THOMPSON, S. M. 1997. Organotypic slice cultures: a technique has come of age. *Trends Neurosci*, 20, 471-7.
- GALVAN, M., DAVID, J. P., DELACOURTE, A., LUNA, J. & MENA, R. 2001. Sequence of neurofibrillary changes in aging and Alzheimer's disease: A confocal study with phospho-tau antibody, AD2. *J Alzheimers Dis*, 3, 417-425.
- GAMBLIN, T. C., KING, M. E., DAWSON, H., VITEK, M. P., KURET, J., BERRY, R. W. & BINDER, L. I. 2000. In vitro polymerization of tau protein monitored by laser light scattering: method and application to the study of FTDP-17 mutants. *Biochemistry*, 39, 6136-44.
- GARCIA, M. L. & CLEVELAND, D. W. 2001. Going new places using an old MAP: tau, microtubules and human neurodegenerative disease. *Curr Opin Cell Biol*, 13, 41-8.
- GASPARINI, L., TERNI, B. & SPILLANTINI, M. G. 2007. Frontotemporal dementia with tau pathology. *Neurodegener Dis*, 4, 236-53.
- GEBARA, E., SULTAN, S., KOCHER-BRAISSANT, J. & TONI, N. 2013. Adult hippocampal neurogenesis inversely correlates with microglia in conditions of voluntary running and aging. *Front Neurosci*, 7, 145.

- GLEESON, J. G., LIN, P. T., FLANAGAN, L. A. & WALSH, C. A. 1999. Doublecortin is a microtubule-associated protein and is expressed widely by migrating neurons. *Neuron*, 23, 257-71.
- GLENNER, G. G. & WONG, C. W. 1984. Alzheimer's disease: initial report of the purification and characterization of a novel cerebrovascular amyloid protein. *Biochem Biophys Res Commun*, 120, 885-90.
- GOEDERT, M., JAKES, R., SPILLANTINI, M. G., HASEGAWA, M., SMITH, M. J. & CROWTHER, R. A. 1996. Assembly of microtubule-associated protein tau into Alzheimer-like filaments induced by sulphated glycosaminoglycans. *Nature*, 383, 550-3.
- GOEDERT, M., SPILLANTINI, M. G., JAKES, R., RUTHERFORD, D. & CROWTHER, R. A. 1989. Multiple isoforms of human microtubule-associated protein tau: sequences and localization in neurofibrillary tangles of Alzheimer's disease. *Neuron*, 3, 519-26.
- GOEDERT, M., WISCHIK, C. M., CROWTHER, R. A., WALKER, J. E. & KLUG, A. 1988. Cloning and sequencing of the cDNA encoding a core protein of the paired helical filament of Alzheimer disease: identification as the microtubule-associated protein tau. *Proc Natl Acad Sci U S A*, 85, 4051-5.
- GOLDBAUM, O., OPPERMANN, M., HANDSCHUH, M., DABIR, D., ZHANG, B., FORMAN, M. S., TROJANOWSKI, J. Q., LEE, V. M. & RICHTER-LANDSBERG, C. 2003. Proteasome inhibition stabilizes tau inclusions in oligodendroglial cells that occur after treatment with okadaic acid. *J Neurosci*, 23, 8872-80.
- GOULD, E. 2007. How widespread is adult neurogenesis in mammals? *Nat Rev Neurosci*, 8, 481-8.
- GOULD, E., BEYLIN, A., TANAPAT, P., REEVES, A. & SHORS, T. J. 1999. Learning enhances adult neurogenesis in the hippocampal formation. *Nat Neurosci*, 2, 260-5.
- GOULD, E. & GROSS, C. G. 2002. Neurogenesis in adult mammals: some progress and problems. *J Neurosci*, 22, 619-23.
- GRUNDKE-IQBAL, I., IQBAL, K., QUINLAN, M., TUNG, Y. C., ZAIDI, M. S. & WISNIEWSKI, H. M. 1986a. Microtubule-associated protein tau. A component of Alzheimer paired helical filaments. *J Biol Chem*, 261, 6084-9.
- GRUNDKE-IQBAL, I., IQBAL, K., TUNG, Y. C., QUINLAN, M., WISNIEWSKI, H. M. & BINDER, L. I. 1986b. Abnormal phosphorylation of the microtubule-associated protein tau (tau) in Alzheimer cytoskeletal pathology. *Proc Natl Acad Sci U S A*, 83, 4913-7.
- GRUNE, T., BOTZEN, D., ENGELS, M., VOSS, P., KAISER, B., JUNG, T., GRIMM, S., ERMAK, G. & DAVIES, K. J. 2010. Tau protein degradation is catalyzed by the ATP/ubiquitin-independent 20S proteasome under normal cell conditions. *Arch Biochem Biophys*, 500, 181-8.
- GU, Y., ARRUDA-CARVALHO, M., WANG, J., JANOSCHKA, S. R., JOSSELYN, S. A., FRANKLAND, P. W. & GE, S. 2012. Optical controlling reveals time-dependent roles for adult-born dentate granule cells. *Nat Neurosci*, 15, 1700-6.
- GUSTKE, N., TRINCZEK, B., BIERNAT, J., MANDELKOW, E. M. & MANDELKOW, E. 1994. Domains of tau protein and interactions with microtubules. *Biochemistry*, 33, 9511-22.

- HANGER, D. P., ANDERTON, B. H. & NOBLE, W. 2009. Tau phosphorylation: the therapeutic challenge for neurodegenerative disease. *Trends Mol Med*, 15, 112-9.
- HANGER, D. P., MANN, D. M., NEARY, D. & ANDERTON, B. H. 1992. Molecular pathology of Alzheimer's disease in sporadic and familial Alzheimer's disease with mutations in the amyloid precursor protein. *Biochem Soc Trans*, 20, 642-5.
- HASEGAWA, M., SMITH, M. J. & GOEDERT, M. 1998. Tau proteins with FTDP-17 mutations have a reduced ability to promote microtubule assembly. *FEBS Lett*, 437, 207-10.
- HIROKAWA, N. 1993. Axonal transport and the cytoskeleton. *Curr Opin Neurobiol*, 3, 724-31.
- HIROKAWA, N. 1994. Microtubule organization and dynamics dependent on microtubule-associated proteins. *Curr Opin Cell Biol*, 6, 74-81.
- HOCHGRAEFE, K. & MANDELKOW, E. M. 2013. Making the brain glow: in vivo bioluminescence imaging to study neurodegeneration. *Mol Neurobiol*, 47, 868-82.
- HONG, M., ZHUKAREVA, V., VOGELBERG-RAGAGLIA, V., WSZOLEK, Z., REED, L., MILLER, B. I., GESCHWIND, D. H., BIRD, T. D., MCKEEL, D., GOATE, A., MORRIS, J. C., WILHELMSSEN, K. C., SCHELLENBERG, G. D., TROJANOWSKI, J. Q. & LEE, V. M. 1998. Mutation-specific functional impairments in distinct tau isoforms of hereditary FTDP-17. *Science*, 282, 1914-7.
- HONG, X. P., PENG, C. X., WEI, W., TIAN, Q., LIU, Y. H., YAO, X. Q., ZHANG, Y., CAO, F. Y., WANG, Q. & WANG, J. Z. 2010. Essential role of tau phosphorylation in adult hippocampal neurogenesis. *Hippocampus*, 20, 1339-49.
- HUR, E. M. & ZHOU, F. Q. 2010. GSK3 signalling in neural development. *Nat Rev Neurosci*, 11, 539-51.
- HUTTON, M., LENDON, C. L., RIZZU, P., BAKER, M., FROELICH, S., HOULDEN, H., PICKERING-BROWN, S., CHAKRAVERTY, S., ISAACS, A., GROVER, A., HACKETT, J., ADAMSON, J., LINCOLN, S., DICKSON, D., DAVIES, P., PETERSEN, R. C., STEVENS, M., DE GRAAFF, E., WAUTERS, E., VAN BAREN, J., HILLEBRAND, M., JOOSSE, M., KWON, J. M., NOWOTNY, P., CHE, L. K., NORTON, J., MORRIS, J. C., REED, L. A., TROJANOWSKI, J., BASUN, H., LANNFELT, L., NEYSTAT, M., FAHN, S., DARK, F., TANNENBERG, T., DODD, P. R., HAYWARD, N., KWOK, J. B., SCHOFIELD, P. R., ANDREADIS, A., SNOWDEN, J., CRAUFURD, D., NEARY, D., OWEN, F., OOSTRA, B. A., HARDY, J., GOATE, A., VAN SWIETEN, J., MANN, D., LYNCH, T. & HEUTINK, P. 1998. Association of missense and 5'-splice-site mutations in tau with the inherited dementia FTDP-17. *Nature*, 393, 702-5.
- HYMAN, B. T. 1997. The neuropathological diagnosis of Alzheimer's disease: clinical-pathological studies. *Neurobiol Aging*, 18, S27-32.
- IHARA, Y., NUKINA, N., MIURA, R. & OGAWARA, M. 1986. Phosphorylated tau protein is integrated into paired helical filaments in Alzheimer's disease. *J Biochem*, 99, 1807-10.
- IKEGAMI, S., HARADA, A. & HIROKAWA, N. 2000. Muscle weakness, hyperactivity, and impairment in fear conditioning in tau-deficient mice. *Neurosci Lett*, 279, 129-32.



- INESTROSA, N. C., MONTECINOS-OLIVA, C. & FUENZALIDA, M. 2012. Wnt signaling: role in Alzheimer disease and schizophrenia. *J Neuroimmune Pharmacol*, 7, 788-807.
- ITTNER, L. M. & GOTZ, J. 2011. Amyloid-beta and tau--a toxic pas de deux in Alzheimer's disease. *Nat Rev Neurosci*, 12, 65-72.
- ITTNER, L. M., KE, Y. D., DELERUE, F., BI, M., GLADBACH, A., VAN EERSEL, J., WOLFING, H., CHIENG, B. C., CHRISTIE, M. J., NAPIER, I. A., ECKERT, A., STAUFENBIEL, M., HARDEMAN, E. & GOTZ, J. 2010. Dendritic function of tau mediates amyloid-beta toxicity in Alzheimer's disease mouse models. *Cell*, 142, 387-97.
- JACK, C. R., JR., PETERSEN, R. C., XU, Y., O'BRIEN, P. C., SMITH, G. E., IVNIK, R. J., TANGALOS, E. G. & KOKMEN, E. 1998. Rate of medial temporal lobe atrophy in typical aging and Alzheimer's disease. *Neurology*, 51, 993-9.
- JACOBS, B. L., VAN PRAAG, H. & GAGE, F. H. 2000. Adult brain neurogenesis and psychiatry: a novel theory of depression. *Mol Psychiatry*, 5, 262-9.
- JAKOBSEN, B., GRAMSBERGEN, J. B., MOLLER DALL, A., ROSENBLAD, C. & ZIMMER, J. 2005. Characterization of organotypic ventral mesencephalic cultures from embryonic mice and protection against MPP toxicity by GDNF. *Eur J Neurosci*, 21, 2939-48.
- JANTZIE, L. L. & TODD, K. G. 2010. Doxycycline inhibits proinflammatory cytokines but not acute cerebral cytogenesis after hypoxia-ischemia in neonatal rats. *J Psychiatry Neurosci*, 35, 20-32.
- JIN, K., PEEL, A. L., MAO, X. O., XIE, L., COTTRELL, B. A., HENSHALL, D. C. & GREENBERG, D. A. 2004. Increased hippocampal neurogenesis in Alzheimer's disease. *Proc Natl Acad Sci U S A*, 101, 343-7.
- JINWAL, U. K., KOREN, J., 3RD, BORYSOV, S. I., SCHMID, A. B., ABISAMBRA, J. F., BLAIR, L. J., JOHNSON, A. G., JONES, J. R., SHULTS, C. L., O'LEARY, J. C., 3RD, JIN, Y., BUCHNER, J., COX, M. B. & DICKEY, C. A. 2010. The Hsp90 cochaperone, FKBP51, increases Tau stability and polymerizes microtubules. *J Neurosci*, 30, 591-9.
- KAMADA, M., LI, R. Y., HASHIMOTO, M., KAKUDA, M., OKADA, H., KOYANAGI, Y., ISHIZUKA, T. & YAWO, H. 2004. Intrinsic and spontaneous neurogenesis in the postnatal slice culture of rat hippocampus. *Eur J Neurosci*, 20, 2499-508.
- KANAI, Y., TAKEMURA, R., OSHIMA, T., MORI, H., IHARA, Y., YANAGISAWA, M., MASAKI, T. & HIROKAWA, N. 1989. Expression of multiple tau isoforms and microtubule bundle formation in fibroblasts transfected with a single tau cDNA. *J Cell Biol*, 109, 1173-84.
- KEE, N., SIVALINGAM, S., BOONSTRA, R. & WOJTOWICZ, J. M. 2002. The utility of Ki-67 and BrdU as proliferative markers of adult neurogenesis. *J Neurosci Methods*, 115, 97-105.
- KEMPERMANN, G. & GAGE, F. H. 1998. Closer to neurogenesis in adult humans. *Nat Med*, 4, 555-7.
- KEMPERMANN, G., JESSBERGER, S., STEINER, B. & KRONENBERG, G. 2004a. Milestones of neuronal development in the adult hippocampus. *Trends Neurosci*, 27, 447-52.

- KEMPERMANN, G., KUHN, H. G. & GAGE, F. H. 1997a. Genetic influence on neurogenesis in the dentate gyrus of adult mice. *Proc Natl Acad Sci U S A*, 94, 10409-14.
- KEMPERMANN, G., KUHN, H. G. & GAGE, F. H. 1997b. More hippocampal neurons in adult mice living in an enriched environment. *Nature*, 386, 493-5.
- KEMPERMANN, G., WISKOTT, L. & GAGE, F. H. 2004b. Functional significance of adult neurogenesis. *Curr Opin Neurobiol*, 14, 186-91.
- KHEIRBEK, M. A., KLEMENHAGEN, K. C., SAHAY, A. & HEN, R. 2012. Neurogenesis and generalization: a new approach to stratify and treat anxiety disorders. *Nat Neurosci*, 15, 1613-20.
- KHLISTUNOVA, I., BIERNAT, J., WANG, Y., PICKHARDT, M., VON BERGEN, M., GAZOVA, Z., MANDELKOW, E. & MANDELKOW, E. M. 2006. Inducible expression of Tau repeat domain in cell models of tauopathy: aggregation is toxic to cells but can be reversed by inhibitor drugs. *J Biol Chem*, 281, 1205-14.
- KHLISTUNOVA, I., PICKHARDT, M., BIERNAT, J., WANG, Y., MANDELKOW, E. M. & MANDELKOW, E. 2007. Inhibition of tau aggregation in cell models of tauopathy. *Curr Alzheimer Res*, 4, 544-6.
- KLAUSBERGER, T., MARTON, L. F., O'NEILL, J., HUCK, J. H., DALEZIOS, Y., FUENTEALBA, P., SUEN, W. Y., PAPP, E., KANEKO, T., WATANABE, M., CSICSVARI, J. & SOMOGYI, P. 2005. Complementary roles of cholecystokinin- and parvalbumin-expressing GABAergic neurons in hippocampal network oscillations. *J Neurosci*, 25, 9782-93.
- KLEMPIN, F. & KEMPERMANN, G. 2007. Adult hippocampal neurogenesis and aging. *Eur Arch Psychiatry Clin Neurosci*, 257, 271-80.
- KLEMPIN, F., KRONENBERG, G., CHEUNG, G., KETTENMANN, H. & KEMPERMANN, G. 2011. Properties of doublecortin-(DCX)-expressing cells in the piriform cortex compared to the neurogenic dentate gyrus of adult mice. *PLoS One*, 6, e25760.
- KNOPS, J., KOSIK, K. S., LEE, G., PARDEE, J. D., COHEN-GOULD, L. & MCCONLOGUE, L. 1991. Overexpression of tau in a nonneuronal cell induces long cellular processes. *J Cell Biol*, 114, 725-33.
- KNOTH, R., SINGEC, I., DITTER, M., PANTAZIS, G., CAPETIAN, P., MEYER, R. P., HORVAT, V., VOLK, B. & KEMPERMANN, G. 2010. Murine features of neurogenesis in the human hippocampus across the lifespan from 0 to 100 years. *PLoS One*, 5, e8809.
- KONDRATIUK, I., DEVIJVER, H., LECHAT, B., VAN LEUVEN, F., KACZMAREK, L. & FILIPKOWSKI, R. K. 2013. Glycogen synthase kinase-3beta affects size of dentate gyrus and species-typical behavioral tasks in transgenic and knockout mice. *Behav Brain Res*, 248, 46-50.
- KOSIK, K. S. 1992. Alzheimer's disease: a cell biological perspective. *Science*, 256, 780-3.
- KOSIK, K. S., JOACHIM, C. L. & SELKOE, D. J. 1986. Microtubule-associated protein tau (tau) is a major antigenic component of paired helical filaments in Alzheimer disease. *Proc Natl Acad Sci U S A*, 83, 4044-8.
- KOSIK, K. S., ORECCHIO, L. D., BAKALIS, S. & NEVE, R. L. 1989. Developmentally regulated expression of specific tau sequences. *Neuron*, 2, 1389-97.

- KOWALL, N. W. & KOSIK, K. S. 1987. Axonal disruption and aberrant localization of tau protein characterize the neuropil pathology of Alzheimer's disease. *Ann Neurol*, 22, 639-43.
- KRONENBERG, G., REUTER, K., STEINER, B., BRANDT, M. D., JESSBERGER, S., YAMAGUCHI, M. & KEMPERMANN, G. 2003. Subpopulations of proliferating cells of the adult hippocampus respond differently to physiologic neurogenic stimuli. *J Comp Neurol*, 467, 455-63.
- KUHN, H. G., BIEBL, M., WILHELM, D., LI, M., FRIEDLANDER, R. M. & WINKLER, J. 2005. Increased generation of granule cells in adult Bcl-2-overexpressing mice: a role for cell death during continued hippocampal neurogenesis. *Eur J Neurosci*, 22, 1907-15.
- KUHN, H. G., DICKINSON-ANSON, H. & GAGE, F. H. 1996. Neurogenesis in the dentate gyrus of the adult rat: age-related decrease of neuronal progenitor proliferation. *J Neurosci*, 16, 2027-33.
- KURET, J., CONGDON, E. E., LI, G., YIN, H., YU, X. & ZHONG, Q. 2005. Evaluating triggers and enhancers of tau fibrillization. *Microsc Res Tech*, 67, 141-55.
- L'EPISCOPO, F., TIROLO, C., CANIGLIA, S., TESTA, N., MORALE, M. C., SERAPIDE, M. F., PLUCHINO, S. & MARCHETTI, B. 2014. Targeting Wnt signaling at the neuroimmune interface for dopaminergic neuroprotection/repair in Parkinson's disease. *J Mol Cell Biol*.
- LARSEN, T. R., ROSSEN, S. & GRAMSBERGEN, J. B. 2008. Dopamine release in organotypic cultures of foetal mouse mesencephalon: effects of depolarizing agents, pargyline, nomifensine, tetrodotoxin and calcium. *Eur J Neurosci*, 28, 569-76.
- LEE, G. 1993. Non-motor microtubule-associated proteins. *Curr Opin Cell Biol*, 5, 88-94.
- LEE, V. M., BALIN, B. J., OTVOS, L., JR. & TROJANOWSKI, J. Q. 1991. A68: a major subunit of paired helical filaments and derivatized forms of normal Tau. *Science*, 251, 675-8.
- LEE, V. M., GOEDERT, M. & TROJANOWSKI, J. Q. 2001. Neurodegenerative tauopathies. *Annu Rev Neurosci*, 24, 1121-59.
- LEUNER, B. & GOULD, E. 2010. Structural plasticity and hippocampal function. *Annu Rev Psychol*, 61, 111-40, C1-3.
- LEWIS, S. A., WANG, D. H. & COWAN, N. J. 1988. Microtubule-associated protein MAP2 shares a microtubule binding motif with tau protein. *Science*, 242, 936-9.
- LI, B., YAMAMORI, H., TATEBAYASHI, Y., SHAFIT-ZAGARDO, B., TANIMUKAI, H., CHEN, S., IQBAL, K. & GRUNDKE-IQBAL, I. 2008. Failure of neuronal maturation in Alzheimer disease dentate gyrus. *J Neuropathol Exp Neurol*, 67, 78-84.
- LI, B., ZHONG, L., YANG, X., ANDERSSON, T., HUANG, M. & TANG, S. J. 2011. WNT5A signaling contributes to Abeta-induced neuroinflammation and neurotoxicity. *PLoS One*, 6, e22920.
- LIE, D. C., COLAMARINO, S. A., SONG, H. J., DESIRE, L., MIRA, H., CONSIGLIO, A., LEIN, E. S., JESSBERGER, S., LANSFORD, H., DEARIE, A. R. & GAGE, F. H. 2005. Wnt signalling regulates adult hippocampal neurogenesis. *Nature*, 437, 1370-5.

- LIM, F., HERNANDEZ, F., LUCAS, J. J., GOMEZ-RAMOS, P., MORAN, M. A. & AVILA, J. 2001. FTDP-17 mutations in tau transgenic mice provoke lysosomal abnormalities and Tau filaments in forebrain. *Mol Cell Neurosci*, 18, 702-14.
- LIU, S., WANG, J., ZHU, D., FU, Y., LUKOWIAK, K. & LU, Y. M. 2003. Generation of functional inhibitory neurons in the adult rat hippocampus. *J Neurosci*, 23, 732-6.
- LIU, Y. B., LIO, P. A., PASTERNAK, J. F. & TROMMER, B. L. 1996. Developmental changes in membrane properties and postsynaptic currents of granule cells in rat dentate gyrus. *J Neurophysiol*, 76, 1074-88.
- LLEDO, P. M., ALONSO, M. & GRUBB, M. S. 2006. Adult neurogenesis and functional plasticity in neuronal circuits. *Nat Rev Neurosci*, 7, 179-93.
- LLEDO, P. M. & GHEUSI, G. 2006. [Adult neurogenesis: from basic research to clinical applications]. *Bull Acad Natl Med*, 190, 385-400; discussion 400-2.
- LLORENS-MARTIN, M., HERNANDEZ, F. & AVILA, J. 2011. Expression of frontotemporal dementia with parkinsonism associated to chromosome 17 tau induces specific degeneration of the ventral dentate gyrus and depressive-like behavior in mice. *Neuroscience*, 196, 215-27.
- LLORENS-MARTIN, M., TEIXEIRA, C. M., FUSTER-MATANZO, A., JURADO-ARJONA, J., BORRELL, V., SORIANO, E., AVILA, J. & HERNANDEZ, F. 2012. Tau isoform with three microtubule binding domains is a marker of new axons generated from the subgranular zone in the hippocampal dentate gyrus: implications for Alzheimer's disease. *J Alzheimers Dis*, 29, 921-30.
- LOOMIS, P. A., HOWARD, T. H., CASTLEBERRY, R. P. & BINDER, L. I. 1990. Identification of nuclear tau isoforms in human neuroblastoma cells. *Proc Natl Acad Sci U S A*, 87, 8422-6.
- LOPRESTI, P., SZUCHET, S., PAPASOZOMENOS, S. C., ZINKOWSKI, R. P. & BINDER, L. I. 1995. Functional implications for the microtubule-associated protein tau: localization in oligodendrocytes. *Proc Natl Acad Sci U S A*, 92, 10369-73.
- LOSSI, L., ALASIA, S., SALIO, C. & MERIGHI, A. 2009. Cell death and proliferation in acute slices and organotypic cultures of mammalian CNS. *Prog Neurobiol*, 88, 221-45.
- LU, J., LI, T., HE, R., BARTLETT, P. F. & GOTZ, J. 2014. Visualizing the microtubule-associated protein tau in the nucleus. *Sci China Life Sci*, 57, 422-31.
- LUCASSEN, P. J., NANINCK, E. F., VAN GOUDOEVER, J. B., FITZSIMONS, C., JOELS, M. & KOROSI, A. 2013. Perinatal programming of adult hippocampal structure and function; emerging roles of stress, nutrition and epigenetics. *Trends Neurosci*, 36, 621-31.
- LYNCH, M. A. 2004. Long-term potentiation and memory. *Physiol Rev*, 84, 87-136.
- MADSEN, J. T., JANSEN, P., HESSLINGER, C., MEYER, M., ZIMMER, J. & GRAMSBERGEN, J. B. 2003. Tetrahydrobiopterin precursor sepiapterin provides protection against neurotoxicity of 1-methyl-4-phenylpyridinium in nigral slice cultures. *J Neurochem*, 85, 214-23.
- MAEDA, S., SAHARA, N., SAITO, Y., MURAYAMA, M., YOSHIKE, Y., KIM, H., MIYASAKA, T., MURAYAMA, S., IKAI, A. & TAKASHIMA, A. 2007. Granular tau oligomers as intermediates of tau filaments. *Biochemistry*, 46, 3856-61.

- MAEDA, S., SAHARA, N., SAITO, Y., MURAYAMA, S., IKAI, A. & TAKASHIMA, A. 2006. Increased levels of granular tau oligomers: an early sign of brain aging and Alzheimer's disease. *Neurosci Res*, 54, 197-201.
- MAGUIRE, E. A., GADIAN, D. G., JOHNSRUDE, I. S., GOOD, C. D., ASHBURNER, J., FRACKOWIAK, R. S. & FRITH, C. D. 2000. Navigation-related structural change in the hippocampi of taxi drivers. *Proc Natl Acad Sci U S A*, 97, 4398-403.
- MALBERG, J. E., EISCH, A. J., NESTLER, E. J. & DUMAN, R. S. 2000. Chronic antidepressant treatment increases neurogenesis in adult rat hippocampus. *J Neurosci*, 20, 9104-10.
- MANDELKOW, E. 1999. Alzheimer's disease. The tangled tale of tau. *Nature*, 402, 588-9.
- MANDELKOW, E., VON BERGEN, M., BIERNAT, J. & MANDELKOW, E. M. 2007. Structural principles of tau and the paired helical filaments of Alzheimer's disease. *Brain Pathol*, 17, 83-90.
- MANDELKOW, E. M. & MANDELKOW, E. 1998. Tau in Alzheimer's disease. *Trends Cell Biol*, 8, 425-7.
- MASTERS, C. L., MULTHAUP, G., SIMMS, G., POTTGIESSER, J., MARTINS, R. N. & BEYREUTHER, K. 1985. Neuronal origin of a cerebral amyloid: neurofibrillary tangles of Alzheimer's disease contain the same protein as the amyloid of plaque cores and blood vessels. *EMBO J*, 4, 2757-63.
- MAYFORD, M., BACH, M. E., HUANG, Y. Y., WANG, L., HAWKINS, R. D. & KANDEL, E. R. 1996a. Control of memory formation through regulated expression of a CaMKII transgene. *Science*, 274, 1678-83.
- MAYFORD, M., BARANES, D., PODSYPANINA, K. & KANDEL, E. R. 1996b. The 3'-untranslated region of CaMKII alpha is a cis-acting signal for the localization and translation of mRNA in dendrites. *Proc Natl Acad Sci U S A*, 93, 13250-5.
- MESSING, L., DECKER, J. M., JOSEPH, M., MANDELKOW, E. & MANDELKOW, E. M. 2013. Cascade of tau toxicity in inducible hippocampal brain slices and prevention by aggregation inhibitors. *Neurobiol Aging*, 34, 1343-54.
- MING, G. L. & SONG, H. 2005. Adult neurogenesis in the mammalian central nervous system. *Annu Rev Neurosci*, 28, 223-50.
- MING, G. L. & SONG, H. 2011. Adult neurogenesis in the mammalian brain: significant answers and significant questions. *Neuron*, 70, 687-702.
- MOCANU, M. M., NISSEN, A., ECKERMANN, K., KHLISTUNOVA, I., BIERNAT, J., DREXLER, D., PETROVA, O., SCHONIG, K., BUJARD, H., MANDELKOW, E., ZHOU, L., RUNE, G. & MANDELKOW, E. M. 2008. The potential for beta-structure in the repeat domain of tau protein determines aggregation, synaptic decay, neuronal loss, and coassembly with endogenous Tau in inducible mouse models of tauopathy. *J Neurosci*, 28, 737-48.
- MORRENS, J., VAN DEN BROECK, W. & KEMPERMANN, G. 2012. Glial cells in adult neurogenesis. *Glia*, 60, 159-74.
- MORRIS, R. G., GARRUD, P., RAWLINS, J. N. & O'KEEFE, J. 1982. Place navigation impaired in rats with hippocampal lesions. *Nature*, 297, 681-3.

- MORRIS, R. G., HAGAN, J. J. & RAWLINS, J. N. 1986. Allocentric spatial learning by hippocampectomised rats: a further test of the "spatial mapping" and "working memory" theories of hippocampal function. *Q J Exp Psychol B*, 38, 365-95.
- MOSER, M. B. & MOSER, E. I. 1998. Functional differentiation in the hippocampus. *Hippocampus*, 8, 608-19.
- MOSHER, K. I., ANDRES, R. H., FUKUHARA, T., BIERI, G., HASEGAWA-MORIYAMA, M., HE, Y., GUZMAN, R. & WYSS-CORAY, T. 2012. Neural progenitor cells regulate microglia functions and activity. *Nat Neurosci*, 15, 1485-7.
- MULLEN, R. J., BUCK, C. R. & SMITH, A. M. 1992. NeuN, a neuronal specific nuclear protein in vertebrates. *Development*, 116, 201-11.
- MURRELL, J., FARLOW, M., GHETTI, B. & BENSON, M. D. 1991. A mutation in the amyloid precursor protein associated with hereditary Alzheimer's disease. *Science*, 254, 97-9.
- NAGY, Z., ESIRI, M. M., CATO, A. M. & SMITH, A. D. 1997. Cell cycle markers in the hippocampus in Alzheimer's disease. *Acta Neuropathol*, 94, 6-15.
- NAKATOMI, H., KURIU, T., OKABE, S., YAMAMOTO, S., HATANO, O., KAWAHARA, N., TAMURA, A., KIRINO, T. & NAKAFUKU, M. 2002. Regeneration of hippocampal pyramidal neurons after ischemic brain injury by recruitment of endogenous neural progenitors. *Cell*, 110, 429-41.
- NAMBA, T., MOCHIZUKI, H., ONODERA, M., MIZUNO, Y., NAMIKI, H. & SEKI, T. 2005. The fate of neural progenitor cells expressing astrocytic and radial glial markers in the postnatal rat dentate gyrus. *Eur J Neurosci*, 22, 1928-41.
- NAMBA, T., MOCHIZUKI, H., ONODERA, M., NAMIKI, H. & SEKI, T. 2007. Postnatal neurogenesis in hippocampal slice cultures: early in vitro labeling of neural precursor cells leads to efficient neuronal production. *J Neurosci Res*, 85, 1704-12.
- NJIE, E. G., BOELEN, E., STASSEN, F. R., STEINBUSCH, H. W., BORCHELT, D. R. & STREIT, W. J. 2012. Ex vivo cultures of microglia from young and aged rodent brain reveal age-related changes in microglial function. *Neurobiol Aging*, 33, 195 e1-12.
- NORABERG, J., KRISTENSEN, B. W. & ZIMMER, J. 1999. Markers for neuronal degeneration in organotypic slice cultures. *Brain Res Brain Res Protoc*, 3, 278-90.
- NORABERG, J., POULSEN, F. R., BLAABJERG, M., KRISTENSEN, B. W., BONDE, C., MONTERO, M., MEYER, M., GRAMSBERGEN, J. B. & ZIMMER, J. 2005. Organotypic hippocampal slice cultures for studies of brain damage, neuroprotection and neurorepair. *Curr Drug Targets CNS Neurol Disord*, 4, 435-52.
- NOWAKOWSKI, R. S., LEWIN, S. B. & MILLER, M. W. 1989. Bromodeoxyuridine immunohistochemical determination of the lengths of the cell cycle and the DNA-synthetic phase for an anatomically defined population. *J Neurocytol*, 18, 311-8.
- O'KANE, G., KENSINGER, E. A. & CORKIN, S. 2004. Evidence for semantic learning in profound amnesia: an investigation with patient H.M. *Hippocampus*, 14, 417-25.

- O'KEEFE, J. & DOSTROVSKY, J. 1971. The hippocampus as a spatial map. Preliminary evidence from unit activity in the freely-moving rat. *Brain Res*, 34, 171-5.
- O'KEEFE, J., NADEL, L. & WILLNER, J. 1979. Tuning out irrelevancy? Comments on Solomon's temporal mapping view of the hippocampus. *Psychol Bull*, 86, 1280-9.
- ODAWARA, T., ISEKI, E., KOSAKA, K., AKIYAMA, H., IKEDA, K. & YAMAMOTO, T. 1995. Investigation of tau-2 positive microglia-like cells in the subcortical nuclei of human neurodegenerative disorders. *Neurosci Lett*, 192, 145-8.
- OHM, T. G. 2007. The dentate gyrus in Alzheimer's disease. *Prog Brain Res*, 163, 723-40.
- PAOLICELLI, R. C., BOLASCO, G., PAGANI, F., MAGGI, L., SCIANNI, M., PANZANELLI, P., GIUSTETTO, M., FERREIRA, T. A., GUIDUCCI, E., DUMAS, L., RAGOZZINO, D. & GROSS, C. T. 2011. Synaptic pruning by microglia is necessary for normal brain development. *Science*, 333, 1456-8.
- PAOLICELLI, R. C. & GROSS, C. T. 2011. Microglia in development: linking brain wiring to brain environment. *Neuron Glia Biol*, 7, 77-83.
- PAPASOZOMENOS, S. C. & BINDER, L. I. 1987. Phosphorylation determines two distinct species of Tau in the central nervous system. *Cell Motil Cytoskeleton*, 8, 210-26.
- PEREZ-ASENSIO, F. J., PERPINA, U., PLANAS, A. M. & POZAS, E. 2013. Interleukin-10 regulates progenitor differentiation and modulates neurogenesis in adult brain. *J Cell Sci*, 126, 4208-19.
- PLUMPE, T., EHNINGER, D., STEINER, B., KLEMPIN, F., JESSBERGER, S., BRANDT, M., ROMER, B., RODRIGUEZ, G. R., KRONENBERG, G. & KEMPERMANN, G. 2006. Variability of doublecortin-associated dendrite maturation in adult hippocampal neurogenesis is independent of the regulation of precursor cell proliferation. *BMC Neurosci*, 7, 77.
- POORKAJ, P., BIRD, T. D., WIJSMAN, E., NEMENS, E., GARRUTO, R. M., ANDERSON, L., ANDREADIS, A., WIEDERHOLT, W. C., RASKIND, M. & SCHELLENBERG, G. D. 1998. Tau is a candidate gene for chromosome 17 frontotemporal dementia. *Ann Neurol*, 43, 815-25.
- POPPEK, D., KECK, S., ERMAK, G., JUNG, T., STOLZING, A., ULLRICH, O., DAVIES, K. J. & GRUNE, T. 2006. Phosphorylation inhibits turnover of the tau protein by the proteasome: influence of RCAN1 and oxidative stress. *Biochem J*, 400, 511-20.
- POULSEN, F. R., BLAABJERG, M., MONTERO, M. & ZIMMER, J. 2005. Glutamate receptor antagonists and growth factors modulate dentate granule cell neurogenesis in organotypic, rat hippocampal slice cultures. *Brain Res*, 1051, 35-49.
- PRINGLE, A. K., SUNDSTROM, L. E., WILDE, G. J., WILLIAMS, L. R. & IANNOTTI, F. 1996. Brain-derived neurotrophic factor, but not neurotrophin-3, prevents ischaemia-induced neuronal cell death in organotypic rat hippocampal slice cultures. *Neurosci Lett*, 211, 203-6.
- PRISTERA, A., SARAULLI, D., FARIOLI-VECCHIOLI, S., STRIMPAKOS, G., COSTANZI, M., DI CERTO, M. G., CANNAS, S., CIOTTI, M. T., TIRONE, F., MATTEI, E., CESTARI, V. & CANU, N. 2013. Impact of N-tau on adult hippocampal neurogenesis, anxiety, and memory. *Neurobiol Aging*, 34, 2551-63.

- RAINETEAU, O., HUGEL, S., OZEN, I., RIETSCHIN, L., SIGRIST, M., ARBER, S. & GAHWILER, B. H. 2006. Conditional labeling of newborn granule cells to visualize their integration into established circuits in hippocampal slice cultures. *Mol Cell Neurosci*, 32, 344-55.
- RAY, A. M., OWEN, D. E., EVANS, M. L., DAVIS, J. B. & BENHAM, C. D. 2000. Caspase inhibitors are functionally neuroprotective against oxygen glucose deprivation induced CA1 death in rat organotypic hippocampal slices. *Brain Res*, 867, 62-9.
- REIF, A., FRITZEN, S., FINGER, M., STROBEL, A., LAUER, M., SCHMITT, A. & LESCH, K. P. 2006. Neural stem cell proliferation is decreased in schizophrenia, but not in depression. *Mol Psychiatry*, 11, 514-22.
- REIS, D. J., YANG, X. C. & MILNER, T. A. 1998. Agmatine containing axon terminals in rat hippocampus form synapses on pyramidal cells. *Neurosci Lett*, 250, 185-8.
- RIZZU, P., VAN SWIETEN, J. C., JOOSSE, M., HASEGAWA, M., STEVENS, M., TIBBEN, A., NIERMEIJER, M. F., HILLEBRAND, M., RAVID, R., OOSTRA, B. A., GOEDERT, M., VAN DUIJN, C. M. & HEUTINK, P. 1999. High prevalence of mutations in the microtubule-associated protein tau in a population study of frontotemporal dementia in the Netherlands. *Am J Hum Genet*, 64, 414-21.
- ROBERSON, E. D., HALABISKY, B., YOO, J. W., YAO, J., CHIN, J., YAN, F., WU, T., HAMTO, P., DEVIDZE, N., YU, G. Q., PALOP, J. J., NOEBELS, J. L. & MUCKE, L. 2011. Amyloid-beta/Fyn-induced synaptic, network, and cognitive impairments depend on tau levels in multiple mouse models of Alzheimer's disease. *J Neurosci*, 31, 700-11.
- ROBERSON, E. D., SCEARCE-LEVIE, K., PALOP, J. J., YAN, F., CHENG, I. H., WU, T., GERSTEIN, H., YU, G. Q. & MUCKE, L. 2007. Reducing endogenous tau ameliorates amyloid beta-induced deficits in an Alzheimer's disease mouse model. *Science*, 316, 750-4.
- ROCHE, R. A., MANGAOANG, M. A., COMMINS, S. & O'MARA, S. M. 2005. Hippocampal contributions to neurocognitive mapping in humans: a new model. *Hippocampus*, 15, 622-41.
- ROGAEV, E. I., SHERRINGTON, R., ROGAEVA, E. A., LEVESQUE, G., IKEDA, M., LIANG, Y., CHI, H., LIN, C., HOLMAN, K., TSUDA, T. & ET AL. 1995. Familial Alzheimer's disease in kindreds with missense mutations in a gene on chromosome 1 related to the Alzheimer's disease type 3 gene. *Nature*, 376, 775-8.
- ROMER, B., KREBS, J., OVERALL, R. W., FABEL, K., BABU, H., OVERSTREET-WADICHE, L., BRANDT, M. D., WILLIAMS, R. W., JESSBERGER, S. & KEMPERMANN, G. 2011. Adult hippocampal neurogenesis and plasticity in the infrapyramidal bundle of the mossy fiber projection: I. Co-regulation by activity. *Front Neurosci*, 5, 107.
- SAHAY, A., SCOBIE, K. N., HILL, A. S., O'CARROLL, C. M., KHEIRBEK, M. A., BURGHARDT, N. S., FENTON, A. A., DRANOVSKY, A. & HEN, R. 2011. Increasing adult hippocampal neurogenesis is sufficient to improve pattern separation. *Nature*, 472, 466-70.
- SANDER, J. W. & SHORVON, S. D. 1996. Epidemiology of the epilepsies. *J Neurol Neurosurg Psychiatry*, 61, 433-43.
- SANTACRUZ, K., LEWIS, J., SPIRES, T., PAULSON, J., KOTILINEK, L., INGELSSON, M., GUIMARAES, A., DETURE, M., RAMSDEN, M., MCGOWAN, E., FORSTER, C., YUE,



- M., ORNE, J., JANUS, C., MARIASH, A., KUSKOWSKI, M., HYMAN, B., HUTTON, M. & ASHE, K. H. 2005. Tau suppression in a neurodegenerative mouse model improves memory function. *Science*, 309, 476-81.
- SCHLESSINGER, A. R., COWAN, W. M. & GOTTLIEB, D. I. 1975. An autoradiographic study of the time of origin and the pattern of granule cell migration in the dentate gyrus of the rat. *J Comp Neurol*, 159, 149-75.
- SEKI, T. & ARAI, Y. 1993. Highly polysialylated NCAM expression in the developing and adult rat spinal cord. *Brain Res Dev Brain Res*, 73, 141-5.
- SENNVIK, K., BOEKHOORN, K., LASRADO, R., TERWEL, D., VERHAEGHE, S., KORR, H., SCHMITZ, C., TOMIYAMA, T., MORI, H., KRUGERS, H., JOELS, M., RAMAKERS, G. J., LUCASSEN, P. J. & VAN LEUVEN, F. 2007. Tau-4R suppresses proliferation and promotes neuronal differentiation in the hippocampus of tau knockin/knockout mice. *FASEB J*, 21, 2149-61.
- SERI, B., GARCIA-VERDUGO, J. M., MCEWEN, B. S. & ALVAREZ-BUYLLA, A. 2001. Astrocytes give rise to new neurons in the adult mammalian hippocampus. *J Neurosci*, 21, 7153-60.
- SHERRINGTON, R., ROGAEV, E. I., LIANG, Y., ROGAEVA, E. A., LEVESQUE, G., IKEDA, M., CHI, H., LIN, C., LI, G., HOLMAN, K., TSUDA, T., MAR, L., FONCIN, J. F., BRUNI, A. C., MONTESI, M. P., SORBI, S., RAINERO, I., PINESSI, L., NEE, L., CHUMAKOV, I., POLLEN, D., BROOKES, A., SANSEAU, P., POLINSKY, R. J., WASCO, W., DA SILVA, H. A., HAINES, J. L., PERKICAK-VANCE, M. A., TANZI, R. E., ROSES, A. D., FRASER, P. E., ROMMENS, J. M. & ST GEORGE-HYSLOP, P. H. 1995. Cloning of a gene bearing missense mutations in early-onset familial Alzheimer's disease. *Nature*, 375, 754-60.
- SHRUSTER, A. & OFFEN, D. 2014. Targeting neurogenesis ameliorates danger assessment in a mouse model of Alzheimer's disease. *Behav Brain Res*, 261, 193-201.
- SMITH, D. L., POZUETA, J., GONG, B., ARANCIO, O. & SHELANSKI, M. 2009. Reversal of long-term dendritic spine alterations in Alzheimer disease models. *Proc Natl Acad Sci U S A*, 106, 16877-82.
- SONG, J., SUN, J., MOSS, J., WEN, Z., SUN, G. J., HSU, D., ZHONG, C., DAVOUDI, H., CHRISTIAN, K. M., TONI, N., MING, G. L. & SONG, H. 2013. Parvalbumin interneurons mediate neuronal circuitry-neurogenesis coupling in the adult hippocampus. *Nat Neurosci*, 16, 1728-30.
- SONG, J., ZHONG, C., BONAGUIDI, M. A., SUN, G. J., HSU, D., GU, Y., MELETIS, K., HUANG, Z. J., GE, S., ENIKOLOPOV, G., DEISSEROTH, K., LUSCHER, B., CHRISTIAN, K. M., MING, G. L. & SONG, H. 2012. Neuronal circuitry mechanism regulating adult quiescent neural stem-cell fate decision. *Nature*, 489, 150-4.
- SPALDING, K. L., BERGMANN, O., ALKASS, K., BERNARD, S., SALEHPOUR, M., HUTTNER, H. B., BOSTROM, E., WESTERLUND, I., VIAL, C., BUCHHOLZ, B. A., POSSNERT, G., MASH, D. C., DRUID, H. & FRISEN, J. 2013. Dynamics of hippocampal neurogenesis in adult humans. *Cell*, 153, 1219-27.
- SPILLANTINI, M. G., BIRD, T. D. & GHETTI, B. 1998. Frontotemporal dementia and Parkinsonism linked to chromosome 17: a new group of tauopathies. *Brain Pathol*, 8, 387-402.

- SPILLANTINI, M. G. & GOEDERT, M. 2000. Tau mutations in familial frontotemporal dementia. *Brain*, 123 ( Pt 5), 857-9.
- SQUIRE, L. R. 1992. Memory and the hippocampus: a synthesis from findings with rats, monkeys, and humans. *Psychol Rev*, 99, 195-231.
- STOPPINI, L., BUCHS, P. A. & MULLER, D. 1991. A simple method for organotypic cultures of nervous tissue. *J Neurosci Methods*, 37, 173-82.
- STORGAARD, J., KORNBLOT, B. T., ZIMMER, J. & GRAMSBERGEN, J. B. 2000. 3-Nitropropionic acid neurotoxicity in organotypic striatal and corticostriatal slice cultures is dependent on glucose and glutamate. *Exp Neurol*, 164, 227-35.
- SU, X., GUAN, W., YU, Y. C. & FU, Y. 2014. Cerebellar stem cells do not produce neurons and astrocytes in adult mouse. *Biochem Biophys Res Commun*, 450, 378-83.
- SULTAN, A., NESSLANY, F., VIOLET, M., BEGARD, S., LOYENS, A., TALAHARI, S., MANSUROGLU, Z., MARZIN, D., SERGEANT, N., HUMEZ, S., COLIN, M., BONNEFOY, E., BUEE, L. & GALAS, M. C. 2011. Nuclear tau, a key player in neuronal DNA protection. *J Biol Chem*, 286, 4566-75.
- SULTAN, S., GEBARA, E. & TONI, N. 2013. Doxycycline increases neurogenesis and reduces microglia in the adult hippocampus. *Front Neurosci*, 7, 131.
- SUN, G. J., SAILOR, K. A., MAHMOOD, Q. A., CHAVALI, N., CHRISTIAN, K. M., SONG, H. & MING, G. L. 2013. Seamless reconstruction of intact adult-born neurons by serial end-block imaging reveals complex axonal guidance and development in the adult hippocampus. *J Neurosci*, 33, 11400-11.
- SUNDSTROM, L., MORRISON, B., 3RD, BRADLEY, M. & PRINGLE, A. 2005. Organotypic cultures as tools for functional screening in the CNS. *Drug Discov Today*, 10, 993-1000.
- SYDOW, A., VAN DER JEUGD, A., ZHENG, F., AHMED, T., BALSCHUN, D., PETROVA, O., DREXLER, D., ZHOU, L., RUNE, G., MANDELKOW, E., D'HOOGHE, R., ALZHEIMER, C. & MANDELKOW, E. M. 2011. Tau-induced defects in synaptic plasticity, learning, and memory are reversible in transgenic mice after switching off the toxic Tau mutant. *J Neurosci*, 31, 2511-25.
- TAKASHIMA, A., MURAYAMA, M., MURAYAMA, O., KOHNO, T., HONDA, T., YASUTAKE, K., NIHONMATSU, N., MERCKEN, M., YAMAGUCHI, H., SUGIHARA, S. & WOLOZIN, B. 1998. Presenilin 1 associates with glycogen synthase kinase-3beta and its substrate tau. *Proc Natl Acad Sci U S A*, 95, 9637-41.
- TASHIRO, K., HASEGAWA, M., IHARA, Y. & IWATSUBO, T. 1997. Somatodendritic localization of phosphorylated tau in neonatal and adult rat cerebral cortex. *Neuroreport*, 8, 2797-801.
- THOMPSON, S. M. 1993. Consequence of epileptic activity in vitro. *Brain Pathol*, 3, 413-9.
- TONI, N., LAPLAGNE, D. A., ZHAO, C., LOMBARDI, G., RIBAK, C. E., GAGE, F. H. & SCHINDER, A. F. 2008. Neurons born in the adult dentate gyrus form functional synapses with target cells. *Nat Neurosci*, 11, 901-7.
- TONI, N. & SULTAN, S. 2011. Synapse formation on adult-born hippocampal neurons. *Eur J Neurosci*, 33, 1062-8.

- TONI, N., TENG, E. M., BUSHONG, E. A., AIMONE, J. B., ZHAO, C., CONSIGLIO, A., VAN PRAAG, H., MARTONE, M. E., ELLISMAN, M. H. & GAGE, F. H. 2007. Synapse formation on neurons born in the adult hippocampus. *Nat Neurosci*, 10, 727-34.
- ULLIAN, E. M., SAPPERSTEIN, S. K., CHRISTOPHERSON, K. S. & BARRES, B. A. 2001. Control of synapse number by glia. *Science*, 291, 657-61.
- URLINGER, S., BARON, U., THELLMANN, M., HASAN, M. T., BUJARD, H. & HILLEN, W. 2000. Exploring the sequence space for tetracycline-dependent transcriptional activators: novel mutations yield expanded range and sensitivity. *Proc Natl Acad Sci U S A*, 97, 7963-8.
- VAN DER JEUGD, A., HOCHGRAFE, K., AHMED, T., DECKER, J. M., SYDOW, A., HOFMANN, A., WU, D., MESSING, L., BALSCHUN, D., D'HOOGHE, R. & MANDELKOW, E. M. 2012. Cognitive defects are reversible in inducible mice expressing pro-aggregant full-length human Tau. *Acta Neuropathol*, 123, 787-805.
- VAN PAESSCHEN, W., CONNELLY, A., KING, M. D., JACKSON, G. D. & DUNCAN, J. S. 1997. The spectrum of hippocampal sclerosis: a quantitative magnetic resonance imaging study. *Ann Neurol*, 41, 41-51.
- VAN PRAAG, H., SCHINDER, A. F., CHRISTIE, B. R., TONI, N., PALMER, T. D. & GAGE, F. H. 2002. Functional neurogenesis in the adult hippocampus. *Nature*, 415, 1030-4.
- VAN SWIETEN, J. & SPILLANTINI, M. G. 2007. Hereditary frontotemporal dementia caused by Tau gene mutations. *Brain Pathol*, 17, 63-73.
- VANELZAKKER, M., FEVURLY, R. D., BREINDEL, T. & SPENCER, R. L. 2008. Environmental novelty is associated with a selective increase in Fos expression in the output elements of the hippocampal formation and the perirhinal cortex. *Learn Mem*, 15, 899-908.
- VARELA-NALLAR, L., GRABOWSKI, C. P., ALFARO, I. E., ALVAREZ, A. R. & INESTROSA, N. C. 2009. Role of the Wnt receptor Frizzled-1 in presynaptic differentiation and function. *Neural Dev*, 4, 41.
- VON BERGEN, M., BARGHORN, S., LI, L., MARX, A., BIERNAT, J., MANDELKOW, E. M. & MANDELKOW, E. 2001. Mutations of tau protein in frontotemporal dementia promote aggregation of paired helical filaments by enhancing local beta-structure. *J Biol Chem*, 276, 48165-74.
- VON BERGEN, M., FRIEDHOFF, P., BIERNAT, J., HEBERLE, J., MANDELKOW, E. M. & MANDELKOW, E. 2000. Assembly of tau protein into Alzheimer paired helical filaments depends on a local sequence motif ((306)VQIVYK(311)) forming beta structure. *Proc Natl Acad Sci U S A*, 97, 5129-34.
- WAHAB, A., ALBUS, K., GABRIEL, S. & HEINEMANN, U. 2010. In search of models of pharmacoresistant epilepsy. *Epilepsia*, 51 Suppl 3, 154-9.
- WANG, D. D. & BORDEY, A. 2008. The astrocyte odyssey. *Prog Neurobiol*, 86, 342-67.
- WANG, L. P., KEMPERMANN, G. & KETTENMANN, H. 2005. A subpopulation of precursor cells in the mouse dentate gyrus receives synaptic GABAergic input. *Mol Cell Neurosci*, 29, 181-9.
- WANG, Y. P., BIERNAT, J., PICKHARDT, M., MANDELKOW, E. & MANDELKOW, E. M. 2007. Stepwise proteolysis liberates tau fragments that nucleate the Alzheimer-

- like aggregation of full-length tau in a neuronal cell model. *Proc Natl Acad Sci U S A*, 104, 10252-7.
- WEBER, T., BAIER, V., PAULY, R., SAHAY, A., BAUR, M., HERRMANN, E., CICCOLINI, F., HEN, R., KRONENBERG, G. & BARTSCH, D. 2011. Inducible gene expression in GFAP+ progenitor cells of the SGZ and the dorsal wall of the SVZ-A novel tool to manipulate and trace adult neurogenesis. *Glia*, 59, 615-26.
- WEIMER, J. M. & ANTON, E. S. 2006. Doubling up on microtubule stabilizers: synergistic functions of doublecortin-like kinase and doublecortin in the developing cerebral cortex. *Neuron*, 49, 3-4.
- WEINGARTEN, M. D., LOCKWOOD, A. H., HWO, S. Y. & KIRSCHNER, M. W. 1975. A protein factor essential for microtubule assembly. *Proc Natl Acad Sci U S A*, 72, 1858-62.
- WILLE, H., DREWES, G., BIERNAT, J., MANDELKOW, E. M. & MANDELKOW, E. 1992. Alzheimer-like paired helical filaments and antiparallel dimers formed from microtubule-associated protein tau in vitro. *J Cell Biol*, 118, 573-84.
- WILLIAMS, J. H., LI, Y. G., NAYAK, A., ERRINGTON, M. L., MURPHY, K. P. & BLISS, T. V. 1993. The suppression of long-term potentiation in rat hippocampus by inhibitors of nitric oxide synthase is temperature and age dependent. *Neuron*, 11, 877-84.
- WITTER, M. P., NABER, P. A., VAN HAEFTEN, T., MACHIELSEN, W. C., ROMBOUTS, S. A., BARKHOF, F., SCHELTENS, P. & LOPES DA SILVA, F. H. 2000. Cortico-hippocampal communication by way of parallel parahippocampal-subicular pathways. *Hippocampus*, 10, 398-410.
- WOLF, H. K., BUSLEI, R., SCHMIDT-KASTNER, R., SCHMIDT-KASTNER, P. K., PIETSCH, T., WIESTLER, O. D. & BLUMCKE, I. 1996. NeuN: a useful neuronal marker for diagnostic histopathology. *J Histochem Cytochem*, 44, 1167-71.
- WOODGETT, J. R. 2001. Judging a protein by more than its name: GSK-3. *Sci STKE*, 2001, re12.
- XU, Q., D'AMORE, P. A. & SOKOL, S. Y. 1998. Functional and biochemical interactions of Wnts with FrzA, a secreted Wnt antagonist. *Development*, 125, 4767-76.
- ZEMPEL, H., LUEDTKE, J., KUMAR, Y., BIERNAT, J., DAWSON, H., MANDELKOW, E. & MANDELKOW, E. M. 2013. Amyloid-beta oligomers induce synaptic damage via Tau-dependent microtubule severing by TTLL6 and spastin. *EMBO J*, 32, 2920-37.
- ZEMPEL, H. & MANDELKOW, E. M. 2012. Linking amyloid-beta and tau: amyloid-beta induced synaptic dysfunction via local wreckage of the neuronal cytoskeleton. *Neurodegener Dis*, 10, 64-72.
- ZHANG, X., SMITH, D. L., MERIIN, A. B., ENGEMANN, S., RUSSEL, D. E., ROARK, M., WASHINGTON, S. L., MAXWELL, M. M., MARSH, J. L., THOMPSON, L. M., WANKER, E. E., YOUNG, A. B., HOUSMAN, D. E., BATES, G. P., SHERMAN, M. Y. & KAZANTSEV, A. G. 2005. A potent small molecule inhibits polyglutamine aggregation in Huntington's disease neurons and suppresses neurodegeneration in vivo. *Proc Natl Acad Sci U S A*, 102, 892-7.

- ZHAO, C., TENG, E. M., SUMMERS, R. G., JR., MING, G. L. & GAGE, F. H. 2006. Distinct morphological stages of dentate granule neuron maturation in the adult mouse hippocampus. *J Neurosci*, 26, 3-11.
- ZHOU, F. Q. & SNIDER, W. D. 2005. Cell biology. GSK-3beta and microtubule assembly in axons. *Science*, 308, 211-4.
- ZIMMER, J. & GAHWILER, B. H. 1987. Growth of hippocampal mossy fibers: a lesion and coculture study of organotypic slice cultures. *J Comp Neurol*, 264, 1-13.

## Acknowledgment

I would like to thank my mentors, Prof. Dr. Eckhard Mandelkow and Dr. Eva-Maria Mandelkow for giving me an opportunity to conduct my Ph.D. thesis in their laboratory and for continuous advice.

I express my gratitude to my lab colleagues Dr. Lars Krueger, Dr. Marta Anglada-Huguet, Dr. Frank Dennissen, Dr. Jochen Decker and Katharina Paesler for their interest, valuable scientific input and technical advice while working in this project. Thanks also to the members of the mouse team in Hamburg, Dr. Astrid Sydow, Dr. Katja Hochgräfe, Anne Hofmann and Stefanie Könen for the generation of transgenic mouse lines which allowed me to carry out my research.

I take this opportunity to thank the people who have contributed to the development of my academic career over the years, notably my teachers from school and my professors at the University of Madras, Department of Medical Biochemistry, Prof. Dr. C. Panneerselvam and Prof. Dr. P. Sachdanandham for their advice and encouragement.

Last but not least I would like to extend my gratitude for my family for their constant love and support.

Chris Maria Renny Joseph

## **Declaration**

I declare that the work in this thesis contains original results of my own investigation, except where otherwise stated. This work was carried out at the Max-Planck-Unit for Structural Molecular Biology at DESY, Hamburg, and at the German Center for Neurodegenerative Diseases, Bonn, under the supervision of Prof. Dr. Eckhard Mandelkow and in partial fulfillment of the requirements of the doctoral degree of the University of Hamburg, Department of Biology. I further declare that this work has not been submitted to any university or institution towards the partial fulfillment of any degree.

Chris Maria Renny Joseph

Hamburg, 2014

